



EDITORIAL

Dear readers,

We have the pleasure to present to you the new regular issue of the Bulgarian Journal of Meteorology and Hydrology (BJMH). It consists of ten original papers by Bulgarian, Albanian, Bosnian and Ukrainian meteorologists and hydrologists.

The authors of the first three papers were participants in the target group of the project BG051PO001-3.3.06-0063 under the “Programme for multidisciplinary training of PhD students, post-docs, post graduate students and young scientists”, funded by the Operational Programme “Human Resources Development”, co-financed by the European Social Fund of the European Union 2007-2013, with beneficiary the National Institute of Meteorology and Hydrology. As stated in BJMH Special issue, vol. 20, No 5 from 2015, the studies in these papers were presented at the National Science Workshop, held in Hisar (28.09.-01.10.2015) in the frame of the project.

The fourth paper is dedicated to description and construction of the climate of cyclonic activity in the Mediterranean, proposing original and relatively simple method for calculating the potential vorticity flow.

The fifth paper deals with the macrocirculation processes of the northwest Black sea region, contributing to surface wind strengthening.

The sixth one gives quantitative assessment of water losses of Badovc Lake in Kosovo based on both water balance of the lake and water isotopic composition.

In the seventh paper, through experimental studies within a real water management system in Bulgaria, the author proves the feasibility of the proposed methodological approach and the mathematical model, mainly for improvement and efficiency of the procedure for issuing permits for water abstractions.

The eighth paper gives the latest statistical data from observations on groundwater chemical status of EU Member States in particularly Bulgaria and Belgium.

The last two papers (Part one and two) deal with different numerical simulations of the groundwater level fluctuations in riparian lowlands.

We are currently inviting authors to submit original and high quality works to be published in the journal. We are strongly motivated to assure the regular issuing of BJMH and to raise its popularity among scientific communities both in Bulgaria and abroad.

Ekaterina Batchvarova (Chief Editor)
Tatiana Spassova (Technical Editor)



Spatio-temporal characteristics of some convective induced extreme events in Bulgaria

Lilia Bocheva*, Tsveta Nikolova

*National Institute of Meteorology and Hydrology - BAS,
66, Tsarigradsko shose, 1784 Sofia, Bulgaria*

Abstract: Severe convective storms produce dangerous weather phenomena especially during the warm half of the year like heavy and very intense rainfall, thunderstorms and hail-fall. They are often associated with strong to violent wind gusts and sometimes even with such dangerous events like squall or tornado. The objective of this work is to present the spatial and temporal distribution of torrential convective precipitations during the period 1991-2014 in different regions of Bulgaria. Only days in which there is thunderstorm activity combined with 24-hour precipitation amount above 60 mm are selected and analyzed. The choice of 60 mm/24h as a bottom limit is motivated by the fact that for 90% of all meteorological stations in Bulgaria it is equal or above the climatological monthly precipitation normal. The regional intra-monthly distribution of such extreme events is also presented and results for two 12-year periods 1991–2002 and 2003–2014, are compared and statistically estimated. Second part of the study summarizes general features of the tornado and waterspouts occurrence in Bulgaria (2001-2014) such as the geographical, monthly and diurnal distributions. Characteristics concerning tornado intensity are also presented.

Keywords: convective precipitation; tornado; climate; Bulgaria

1. INTRODUCTION

The aim of the present study is to continue the investigation over potentially dangerous severe storms that lead to abundant precipitation, to severe thunderstorms and hail, and rarely to such violent events as tornado. They are sparse in space and time and have unfavourable influence on the economics and societies causing significant property and infrastructure damages as well as losses of life.

* Lilia.Bocheva@meteo.bg

The first part of this study presents the spatial and temporal distribution of torrential convective precipitations during the last 24 years (1991-2014) in different regions of Bulgaria. Only days in which there is thunderstorm activity combined with 24-hour precipitation amount above 60 mm are selected and analyzed. The choice of 60 mm/24h as a bottom limit is motivated by the fact that for 90% of all meteorological stations in Bulgaria it is equal or above the climatological monthly precipitation normal. The regional intra-monthly distribution of such extreme events is also presented.

The distribution of precipitations across the territory of Bulgaria and its seasonality are mainly caused by the atmospheric circulation patterns and the topography characteristics. The zonal extension of the Stara Planina and the Rila - Rhodope massif present a natural barrier to the invasion of cold air masses towards the southern part of the country. These mountains are also a barrier to warm air masses that are forced to overflow them. Actually the country is divided into North and South Bulgaria by the Stara Planina mountain chain, which affects the precipitation and temperature regime on either side of it. However, a significant difference in the precipitation regime has recently been observed between the western and eastern parts of the country (Bocheva, 2015).

General features of the tornado and waterspouts occurrence in Bulgaria during the last 15 years are also presented. Second part summarizes their geographical, yearly, monthly and diurnal distributions. Characteristics concerning tornado intensity are also presented.

Tornadoes occur relatively rarely in Bulgaria compared to other parts of the world. These events may often remain unreported when they occur in remote and weakly populated mountainous regions of the country or if they leave no significant damage behind. The number of reports of tornadoes in Bulgarian in the last 10-15 years however has significantly increased thanks to the revolutionary development of the information technology.

2. DATA AND METHODS

The study is based on data of torrential convective precipitation events (days with $Q \geq 60$ mm/24h and thunderstorm) from the meteorological database of the National Institute of Meteorology and Hydrology (NIMH) of Bulgaria for the period 1991–2014. We consider all synoptic, climatological and rain-gauge stations, in which regular observations were completed during the whole period or part of it. Their number varies between 555 in 1991 and 371 in 2014. The records for duration and intensity of atmospheric phenomena are available for all cases. Expert quality control of data has been carried out. The automatic stations data is not included in this study, because of their short period of exploitation and different sensors. The distribution of stormy days for each station is analyzed and then summarized for each of the 6 considered regions in Bulgaria during the whole studied period. The selected regions are: North-West (NW),

North-Central (NC), North-East (NE), South-East (SE), South-Central (SC), and South-West (SW) Bulgaria (BG) - see Fig. 1. They are chosen on administrative principle, but also match to some extent the different sub-climate zones of the country.

Intra-monthly distributions of convective torrential precipitations for each region, as well as annual and monthly distributions of large-scale convective storms for whole country are presented and results for two 12-years periods 1991–2002 and 2003–2014, are compared.

Statistical analysis is performed in order to assess the variability and possible differences in the torrential convective precipitation days from long-term data series. For the comparison of the two periods 1991-2002 and 2003-2014 ANOVA with Poisson distribution (StatSoft, 2004) are applicable to such discrete samples of heavy precipitation days.

The present work is based also on a collection of data of 55 tornados and waterspouts in Bulgaria between 2001 and 2014. Data originated from eyewitness reports, site investigations, media news, reports of the local administration of damage in crops and infrastructure. Press and TV are often the richest source of images of the tornadoes and waterspouts themselves or the damage they have caused. Data from site investigations of damage, scientific publications, and the meteorological data base of NIMH and the archives of the Bulgarian Hail Suppression Agency (BAHS) are also included. The analysis of the vertical structure of the atmosphere at the location and the time of occurrence are based on the sounding data from the archives of NIMH. The tornado cases have also been classified by severity according the Fujita scale (Fujita, 1981).

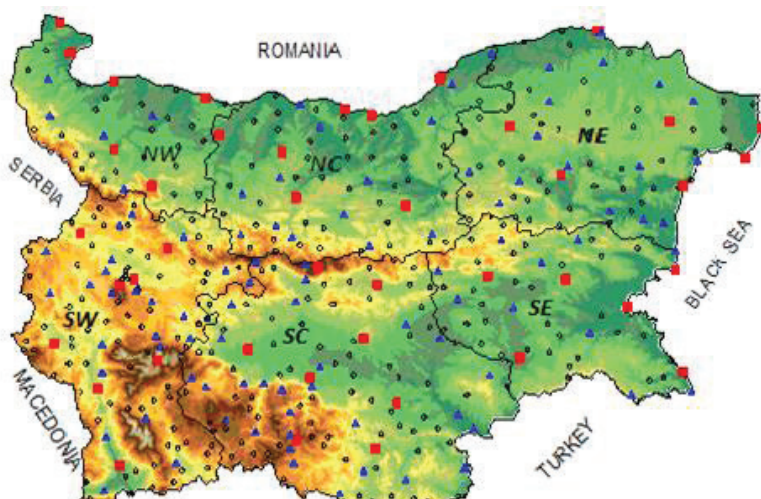


Fig. 1. The present NIMH weather stations network: synoptic (squares), climatological (triangles) and rain-gauge (circles) stations.

3. REGIONAL DISTRIBUTION OF CONVECTIVE PRECIPITATIONS

During the 24-year period of investigation the annual distribution of number of days with convective precipitation $\geq 60\text{mm}/24\text{h}$ shows an increasing trend almost in all regions although the number of meteorological stations in Bulgaria decreases. About 43% of days with dangerous precipitations during the period (1991–2002) are connected with convective storms (from 18.5% for SW Bulgaria to 55% for SC Bulgaria). During the second period (2003-2014) the contribution of torrential convective precipitations increases to 63% (from 40.3% for NC Bulgaria to 69.4% for SC Bulgaria). The increasing of number of convective heavy rain days is statistically significant for NE, SC and especially for SW Bulgaria (Table 1).

Table 1: Statistical comparison between two samples of number of convective precipitation days in different parts of Bulgaria, using the Poisson distribution for the 1991 – 2002 (1) and 2003 – 2014(2) data set.

№ of samples	1	2	1, 2	tail	$(\mu_2 - \mu_1)/\mu_1$
Precipitation days	mean	mean		probability	
Group C2	μ_1	μ_2	χ^2	p	%
NW Bulgaria	1.4	2.1	1.533	0.216	0.46
NC Bulgaria	2.8	2.1	1.107	0.293	-0.24
NE Bulgaria	2.9	4.4	3.708	0.054	0.51
SE Bulgaria	3.8	4.4	0.495	0.482	0.13
SC Bulgaria	6.4	9.1	5.533	0.018	0.41
SW Bulgaria	1.7	4.2	13.28	0.0003	1.50

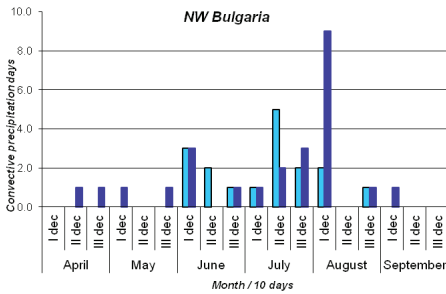
The maximum in annual distribution of stormy days is in the height of summer season in July almost for all regions in Bulgaria (Fig. 2). These results coincide with the observed maximum in monthly distribution of thunderstorm days for East Bulgaria (Bocheva et al., 2013) and are a month later than those for other parts of the country.

The comparison between two periods show differences in intra-monthly distribution of torrential convective precipitations in different regions in warm half of the year especially those from west and east parts of the country. During the second period (2003-2014) the maximum in such type event for the stations from West and SC Bulgaria is observed in first decade of August. In these regions the heavy thunderstorms become more frequent in all decades of September also.

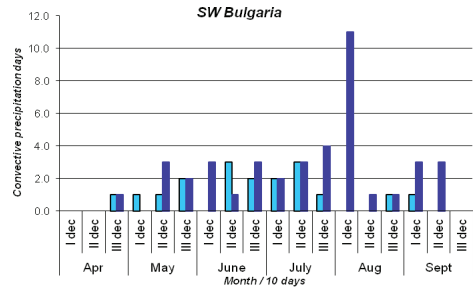
For regions from north part of the country all such days occurred only during the warm season for whole period of investigation 1991-2014. Only in NE Bulgaria, a couple of torrential convective precipitations (bellow 10%), is observed during the second period 2003-2014.

The potential dangerous precipitation events, attended by thunderstorms during the cold half of the year are typical for SC Bulgaria (about 40% of all torrential convective

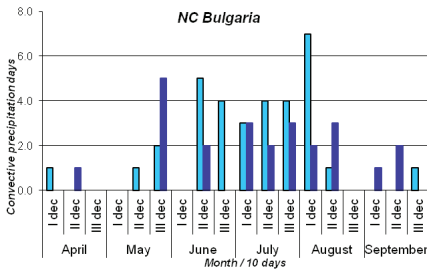
precipitations during the period 2003-2014) and to some extent for SE Bulgaria (26%) and SW Bulgaria (20%). This is connected mostly with the observed changes in atmospheric circulation over the region, especially with the changes in trajectories of Mediterranean cyclones over Balkans (Marinova et al., 2005). More than 80% of high-impact weather events over Bulgaria during the cold period of the year are associated with the behavior of Mediterranean cyclones and the great number of them affected south part of the country. Most Mediterranean cyclones associated with severe storms moved through the southernmost parts of Balkan Peninsula and for large part of motion was attended by a blocking regime in the mid-level mass field (Bocheva et al., 2007).



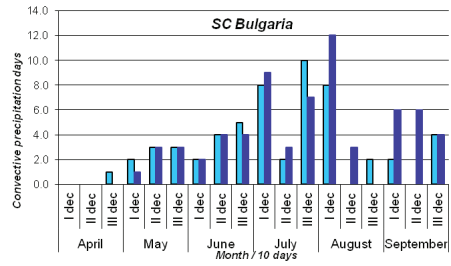
(a) NW Bulgaria



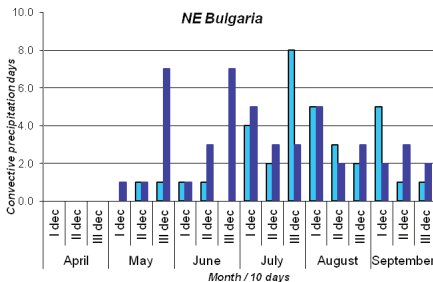
(d) SW Bulgaria



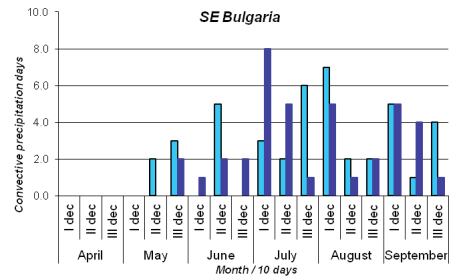
(b) NC Bulgaria



(e) SC Bulgaria



(c) NE Bulgaria



(f) SE Bulgaria

Fig. 2. Inter-monthly regional distribution of number of heavy convective precipitation days during the warm half of the year for periods: 1991-2002 (light blue) and 2003-2014 (dark blue).

5. SPATIAL AND TEMPORAL DISTRIBUTION OF TORNADO EVENTS

All 55 tornado and waterspouts cases registered between 2001 and 2014 in Bulgaria have occurred in 44 days. The average number per year in Bulgaria is 3.9 which therefore makes up a frequency of $P=0.35/10^4 \text{ km}^2 \text{ year}^{-1}$. The similar frequency was published for Austria ($P=0.3/10^4 \text{ km}^2 \text{ year}^{-1}$ – Holzer, 2000) while the one for Greece appears to be 4 times bigger ($P=1.1/10^4 \text{ km}^2 \text{ year}^{-1}$ - Sioutas, 2011).

Only 18 out of 28 administrative regions have registered tornadoes for the 14-year period (Fig. 3). The Sofia-city region has the highest frequency of $2.1/10^4 \text{ km}^2 \text{ year}^{-1}$ followed by Dobrich ($1.2/10^4 \text{ km}^2 \text{ year}^{-1}$) and Razgrad ($1.1/10^4 \text{ km}^2 \text{ year}^{-1}$). The regions of Varna and Burgas ($0.7/10^4 \text{ km}^2 \text{ year}^{-1}$), Plovdiv, Vratsa and Veliko Tarnovo ($0.6/10^4 \text{ km}^2 \text{ year}^{-1}$), Targovishte and Kyustendil ($0.5/10^4 \text{ km}^2 \text{ year}^{-1}$), and Smolyan ($0.4/10^4 \text{ km}^2 \text{ year}^{-1}$) exhibit frequencies greater than the national average. Only waterspouts have been reported in the region of Dobrich which border the Black sea.

All documented tornado cases in Bulgaria from 2001 to 2014 have been classified by severity according to the Fujita scale and by the type of the topography and the land use of the terrain upon which they occurred. There are 14 cases upon mountainous or hilly terrain covered by shrub or grass; 8 cases upon wooded mountainous or hilly terrain; 14 cases over flat terrain (plain); and 17 waterspouts. Almost half (above 40%) of all cases in Bulgaria therefore have occurred over mountainous or hilly terrain which contrasts with other parts of Europe where tornadoes most often form and develop upon flat terrain or near water bodies (Giaiotti et al., 2007; Sioutas, 2011).

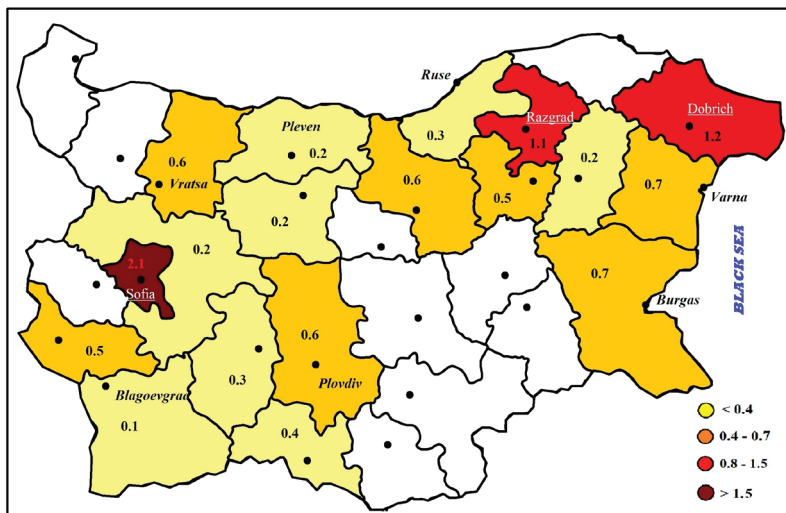


Fig. 3. Mean annual frequency of tornado occurrence in Bulgaria per administrative provinces (2001-2014).

The classification by strength excludes the 17 waterspouts. The reason is that they caused no damage and this inhibits the attempts to classify them according to the Fujita scale. Most of the tornadoes (73%) match or even do not reach the F1 level of the Fujita scale which means that they were weak. About 11% of all cases have been attributed with an intermediate class F1-F2 because the damage data corresponds to the higher class F2 but the wind data suggest only class F1. There have been no documented cases of a class higher than F2 in Bulgaria.

The diurnal distribution of tornadoes and waterspouts in Bulgaria show that most of the cases (about 80%) occurred within the afternoon hours between 15:00 and 19:00 Local time (East European Time (EET) which in summer is 3 hour ahead of the Universal Coordinated Time (UTC) and in winter – 2 h) – Fig. 4a. The monthly distribution of tornado cases (Fig. 4b) show that almost all cases (91%) occurred within the warm half of the year between April and September. The highest frequency of tornado events has occurred in June and July. This corresponds to the statistics for other countries in Central and Eastern Europe. Waterspouts in Bulgaria seem to occur between June and September. This matches the time of year when the sea water is the warmest.

In the list of documented tornadoes in the 14-year period there are 5 “winter” cases which occurred within the cold half of year: 3 of which in Southern Bulgaria and 2- in Northern Bulgaria. They were associated with strong thunderstorms which developed along rapid and intense cold fronts introducing cold and moist air masses in Bulgaria after a prolonged period of unseasonably warm and dry weather.

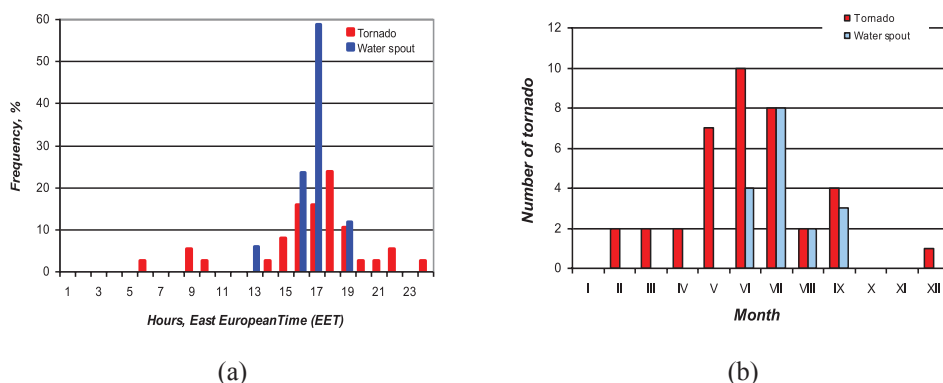


Fig. 4. Diurnal (a) and monthly (b) distribution of tornadoes and waterspouts in Bulgaria (2001-2014).

CONCLUDING REMARKS

- ❖ Statistically significant recent increase in the number of days with torrential convective precipitation is observed in NE, SC and especially in SW Bulgaria.

- ❖ Tornadoes in Bulgaria mainly occur in the north-central, north-eastern and south-central regions of Bulgaria over mountainous terrain but also over plains.
- ❖ The intensity analysis indicated that the majority of the tornadoes in Bulgaria can be classified as F0–F1 of the Fujita scale which is equivalent to “weak” tornadoes.
- ❖ In order to investigate more precisely the risk of severe hydro-meteorological events, it is necessary to build modern national database including the reported damage caused by the different hazardous events for the sectors of the economy. It can be done by restoring and unifying the available archive data in the insurance companies, the national civil-protection service, ministries, the national statistical institute, and others.

AKNOWLEDGEMENT

This document has been prepared with the financial support of the European Social Fund through Project BG051PO001-3.3.06-0063. NIMH - BAS is solely responsible for the content of this document, and under no circumstances it can be considered as an official position of the EU or the Ministry of Education and Science.

REFERENCES

- Bocheva L., Ch. Georgiev and P. Simeonov (2007). A climatic study of severe storms over Bulgaria produced by Mediterranean cyclones in 1990-2001 period. *Atmos. Res.*, 83, 2-4, 284-293.
- Bocheva, L., P. Simeonov, T. Marinova (2013). Variations of thunderstorm activity in non-mountainous regions of Bulgaria (1961 – 2010), *BJMH*, v.18, pp.38-46.
- Bocheva L. (2015). Comparative analysis of heavy precipitation in non-mountainous regions of Bulgaria. 15th International Multidisciplinary scientific GeoConference SGEM 2015, Energy and Clean Technologies, Conference Proceedings, Air Pollution & Climate Change, 889-896, ISBN 978-619-7105-38-4, ISSN 1314-2704, DOI: 10.5593/sgem2015B41
- Fujita, T.T. (1981). Tornadoes and downbursts in the context of generalized planetary scales. *J. Atmos. Sci.*, 38, 1511-1534.
- Giaiotti D., Giovannoni M, Pucillo A, Stel F. (2007). The climatology of tornadoes and waterspouts in Italy. *Atmos. Res.*, 83, 534-541.
- Holzer A. M. (2000). Tornado Climatology of Austria. *Atmos. Res.* 56, 203–212.
- Marinova, T., L. Bocheva, V. Sharov (2005). On Some Climatic Changes in the Circulation over the Mediterranean Area. *Idojaras*, vol.109, No 1, pp.98-104
- Sioutas M. (2011). A tornado and waterspout climatology for Greece. *Atmos. Res.* 100, 344-356.
- StatSoft, Inc., STATISTICA (data analysis software system), version 6, 2004 (www.statsoft.com).



Operational storm surge modelling in the Western Black Sea: one way coupling with a wave model

Vasko Galabov*

*National Institute of Meteorology and Hydrology- Bulgarian Academy of Sciences (NIMH- BAS),
Tsarigradsko shose 66, 1784 Sofia*

Abstract. We present the progress in the operational modelling of storm surges along the Western Black Sea coast with a focus on the Bulgarian coast. A one way coupling of such model with an operational wave model is implemented. The wave model provides information about the wave induced stress on the sea surface and the wind drag coefficient. The validation of the system of these two models during several storms with strong winds and surges above 1m shows that the influence of the wave induced stress is not significant because of the spatial resolution of the storm surge model. The influence of the sea state on the wind drag coefficient is significant and leads to improvement: prevention of overestimation of the surge for severe storm cases. Two alternative approaches to parameterize the wind drag coefficient dependency of the wave parameters are tested: direct usage of the friction velocity from the wave spectra and the use of wave steepness output from the wave model. The use of the wave steepness information in the storm surge model leads to improvements of the simulation results, while the usage of the friction velocity leads to further overestimation of the surges. The approach with the wave steepness was implemented in the storm surge forecasting system of NIMH-BAS.

Keywords: storm surge, Black Sea, wind drag coefficient, waves

1. INTRODUCTION

Storm surges in the Black Sea are events that happen with much lower frequency and amplitude than in the ocean, however during the last 50 years there are more than 20 events with sea level rise more than 80 cm for the Bulgarian coast and about 10 cases with peak level rise of more than 1m and the most extreme recorded one is the storm surge during the storm of February 1979 when the sea level rise reached 1.5m at some locations around the Bulgarian coast and caused very significant damages. Other

* vasko.galabov@meteo.bg

notable storms are the storms of 1976, 1977, 1981, 1996, 1997, 1998, 2006, 2010, 2012 and others. The first numerical prediction of storm surges by a hydrodynamic model and a prediction by statistical modeling was implemented by Mungov back in the 80's. After 1990 the storm surge model of Meteo France (Mungov and Daniel, 2000) was adapted to the Black Sea in the frame of the bilateral cooperation between Meteo France and NIMH. It was found that the model generally underestimates the storm surges, fact explained with the low spatial and temporal resolution of the atmospheric forcing. Another approach to the storm surge prediction by using neural networks technique was tested by Pashova and Popova (2011). The present article describes an approach to implement a one way coupling of the storm surge model with the operational wave model of NIMH (National Institute of Meteorology and Hydrology) by exchange of information about the sea state and wave radiation stress from the wave model to the storm surge model. As it was found that the influence of the wave radiation stress on the storm surge prediction is negligible, the study is focused mainly on the influence of the sea state parameters on the wind drag coefficient and therefore on the sea level predictions of the model. We evaluate the influence of the replacement of the bulk definitions with definitions of the wind drag coefficient depending on the wave parameters- wave age or wave steepness. The article may be considered as a continuation of the work of Mungov (Mungov and Daniel, 2000) on the operational storm surge modeling in the Western Black Sea, showing the recent improvements of this operational system.

2. DEPENDENCE OF THE WIND DRAG COEFFICIENT ON THE SEA STATE PARAMETERS

The wind driven surge is determined by the transfer of momentum from the atmosphere to the sea surface that generates a drift current. The transfer of momentum is expressed in the storm surge model using the wind shear stress (the shear force per unit of the contact area):

$$|\tau| = \rho_a * C_d * U_{10}^2 = \rho_a * u_*^2 \quad (1)$$

where C_d is the wind drag coefficient, ρ_a is the air density and U_{10} is the wind speed at 10m height above the sea surface. According to Monin- Obukhov similarity theory of the atmospheric boundary layer:

$$C_d = k^2 * \ln^{-2} \left(\frac{z}{z_0} \right) \quad (2)$$

where k is the von Karman constant, z is 10m in the case of the usage of 10m winds and z_0 is the aerodynamic roughness length of the sea surface. One may naturally expect that

the sea surface roughness length depends on the sea state. According to Charnock model (Charnock, 1955):

$$z_0 = \alpha * \frac{uZ}{g} \quad (3)$$

where α is the Charnock parameter, varying from 0.012 to 0.0185 according to different estimations and experiments.

Typically in the wave and circulation models the value of C_d is parameterized using linear functions of the 10m wind speed (the so called bulk formulations):

$$C_d = 0.001 * (a + b * U_{10}) \quad (4)$$

The coefficients a and b in 4) are usually determined by experimental in situ measurements in different oceans, wind speed ranges and atmospheric conditions. According to Wu (1975) $a = 0.8$ and $b = 0.065$ and according to Smith and Banke(1975) $a = 0.63$ and $b = 0.066$. The bulk formulations mean that the drag coefficient rises continuously with the rise of the wind speed. However the experimental measurements show that above 30m the behaviour of the drag coefficient is totally different. The studies of experimental results in situ in tropical cyclones and laboratory experiments by Powell et al (2003), Donelan et al (2004) and others show that above some wind speed (30m/s according to Powell and probably with different thresholds in different areas) the drag coefficient is not increasing, but stays constant and in extreme hurricane conditions above 45m/s even decreases due to the interaction of the wind with waves. Instead of usage of a coupled ocean-boundary layer model, Zijlema, van Vledder and Holthuijsen (2012) recently proposed the usage of a bulk parameterization (further referred as Zijlema formula in the study) that is based on second order polynomial fit:

$$C_d = 0.001 * (0.55 + 2.97 * U - 1.49 * U^2) \quad (5)$$

$$\overline{U} = \frac{U_{10}}{U_{ref}} \quad (6)$$

with a reference wind speed $U_{ref} = 31.5\text{m/s}$. Such function is rising to a maximal value at the reference wind speed and after that is decreasing.

Most of the studies (theoretical and experimental) on the dependence of the drag coefficient focus on two main approaches- expression of C_d as a function of the wave age

$$\beta = \frac{c_p}{u_*} \quad (7)$$

where c_p is phase speed of the waves at the spectral peak, or as a function of the wave steepness or as a combination of wave parameters. Stewart (1974) concluded that in the Charnock model the Charnock parameter is a function of the wave age and the function is

$$\alpha = f(\beta) = \alpha_1 * \beta^m \quad (8)$$

The values of α_1 and m are obtained by experiments. Negative value of m means that the growing wind sea (young waves) is rougher than the developed (mature) wind sea. Positive m means the opposite- the mature wind sea is with higher roughness. The field observations conclude that m is definitely negative.

Taylor and Yelland (2001) found that if the wind speed is above 12 m/s the dependence of C_d on the wave age becomes poor and argued that especially above that wind speed the dependence of the drag coefficient on the wave steepness is far more clearer. In a recent study Wang et al (2013) found, studying experimental measurements that the dependence of the drag coefficient on the wave age is in a good agreement with observations only if the friction velocity is below 0.5. Above that value wave steepness (or an expression based on Reynolds number) describes the behaviour of C_d much better.

Guan and Xie (2004) described a physical interpretation of the existing linear parameterizations of C_d as a function of the wind speed. They combined the logarithmic law of the wind within the atmospheric boundary layer with the Charnock relation and expressed the drag coefficient as a function of the wind speed with the Charnock's "constant" as a parameter. This function is nearly linear within the usually measured ranges of C_d with a slope determined by the value of α (eq.3). If α is not a constant, but a function of the wave parameters, after invoking the 3/2 power law (Toba, 1972):

$$\frac{gH}{u_*^2} = 0.062 \left(\frac{gT}{u_*} \right)^{3/2} \quad (9)$$

This way the authors came to a relation for the wind drag coefficient that is a linear function of the wind speed with a slope determined by a function of the wave steepness:

$$C_d = 0.001 * (0.78 + 0.475 * f(\delta) * U_{10}) \quad (10)$$

where $f(\delta)$ is equal to $0.85^B A^{1/2} \delta^{-B}$ and the meaning of B is the same as the meaning of m in eq.8. The coefficients A and B are experimentally determined. Some of the proposals are listed in Guan and Xie (2004) and in the present study we use the A and B proposed by Smith et al (1992) with $A = 0.5$ and $B = -1$. In the case of Smith's definition we are coming to the next relation:

$$C_d = 0.001 * (0.78 + K * \delta * U_{10}) \quad (11)$$

where K is a tunable parameter. In the case of Smith's definition it is 0.4, note however that the value of 0.475 is a result of a statistical procedure performed by Guan and Xie that will make the relation to provide much lower values of the drag coefficient than the values provided by Wu and Smith and Banke formulations under moderate wind conditions, therefore the user may tune up K in case of usage of (11) to his own model and wind input. It is also possible to use other definitions of B which are negative but not equal to one (therefore the drag coefficient does not depend exactly linear to the wave steepness) – the ranges of B by various authors will lead to a dependence of δ^C with C varying from 1 to 2.

From the practical point of view there are two main ways to take into account the dependence of the drag coefficient on the sea state in a storm surge model – to use the wave steepness and the relation of Guan and Xie in coupled or non-coupled models (the wave steepness is a standard output of the wave models) or to use directly the drag coefficient as it is calculated in the source terms (actually meaning that we are using a drag coefficient dependent on the wave age). In the wave models different parameterizations of the source terms are used and while in some of them the drag coefficient (and so the friction velocity) are calculated using bulk formulations, others are computing the friction velocity in the source terms – for instance the source term of WAM cycle IV using the Janssen's theory (Janssen, 1991).

3. METHODS AND DATA

The storm surge model described in this study is the storm surge model of METEO FRANCE which operational implementation to the Black Sea is described by Mungov and Daniel (2000). The bathymetry is with 1/30° spatial resolution and the grid is a regular longitude-latitude grid.

The model is two-dimensional depth integrating model with equations written in spherical coordinate system:

$$\frac{\partial U}{\partial t} = fV - \frac{g}{R \cos \varphi} \frac{\partial \eta}{\partial \lambda} - \frac{1}{\rho R \cos \varphi} \frac{\partial P_a}{\partial \lambda} - \left[\frac{U}{R \cos \varphi} \frac{\partial U}{\partial \lambda} + \frac{V}{R} \frac{\partial U}{\partial \varphi} \right] + \frac{\tau_{sx} - \tau_{bx}}{\rho H} + A_H \nabla^2 U$$

$$\frac{\partial V}{\partial t} = fU - \frac{g}{R} \frac{\partial \eta}{\partial \varphi} - \frac{1}{\rho R} \frac{\partial P_a}{\partial \varphi} - \left[\frac{U}{R \cos \varphi} \frac{\partial V}{\partial \lambda} + \frac{V}{R} \frac{\partial V}{\partial \varphi} \right] + \frac{\tau_{sy} - \tau_{by}}{\rho H} + A_H \nabla^2 V$$

$$\frac{\partial \eta}{\partial t} = \frac{1}{R \cos \varphi} \left[\frac{\partial}{\partial \lambda} (UH) + \frac{\partial}{\partial \varphi} (VH \cos \varphi) \right]$$

containing advection terms, horizontal turbulence terms, nonlinear bottom friction terms, and surface friction terms. U , V are the depth integrated current velocities, f is the Coriolis parameter, R is the earth radius, P_a is the atmospheric pressure, H is the water depth, η is the water free surface elevation, ρ is the water density and A_H is the horizontal diffusion coefficient, τ_{sx} and τ_{sy} are the components of the wind stress and τ_{bx} , τ_{by} – the components of the bottom friction stress.

The wind stress components are:

$$\tau_{sx} = \rho_A C_d |W_{10}| W_{10x}, \quad \tau_{sy} = \rho_A C_d |W_{10}| W_{10y}$$

where ρ_A is the air density, W_{10x} and W_{10y} are the components of the 10m wind speed W_{10} .

The bottom friction stress components are:

$$\tau_{bx} = \rho C_b (U^2 + V^2)^{1/2} U, \quad \tau_{by} = \rho C_b (U^2 + V^2)^{1/2} V$$

where C_b is the bottom drag coefficient which is set in our model to 0.0015 over the shelf and 0.000015 over liquid bottom. We integrate not down to the actual bottom of the sea but to the mixed layer for the month taking into account the very stable stratification of the Black Sea and treating the surge as a long wave propagating only in the upper dynamical layer of the sea. The mixed layer depth of the Black Sea is very shallow when compared with the other European seas (in order of 40-60m during the winter, compared with the order of 300m for the Mediterranean sea). The data for the monthly mixed layer depth of the Black Sea was taken by the study of Kara et al (2005).

The wave model that is used in the study is SWAN version 40.91.ABC (Booij et al 1999). The computational domain is the same as the computational domain of the storm surge model. SWAN is configured to provide an output of the wave steepness and the friction velocity (applicable only if WAM cycle 4 source terms are set in the namelist). The atmospheric forcing data is available with a temporal resolution of one hour. SWAN provides the wave parameters also with one hour interval between the outputs.

The storm surge model reads the wave model output of friction velocity or steepness and in the case of usage of SWAN the data is directly processed (because the SWAN grid is the same as the storm surge model grid) by the subroutine that calculates the wind drag coefficients and the wind stress components.

Data for comparisons of the surge model output is available for two cases: one for the tide gauge Irakli (the middle part of the Bulgarian coast) and one for the tide gauge Ahtopol (southernmost part of the coast). Both tide gauges are located in areas where the coastline is almost straight and simple bottoms with uniform slope and therefore no significant local topographic effects are expected. The data is from the studies of Mungov (2000) and Andreeva (2011).

The data available at the present moment is the maximal daily surge levels. Hourly data is not available and so the possible time shifts of the peaks of the storms cannot

be determined, but due to the fact that the tide in Black Sea is below 8 cm this is not of primary importance and the most important parameter for the operational storm surge forecast is the maximum daily sea level rise.

The fields wind components at 10m height and the mean sea level pressure for some of the most significant cases of a storm surge at the Bulgarian coast are provided by the Bulgarian regional atmospheric modeling group by a downscaling of the ERA-Interim (Dee et al, 2005) reanalysis using the ALADIN model (Bubnova et al 1995; Bogatchev, 2008). For more details about this specific downscaling see Galabov et al (2015). The domain covers the entire Black Sea. The integration starts several days before the beginning of the historical storm at calm weather and so we may expect the sea level at the beginning of the run of the storm surge model to be equal to the mean undisturbed level.

4. RESULTS

The first presented case is the most important one, because it is the highest ever recorded in the Black Sea storm surge (for more details about this storm see Galabov et al (2015)). Storm caused a surge of 1.43 peak value at the tide gauge Irakli and more than 1.5m at the tide gauges in the ports of Varna and Burgas.

Initially we tested the approach to integrate not to the bottom but to the mixed layer depth.

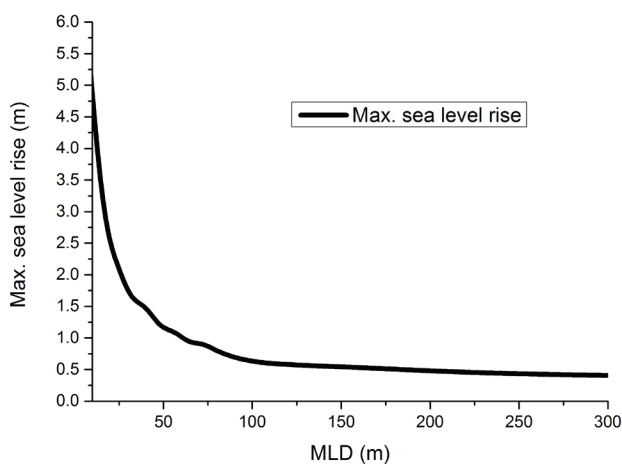


Fig. 1. Dependence of the maximum sea level rise of the depth of integration for the storm of February 1979

We varied the depth of integration and the result is shown on Fig.1. As it may be seen, when integration is down to the bottom of the sea (more than 2000m) the model fails to reproduce any surge above 40cm. On the other hand when the integration is

down to the mixed layer depth (which is 40-50m for February) we obtain realistic simulation result comparable with the tide gauge measurement when using the Smith and Banke formulation of the wind drag coefficient. In the study of Krestenitis et al (2012) the usage of Smith and Banke formulation of C_d results in complete failure to reproduce properly even significantly lower surges (below 1 m) and they are tuning their model with a very high values of $C_d - 8 \cdot 10^{-3}$ when the wind speed is above 20 m/s. The problem is that while it is possible to tune up a model this way, such values of C_d are physically meaningless and taking into account the mentioned previously experiments of Powel and others, such values are much higher than the highest possible in the oceans. Moreover while this is a temporal solution to fit a model to observations, even with such high C_d the model will fail to reproduce the extreme surges like the one in 1979 and after all the important surges are those above 80 cm, while all surges below 50 cm are without practical importance for the operational practice. The conclusion is that the correct way to do storm surge modeling in the Black Sea is to consider the shallow mixed layer and to integrate only to MLD. It is important also to note that climate projections of the storm surges in the Black Sea cannot be performed by the usage of such two dimensional models because of the argument, that the surge is depending strongly on the mixed layer depth. A future change of the temperature of the upper layer of the sea will inevitably change the mixed layer depth and in the case of warming it will lead to a shallower depth of the mixed layer during the winter months and then even weaker storms may result in much higher surges (see Fig. 1 for instance for MLD = 30m for the storm of 1979). Therefore any such projections that ignore the change in the sea stratification underestimate the future extreme events and possibly the underestimation is very serious. This means, that the ONLY way to do a projection of the future storm surges in the Black Sea is to use baroclinic hydrodynamic models and such two dimensional models as the presented one are not applicable for such tasks in order to be able to account the possible increase of storm surge danger even when the storms are weakening.

The first case for which we evaluate the influence of different approaches to define the drag coefficient is the storm of February 1979, which is the highest recorded surge that caused damages and coastal inundation. For a description of this storm see Galabov et al (2015) and Belberov et al (2009). We compare the model simulations with the daily maximum surge, measured at Irakli tide gauge. Fig. 2. shows the performance of the model using three different bulk parameterizations of C_d – the widely used Wu and Smith-Banke formulations and the second order polynomial proposed by Zijlema et al (2012). Both Wu and Smith-Banke formulations result in overestimation of the maximum level by 10–15cm on 19.02.1979 (the peak of the storm) which is in the order of 10% overestimation. The quadratic relation of Zijlema leads to underestimation (that in principle is possible to avoid by rescaling of the relation). The next experiment is using the two approaches to account the dependence of the C_d on the sea state parameters. When we use the drag coefficient obtained by the usage of friction velocity

from SWAN (using the Janssen wind input) we overestimate the surge even higher than the overestimation by the bulk formula. The usage of the formulation based on the wave steepness leads to successful prevention of the overestimation for the highest surge during this storm. The simulations on 20.02.1979 are not successful but this is because of the wind fields and after all the most important is the proper simulation of the storm peak on 19.02.1979 for which the C_d based on wave steepness performs best.

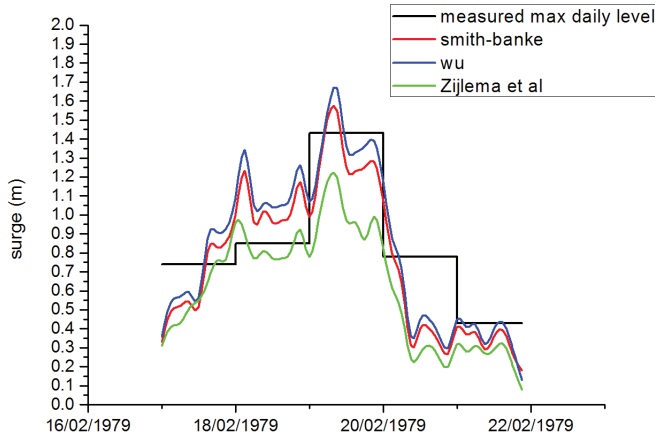


Fig. 2. Comparison of the measured daily maximum surge measured at Irakli tide gauge with model simulations using Smith-Banke and Wu bulk parameterizations of C_d and the second order bulk formula of Zijlema et al (2012).

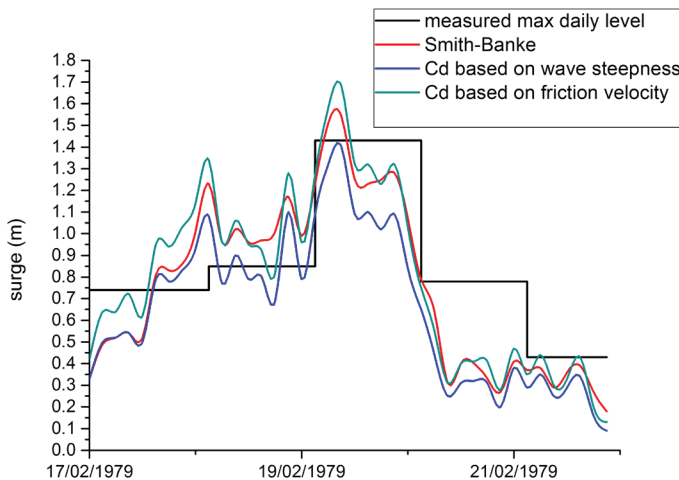


Fig. 3. Comparison of the measured daily maximum surge measured at Irakli tide gauge with model simulations using the default Smith-Banke formula and C_d estimated using the wave steepness and C_d based on the friction velocity obtained by the SWAN wave model.

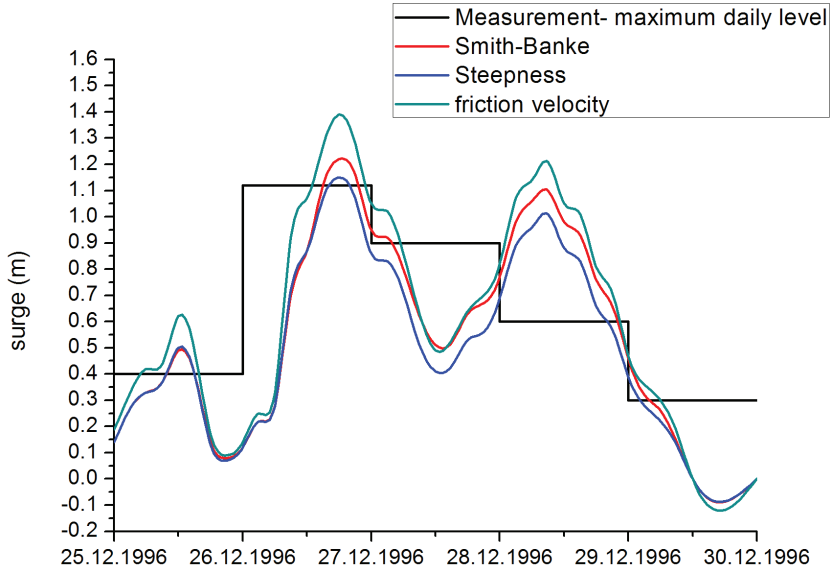


Fig. 4. Comparison of the measured daily maximum surge during the storm of December 1996 measured at Ahtopol tide gauge with model simulations using the default Smith-Banke formula and C_d estimated using the wave steepness and C_d based on the friction velocity obtained by the SWAN wave model.

The next case is the storm of 12.1996. The storm surge model performance was studied in the work of Mungov and Daniel (2000) and an underestimation of the model was found, however in the present study there is no underestimation because the resolution of the wind input is higher and the wind interval between the atmospheric input files is 1h instead of 6h in the study of Mungov and Daniel. The results are presented on Fig. 4 and the conclusions are the same as for the previous case. The highest surge was recorded on 26.12.1996. The model simulates a second peak on 18.12.1996 that was not observed, because of the wind fields downscaling. Otherwise, the usage of the friction velocity again leads to high overestimation, while the usage of the wave steepness prevents the overestimation.

The next case is the storm of January 1998. That storm was also studied by Mungov and Daniel (2000). The results of experimental runs are presented on Fig. 5 and the conclusions are identical to the conclusions for the two previous cases. The lowest overestimation was achieved when using the steepness. Outside of the storm peak the use of the wave steepness leads to identical results to the results using the Smith and Banke formulation. For the peak of the storm however the coupled version of the model lowers the tendency of the model to overestimate.

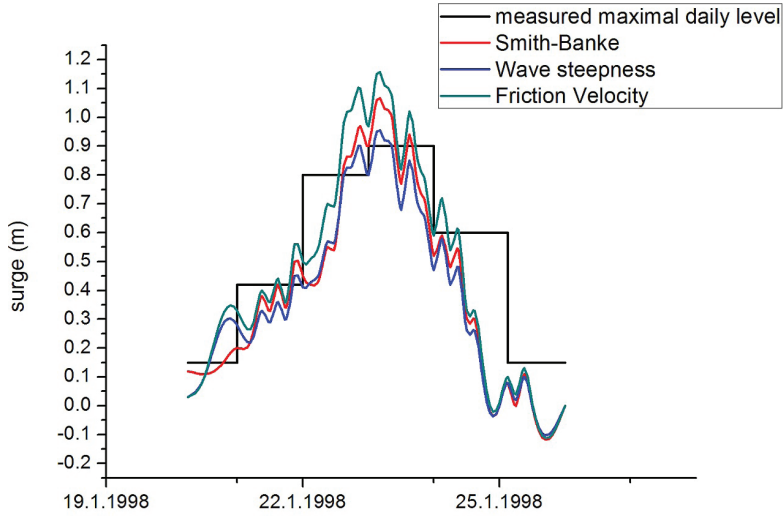


Fig. 5. Comparison of the measured daily maximum surge measured at Irakli tide gauge with model simulations for the storm of January 1998 using the default Smith-Banke formula and C_d estimated using the wave steepness and C_d based on the friction velocity obtained by the SWAN wave model.

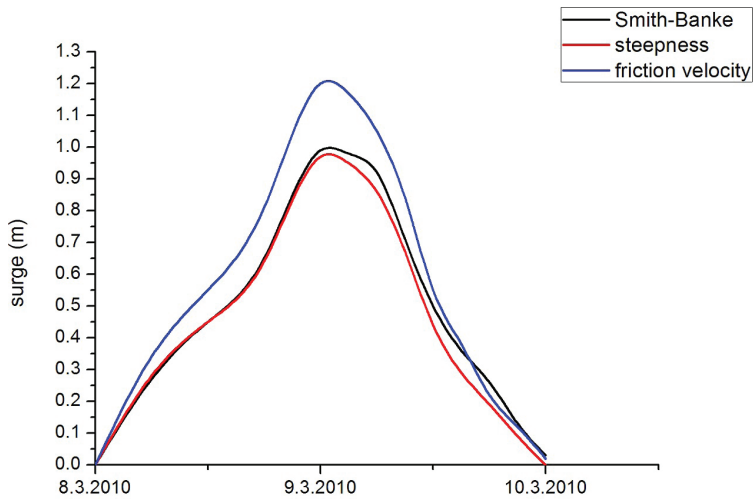


Fig. 6. Model simulations using the default Smith-Banke formula and C_d estimated using the wave steepness and C_d based on the friction velocity obtained by the SWAN wave model- the storm of March 2010.

The next case is a storm during March 2010. For this case there is no significant difference between the result when using the Smith and Banke formula and when using the steepness. The data provided to us by the Bulgarian Oceanological Institute (Valchev et al, 2014) shows that the highest hourly value at Shkorpilovtsi was 1 m, so in this case the model does not overestimate when using the bulk formulation of Smith and Banke. The simulation using the wave steepness is with the same maximum value. Therefore in such cases the use of wave steepness does not lead to underestimation and converge towards the true value better than the bulk formulation and not just permanently produce systematically lower values of the surge. This is an obvious advantage of the use of wave steepness based C_d in the model instead of the bulk formulas and definitions based on friction velocity (wave age).

5. CONCLUSIONS

Quantitative conclusions in the present study are difficult, because we have a limited number of daily maximum sea levels. The storm surges in the Western Black Sea are not a frequent event (especially the extreme ones). While it is possible to obtain the statistical parameters for many cases with sea level rise within the limits of 60 cm, such comparisons are without practical importance because such surges does not lead to coastal inundation and significant hazard. The surges of 1 m and above are with critical importance and the studies of the operational modeling in the Black Sea must be focused on such scenarios of high surges. If we really focus on such cases the conclusions are qualitative rather than quantitative due to their low number. The obvious conclusion however is that the approach using the wave steepness gives much better results than the approach with the friction velocity (which means dependence of the drag coefficient on the wave age). It is likely that the same is valid in other tideless basins with a limited fetch where the wind sea is dominant during the storms that cause significant surges. However, in the oceans it may be the opposite (as it is suggested in some of the referenced studies). There are also hints that the dependence of the drag coefficient on the wave steepness may act as a limiter that prevents the storm surge models from overestimation of the surge. If the model systematically underestimates the surges due to the wind input being with too coarse resolution in space and time, a bulk formulation may be preferable after proper tuning (the quadratic relationship of Zijlema, van Vledder and Holthuijsen may be a better alternative than the linear bulk formulations). The approach presented here is already implemented in the operational system of marine models of NIMH-BAS.

ACKNOWLEDGEMENTS

This document has been prepared with the financial support of the European Social Fund through Project BG051PO001-3.3.06-0063. NIMH - BAS is solely responsible for the content of this document and under no circumstances it can be considered as an official position of the EU or the Ministry of Education and Science.

The study was performed with the help of METEO France- DPREVI/MAR and the author thanks Denis Paradis, Patrick Ohl, Lotfi Aouf and Joel Hoffman and the entire team of the marine division of METEO FRANCE. I wish to express my gratitude to Andrei Bogatchev, Valery Spiridonov and Boryana Tsenova- the team that performed the downscaling and provided the atmospheric data and also to Anna Kortcheva for the support and fruitful discussions.

REFERENCES

- Andreeva, N., Valchev, N., Trifonova, E., Eftimova, P., Kirilova, D., Georgieva, M. (2011). Literary review of historical storm events in the western Black Sea. Proc. of Union of Scientists–Varna, Marine Sciences, 105-112 (In Bulgarian)
- Belberov Z., E. Trifonova, N. Valchev, N. Andreeva, P. Eftimova (2009) Contemporary reconstruction of the historical storm of February 1979 and assessment of its impact on the coastal zone infrastructure. In : Intern. Conf. SGEM, Albena, June 2009, 2, 243-250 (2009)
- Bogatchev A.(2008), Changes in operational suite of ALADIN – BG, ALADIN Newsletter No 34
- Booij, N., R. Ris, L. Holthuijsen,(1999) A third-generation wave model for coastal regions 1. Model description and validation, Journal of geophysical research 104(C4), 7649- 7666
- Bubnová, R., Hello, G., Bénard, P., & Geleyn, J. F. (1995). Integration of the fully elastic equations cast in the hydrostatic pressure terrain-following coordinate in the framework of the ARPEGE/Aladin NWP system. Monthly Weather Review, 123(2), 515-535.
- Charnock H (1955) Wind stress on water surface. Q. J. R. Meteorol. Soc., 81: 639-640
- Dee D.P. and 35 coauthors (2005) The ERA-Interim reanalysis& Configuration and performance of the data assimilation system. Quarterly Journal of the Royal Meteorological Society 137(656), 553-597
- Donelan MA, Haus BK, Reul N, Plant WJ, Stiasnie M, Graber HC, Brown OB, Saltzman ES (2004) On the limiting aerodynamic roughness of the ocean in very strong winds. Geophys. Res. Lett. 31, L18306
- Galabov V, A. Kortcheva, A. Bogatchev, B. Tsenova (2015) Investigation Of The Hydro-Meteorological Hazards Along The Bulgarian Coast Of The Black Sea By Reconstructions Of Historical Storms. Journal of Environmental Protection and Ecology, 16.3, 1005-1015
- Guan C., Xie L. (2004) On the linear parameterization of drag coefficient over sea surface. J. Phys. Oceanogr. 34: 2847-2851
- Janssen PAEM (1991) Quasi-linear theory of wind-wave generation applied to wave forecasting. J Phys Oceanogr.,21,1631–1642

- Kara AB, H.E. Hulbart, A.J. Wallcraft, M.A. Bourassa (2005) Black Sea mixed layer sensitivity to various wind and thermal forcing products on climatological time scales. *Journal of climate*, 18(24), 5266-5293
- Krestenitis Y.N., Androulidakis Y., Kombiadou K. (2012) Storm surge modelling in the Black Sea. In conference: Protection and restoration of the environment XI, Thessaloniki, Greece, DOI: 10.13140/2.1.2163.9042
- Mungov G, Daniel P (2000) Storm surges in the western Black Sea. *Operational forecasting, Mediterranean Marine Science*, 1/1: 45-50
- Pashova L, Popova S (2011) Daily Sea Level forecast at tide gauge Burgas, Bulgaria using artificial neural networks. *Journal of Sea Research*, 66.2: 154-161
- Powell M. D., Vickery P. J., Reinhold T. A. (2003) Reduced drag coefficient for high wind speeds in tropical cyclones. *Nature*, 422(6929), 279-283
- Smith S. D., Banke E. G. (1975) Variation of the sea surface drag coefficient with wind speed. *Quarterly Journal of the Royal Meteorological Society*, 101(429): 665-673.
- Smith, SD, Anderson, RJ, Oost, WA, Kraan, C, Maat, N, Decosmo, J, Katsaros, KB, Davidson, KL, Bumke, K, Hasse, L, and Chadwick (1992) Sea Surface Wind Stress and Drag Coefficients: the HEXOS Results. *Bound Layer Meteorol*, 60, 109-142
- Stewart RW (1974) The air-sea momentum exchange. *Boundary-Layer Meteorol* 16:151-167
- Taylor P.K., Yelland, M.J. 2001. The dependence of sea surface roughness on the height and steepness of the waves. *J. Phys. Oceanogr.* 31: 572-590
- Toba, Y (1972). Local Balance in the Air-Sea Boundary Process. I. On the Growth Process of Wind Waves. *J Oceanogr Soc Japan*, 28, 109-120
- Valchev N., N. Andreeva, P. Eftimova, E. Trifonova (2014) Prototype of Early Warning System for coastal storm hazard (Bulgarian Black Sea Coast). *Comptes Rendus De l'Academie Bulgare des Sciences*, 67(7), 977-988
- Wang J., Song J., Huang Y. (2013) On the parameterization of drag coefficient over sea surface. *Acta Oceanol. Sin.*, 2013, Vol. 32, No. 5, P. 68-74, DOI: 10.1007/s13131-013-0315-3
- Wu J. (1975) Wind-induced drift currents. *J. Fluid Mech.*, 68: 49-70
- Zijlema M, van Vledder G, Holthuisen L.H. (2012) Bottom friction and wind drag for wave models. *Coastal Engineering* 65, 19-26



Wave-current interactions in the Black Sea and Mediterranean sea: tests with two operational models

Vasko Galabov*

*National Institute of Meteorology and Hydrology- Bulgarian Academy of Sciences,
Tsarigradsko shose 66, 1784 Sofia*

Abstract. The influence of the wave-current interactions on the operational wave forecasting in the Black Sea and Mediterranean Sea was tested. We used two operational wave models: the SWAN wave model implemented operationally at NIMH-BAS and MFWAM (the operational implementation of the WAM wave model of METEO-FRANCE). The model outputs for the runs with and without wave-current interactions are compared with satellite altimetry data. The comparison shows that the overall influence of the wave-current interactions in these two semi enclosed seas is very limited and their implementation in the operational wave models may be justified only for some specific areas in the Mediterranean Sea.

Keywords: wave current interaction, Black Sea, SWAN, WAM, Mediterranean sea

1. INTRODUCTION

The operational spectral wave models take into account the processes of wave generation by wind, wave dissipation due to wave breaking (whitecapping), nonlinear wave-wave interactions, processes in shallow water such as depth induced wave breaking, bottom friction and sometimes other processes such as wave damping due to vegetation, refraction, diffraction etc. A process that is currently not taken into account by the operational wave models of NIMH (National Institute of Meteorology and Hydrology) is the interaction between waves and surface currents. The currents depending on their velocity and direction in relation with the wave direction may lead potentially to significant changes in the wave parameters. For instance strong currents opposite to the waves may reshape the wave spectra and also increase the wave steepness and the significant wave height. The steeper waves are more dangerous for the ships and

* vasko.galabov@meteo.bg

especially boats. This is one of the reasons to study the effects of inclusion of the wave-current interactions in the operational model of NIMH for the Black sea and the operational model of METEO FRANCE for the Mediterranean Sea. The wave-current interactions for the Black Sea have been studied by Rusu (2010) and Ivan et al (2012). Their conclusions are that there are conditions for strong influence of opposite currents on waves close to the Danube Delta and entrance of the Sulina Chanel due to existing strong currents that may lead to generation of unusually high steep waves. The goal of the present article, however is to test the inclusion of such interactions in operational context and to evaluate the influence on the wave simulation quality in larger context.

2. METHODS AND DATA

The wave models used in the study are the operational wave model of METEO FRANCE MFWAM based on the WAM wave model (WAMDI Group, 1988) with wave breaking parameterization that is not the default for WAM cycle 4- the parameterisation of Ardhuin (Ardhuin et al, 2008) and also the SWAN wave model (Booij et al, 1999) that is operational at NIMH. The setup of the Bulgarian implementation of SWAN is presented in Galabov et al (2015). The wind data is from ARPEGE model for the Mediterranean Sea and ALADIN for the Black Sea (Bubnova et al, 1995; Bogatchev, 2008). The currents are obtained from the MERCATOR OCEAN system with a spatial resolution of 0.1° . We compare the modelled significant wave heights using satellite altimetry data from JASON2 and SARAL/ ALTIKA satellite.

3. RESULTS

The wave model runs are with and without included wave- current. For the coast of France the runs are for October and November 2014- the currents are stronger during these months and that is the reason for the selection of months. We found that there is an area close to Nice (eastern part of the French Mediterranean coast) where there are conditions for wave propagation opposite to the surface currents and with significant difference between the runs with and without wave-current interaction. Fig.1. shows a case with interaction between waves and opposite currents for the coast of France and Fig.2 shows the influence on the wave steepness- there is a relatively small area were the wave steepness increases but it is close to the coast. Different definitions of warning criteria for the shipping include the steepness and therefore inclusion of wave-current interactions may be important for such specific areas. The simulation of the same case with MFWAM leads to qualitatively the same result.

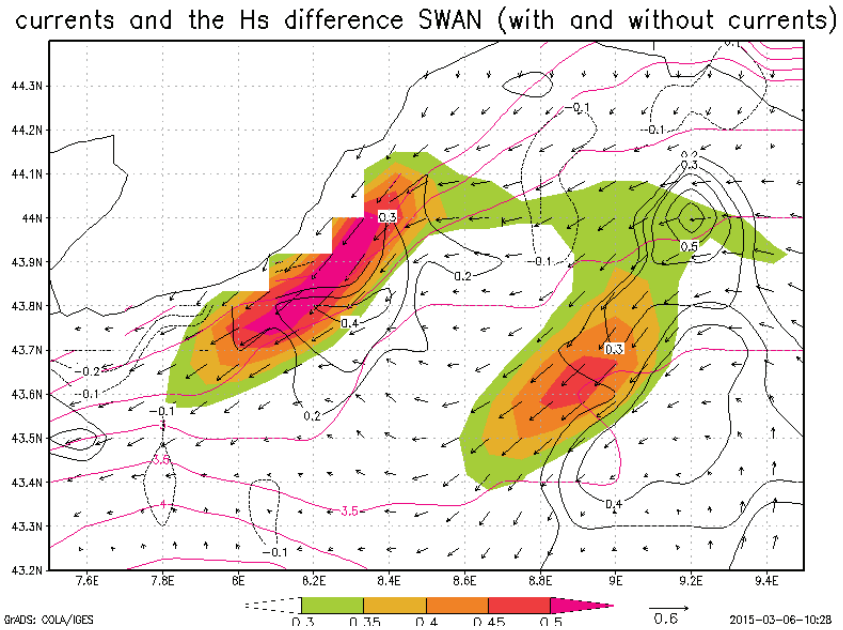


Fig.1. Surface currents (vectors), currents speed (black contours), significant wave height without wave-current interaction (purple contours), the difference in significant wave heights with and without wave-current interaction (colour range). Simulation with SWAN for a case in October 2014.

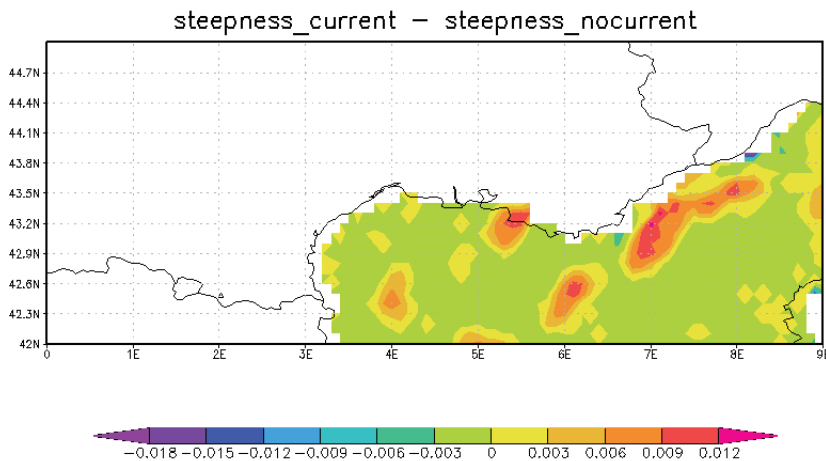


Fig. 2. Wave steepness difference between simulations with and without wave-current interactions.

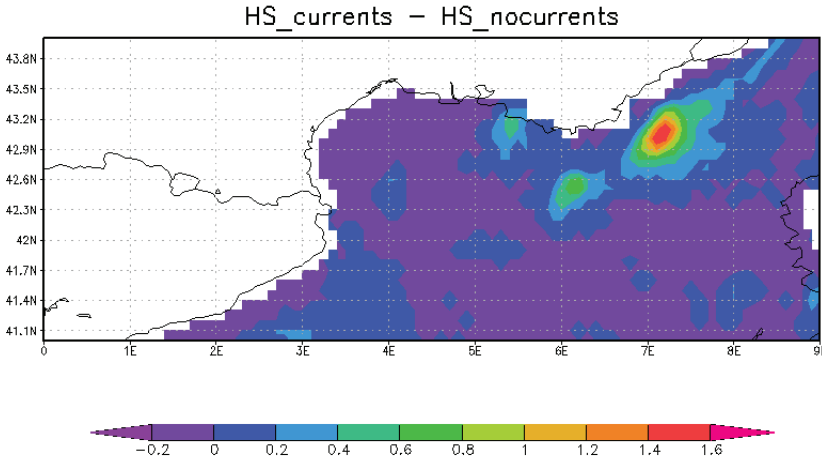


Fig. 3. Significant wave height [m] difference between simulations with and without wave-current interactions.

Fig.3. shows the difference for the significant wave height for the same case- there is an increase of the significant wave height by more than 1m in a small area with strong opposite currents. The problem is the lack of wave measurements in such small areas and lack of possibility to compare with actual measurements in this area. The area is too small to rely on satellite data- the probability to have a satellite track during such case in this area is practically zero.

Next we evaluate the wave-current interactions on a larger scale (the entire Mediterranean Sea). Fig.4. shows the maximal differences between the significant wave heights with and without the influence of currents. The areas with significant differences are the coast of France, Algerian coast, Adriatic Sea and the area south of Greece. Table 1 shows comparison with satellite measurements for October 2014 of the wave simulations with WAM and SWAN wave model with and without wave-current interaction. The statistical indicators are the bias, the scatter index and the root mean square error (RMSE). Generally WAM performs slightly better than SWAN, however the differences between the simulations with and without currents are small and the improvement is marginal. The results for November 2014 are without any significant difference- they are qualitatively the same.

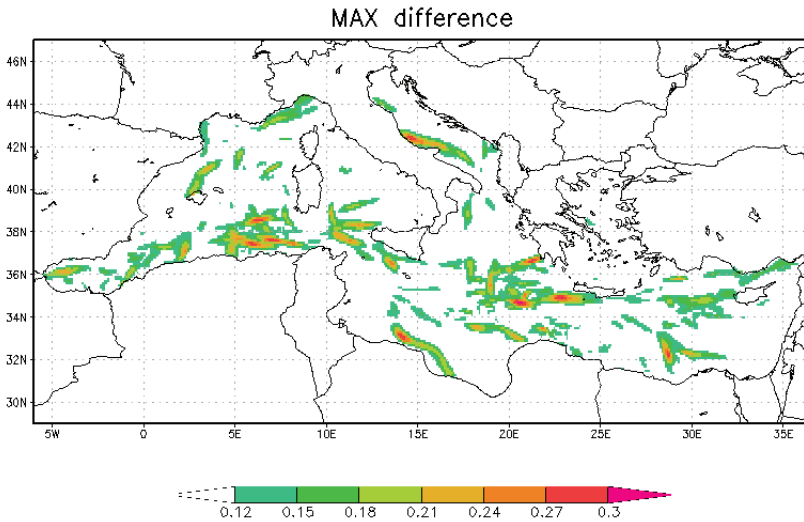


Fig. 4. The highest positive differences for the entire October 2014 (MFWAM simulation)- the difference for each 3 hours is taken and then the highest for each grid cell is extracted and plotted.

Table 1. Comparison of MFWAM and SWAN with and without currents with satellite altimetry data- October 2014.

Model	Currents	Obs. Mean [m]	Model Mean [m]	Bias [m]	RMSE [m]	Scatter Index
MFWAM	yes	1.242	1.127	-0.115	0.281	0.175
	no		1.123	-0.119	0.283	0.175
SWAN	yes	1.241	1.112	-0.129	0.308	0.191
	no		1.100	-0.141	0.322	0.197

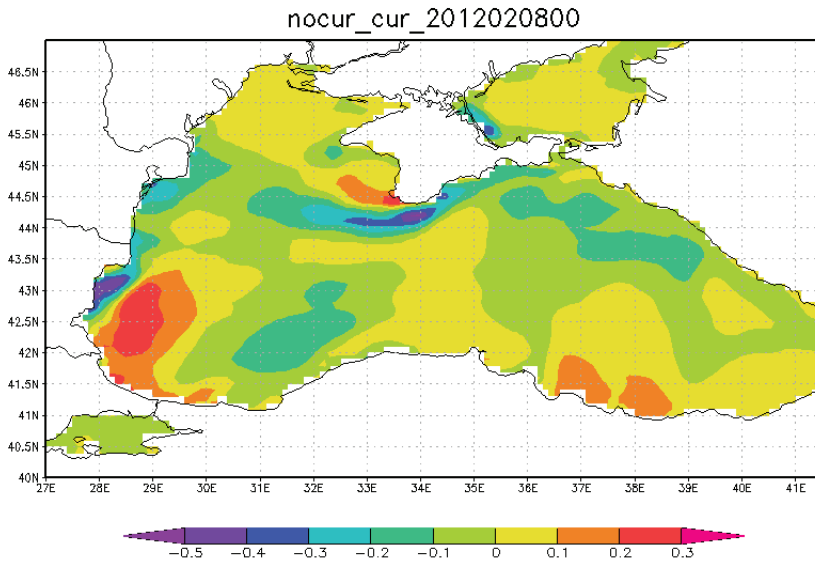


Fig. 5. Difference between the modelled significant wave heights for the Black Sea with and without wave-current interaction during the storm of February 2012. SWAN wave model with WAM cycle 4 physics.

Table 2. Comparison of MFWAM and SWAN with and without currents with satellite altimetry data- January-February 2012 for the Black Sea.

Model	Currents	Obs. Mean [m]	Model Mean [m]	Bias [m]	RMSE [m]	Scatter Index
MFWAM	yes	2.908	2.595	-0.313	0.552	0.141
	no		2.585	-0.323		
SWAN- WAM cycle 4 physics	yes	2.910	2.53	-0.38	0.93	0.26
	no		2.47	-0.44	0.95	
SWAN- WAM cycle 3 physics	yes		2.73	-0.18	0.82	0.27
	no		2.72	-0.19	0.90	

The tests for the Black Sea are performed for the period January- February 2012 that includes many storms with an extreme one among them. Fig.5. shows the difference of

the simulated significant wave heights for this storm. Taking into account that the waves in the open sea were above 6 m for the selected period that is visualized, the difference is in order of 5%. There is some increase of the wave heights when currents are included for the Southern Black Sea (the Turkish coast) however for the Bulgarian coast there are hardly any advantages of the simulation with wave-current interaction. The statistics of comparison with satellite data are shown on Table 2. As it may be seen the bias is lowest when we use WAM cycle 3 physics in SWAN (Komen parameterizations) however the scatter index is significantly lower when we use MFWAM wave model which shows the advantages of the whitecapping parameterization of Ardhuin over the parameterizations available in SWAN (the advantage of MFWAM is significant when we take into account the root mean square error and the scatter index). The wave-current interaction leads to only marginal improvement and in operational mode the inclusion of currents data into the wave model is not expected to improve the predictions.

4. CONCLUSIONS

The overall conclusion is that in the Black Sea and the Mediterranean Sea the inclusion of wave-current interactions in the operational wave models is not expected to lead to significant improvements. While it has some importance at some specific areas, it is presently impossible to verify the models for such small areas without measurements. Some improvement may be observed in smaller domains with very high resolutions but only if currents data with corresponding high resolutions are available which presently is not the case.

ACKNOWLEDGEMENTS

This document has been prepared with the financial support of the European Social Fund through Project BG051PO001-3.3.06-0063.NIMH - BAS is solely responsible for the content of this document, and under no circumstances it can be considered as an official position of the EU or the Ministry of Education and Science.

The study was performed with the help of METEO France- DPREVI/MAR and the author thanks Lotfi Aouf . I also wish to express my gratitude to Anna Kortcheva for the continuous support and fruitful discussions.

REFERENCES

Ardhuin, F., Collard, F., Chapron, B., Queffelec, P., Filipot, J.-F., Hamon, M. (2008) Spectral wave dissipation based on observations : a global validation. In: Proceedings of Chinese-German Joint Symposium, on Hydraulics and Ocean Engineering, Darmstadt, Germany

- Bogatchev A.(2008), Changes in operational suite of ALADIN – BG, ALADIN Newsletter No 34
- Booij, N., R. Ris, L. Holthuijsen,(1999) A third-generation wave model for coastal regions 1. Model description and validation, *Journal of geophysical research* 104(C4), 7649- 7666
- Bubnová, R., Hello, G., Bénard, P., & Geleyn, J. F. (1995). Integration of the fully elastic equations cast in the hydrostatic pressure terrain-following coordinate in the framework of the ARPEGE/Aladin NWP system. *Monthly Weather Review*, 123(2), 515-535.
- Galabov V, A. Kortcheva, A. Bogatchev, B. Tsenova (2015) Investigation Of The Hydro-Meteorological Hazards Along The Bulgarian Coast Of The Black Sea By Reconstructions Of Historical Storms. *Journal of Environmental Protection and Ecology*, 16.3, 1005-1015
- Ivan A.S., C. Gasparotti, E.Rusu (2012) Influence of the interaction between waves and currents on the navigation at the entrance of the Danube Delta. *Journal of Environmental Protection and Ecology*, 13(3A), 1673-1682
- Rusu E. (2010) Modelling of wave-current interaction at the Mouths of the Danube. *Journal of Marine Science and Technology*, 15, 143-1559
- WAMDI Group (1988) The WAM model – A third generation ocean wave prediction model. *Journal of Physical Oceanography*,18, 1775-1810



Objective Climatology of the Cyclonic Circulation over the Mediterranean Based on Relative Vorticity Flux Estimation

Hristo Chervenkov*

*National Institute of Meteorology and Hydrology- Bulgarian Academy of Sciences,
Tsarigradsko shose 66, 1784 Sofia*

Abstract. A general climatological approach for estimation of the cyclonic circulation intensity is proposed and demonstrated. The method is based on a relatively simple, not concerning individual systems, scheme for calculation of the vorticity flux, which is physically one of the most adequate quantitative measures of circulation. The method is applied over the whole 66-year-long NCEP-NCAR gridded reanalysis dataset with the original time resolution over model domain covering entirely the Mediterranean Sea and the surrounding territories, which is a well-known secondary maximum of the cyclonic activity in the Northern hemisphere. Main aims of this long-term hindcast study is to demonstrate the possibilities of the proposed approach, revealing the spatial distribution of the circulation activity, its seasonal variations and possible presence of decadal trends. Most results confirm the facts known from other similar studies, but also others, newly or seldom treated, are pointed out.

Keywords: objective climatology, cyclonic vorticity flux, Mediterranean, long-term variations

The present paper is dedicated to the 60th anniversary of the work of A. Pissarski and in memory of prof. E. Syrakov.

1. INTRODUCTION

Extra-tropical cyclones, their paths and intensity, have been the subject of climatological and synoptical studies for more than a century. They are dominant synoptic-scale features of the atmospheric circulation in the mid-latitudes influencing strongly the local weather, in particular causing severe weather events.

* hristo.tchervenkov@meteo.bg

Due to the significant advantages of the automatic and semi-automatic objective methodologies, they have almost entirely replaced the manual synoptic-chart analysis in the past two decades. It has been proven that the application of numerical algorithms of gridded data, mainly from different reanalysis projects, is an effective approach for obtaining detailed storm statistics and, more generally, a spatially and temporally consistent picture of weather systems. The Lagrangian storm tracking has been widely recognized as an effective approach for analyzing detailed statistics of extratropical weather systems. Lagrangian approach provides information on the preferred locations of cyclone genesis and lysis, the average moving speed and lifetime of weather systems, and the difference between cyclone and anticyclone statistics. With advances in computer resources in recent decades, researchers have developed state-of-the-art automatic algorithms. The high socio-economic and theoretical relevance of such phenomena is the main motivator for the increased scientific interest. Consequently, a large number of research papers have been published in recent years, based either on reanalysis data or on Global Circulation Model (GCM) data (see Ulbrich et al., 2009 for a comprehensive review). Different thresholds, different physical quantities, and considerations of different atmospheric vertical levels add to a picture that is difficult to combine into a common view of cyclones, their variability and trends. An expression of the common drive for estimation of the current progress in the field was the IMILAST project - a community effort to intercompare extratropical cyclone detection and tracking algorithms, whose main aim was to reveal those cyclone characteristics that have been robust between different schemes and those that differ markedly (e.g., Neu et al. 2013).

As distinct hemispheric secondary center of cyclonic activity (Ulbrich et al., 2009), the Mediterranean is one of the most discernible focal points of this intensive interest. Pioneering studies for this region that include climatology of cyclones and cyclogenesis are those by Pisarski (1955), Pettersen (1956) and Klein (1957). Subsequent studies, using the same manual analyses and subjective detection, were able to investigate smaller scales, including also mesoscale features (Radinovic and Lalic, 1959; Radinovic, 1978; Genoves and Jansa, 1989). Objective cyclone identification and tracking methods have been first developed in this area by Alpert et al. (1990a and 1990b). Several studies have focused on dynamics, locations, frequency and temporal variability of genesis of the cyclones in the Mediterranean (Buzzi and Tosi, 1989; Tosi and Buzzi, 1989) and more recently the works of Trigo et al. (1999), Campins et al., (2000) Jansà et al (2001b), Maheras et al., 2001, 2002, Lionello et al., 2002 Picornell et al. (2001), Musculus and Jacob (2005), as well as many others. The study of the Mediterranean cyclones from a climatological point of view has been one of the objectives of the first phase of the WMO WWRP MEDEX (MEDiterranean EXperiment) project (Genovés et al. 2006, Jansà et al 2001b).

The main difference between the present study and most other dynamically oriented climatologies is the attempt to estimate the circulation activity, defined in terms of the relative vorticity flux for fixed time intervals, without inspecting features of individual

cyclones and the related metrics (cyclone centers and tracks, track densities and cyclone frequencies, etc.).

The paper is structured as follows: the second chapter is dedicated to the motivation of the used methodology followed by the description itself. The third chapter describes the choice of the dataset as well as the performed calculations. The proposed novel approach is illustrated by one example. The core of the paper is in the fourth chapter, where the results are exposed and discussed. Summarizing remarks are listed and briefly commented on in the conclusion.

2. METHOD

Following the approaches based on an inspection of weather maps, many authors use cyclone core pressure at isobaric height of medium sea-level pressure (MSLP) or relative minima 1,000-hPa geopotential height fields as a mean measure of a low's intensity. Additional quantification of the cyclone intensity is implemented in several studies: the mean radial gradient (Blender et al. 1997, Trigo 2006, Raible et al. 2007, Rudeva and Gulev 2007) and/or, for example, the Laplacian of MSLP computed with a certain radius around the cyclone centre, as in Murray and Simmonds (1991) and Simmonds (2003). Musculus and Jacob (2005) find an 'area under the cyclone's influence' using a scheme originally designed for the identification of watersheds, applied on high resolution data. Such tessellation of the flow of strictly neighboring 'cyclonic' and 'anticyclonic' segments seems at least unusual in the synoptic scale dynamics, where these systems are frequently separated by large vorticity-free (i.e. 'neutral') zones.

Alternatively (or in some studies as an addition) to the consideration of MSLP minima, a number of schemes identify maxima in low-level (e.g., 850 hPa) vorticity (Hodges 1994, Sinclair 1997, Hewson and Titley 2010). The use of this metric implies an extension to the definition of cyclones, so that not only features with closed isobars are considered. Many authors state (for instance Hodges et al. 2003) that vorticity is more focused at the high-frequency end of the synoptic range, while SLP is better at capturing the low-frequency margin. A problem in using vorticity as the only parameter is the larger number of small-scale maxima (compared to MSLP minima), which makes the procedure much more dependent on the spatial resolution of the data.

A common weakness of all single-point intensity diagnostics is the attempt to assess intensity by only one value, ignoring the spatial (even the planar!) extent of the systems. The author's opinion is that this approach for such vast and asymmetric structures as the mid-latitude cyclones seems physically not sufficient. Emphasizing this fact, Sinclair (Sinclair 1997) presents two examples, in which the systems have similar core-point vorticities, but distinguishably different strengths. He states, that the circulation, equivalent to the area enclosed by a curve times the mean vorticity over the area (i.e. the flux of the vorticity which is equivalent to the line integral of velocity around the boundary of the area – see further), is a more realistic measure of cyclone

strength because it takes into account both the size and rotation rate of the system. The unit of measure of the vorticity flux is m^2s^{-1} or, for convenience, CU, where $1 \text{ CU} = 10^7 \text{ m}^2\text{s}^{-1}$. Following Radinovic (1997) the horizontal domain of a cyclone can be defined as the area of positive (relative) vorticity around the cyclone centre, bounded by the zero-vorticity line. In this manner the vorticity distribution field presents the natural way for distinction between the cyclone domain and its surrounding region (vorticity-free or anticyclonic areas). So, a more concise definition of the cyclone intensity or strength could be: *The cyclone intensity is equal to the flux of the cyclonic (i.e. positive in the Northern and negative in the Southern hemisphere) relative vorticity trough the area around the cyclone centre, bounded by the zero-vorticity line (see the Appendix for the mathematical description)*. The main difficulty with circulation calculations lies in defining the region of cyclonic airflow associated with each vortex, especially in cases of multi-core depressions, when many centers share a common zero-vorticity line. Nevertheless, the physical richness and consistency of the vorticity flux as an objective cyclone intensity estimator, determines the increased use of this measure (see, for example, Picornell et al. 2001). Many computational procedures exist, one of the most elaborated is proposed by Sinclair (Sinclair, 1997).

Main goal of the present study is to estimate the cyclonic circulation over the model domain without identification of individual systems. As a result we can obtain the spatial and temporal distribution of the cyclonic flux trough this area as a general (i.e. without accounting the contribution of every cyclone) measure of the cyclonic *circulation intensity* over the region of interest.

Let n_{ij} be the number of corners of the gridcell with lower left corner at the grid point with indexes i and j , where the vorticity ζ_{ij} is positive. Obviously, n_{ij} can take only five values: 0, 1, 2, 3 and 4, where the values 0 and 4 are in the cases when this gridcell is completely in or out of the area, occupied by the cyclonic flow. If n_{ij} is equal to 1, 2 or 3, the zero-vorticity line, whose exact position is not known, splits the gridcell. The idea is to estimate the ‘cyclonic part’ of the gridcell’s area as:

$$\Delta s_{ij}^c := \frac{n_{ij} \Delta s_{ij}}{4} \approx \frac{n_{ij} \Delta y (\Delta x_j + \Delta x_{j+1})}{8} \quad (1)$$

Here Δy is the cell side along the meridian, Δx_j and Δx_{j+1} are the cell sides along the model’s parallel with index j and $j+1$.

Continuing the upper idea, the average positive (cyclonic) vorticity in the gridcell is equal to:

$$\overline{\xi}_{ij}^c := \begin{cases} \frac{\sum_{i,j,\xi_{ij}^c > 0} \xi_{ij}^c}{n_{ij}}, & n_{ij} \neq 0 \\ 0, & n_{ij} = 0 \end{cases} \quad (2)$$

Finally, we can obtain the cyclonic vorticity flux trough the gridcell:

$$\Phi_{ij}^c = \overline{\xi}_{ij}^c \cdot \Delta s_{ij}^c \quad (3)$$

Keeping in mind that the flux is an additive quantity, the total one over a certain region can be obtained by simple summing of single shares over the calculated by equation (3) contributions for all gridcells included in this region. In particular, it is possible to estimate the flux of an individual cyclone by summing the fluxes for all gridcells inside the zero-vorticity line around the corresponding vertex. Such a task, however, is not the subject of the paper.

The described novel approach differs relevantly from most other studies (Neu et al. 2013), which core is set of algorithms for calculation of the characteristics (vertex centers, trajectories, life-time aspects, etc.) cyclone-by-cyclone. Usually further, to obtain long-term climatologies, statistical and ensemble analysis is performed. Main advantage of the proposed method is its conceptual and mathematical simplicity. This allows in particular escaping from a lot of sophisticated and demanding procedures such as individual cyclone identification and calculation of the intensity cyclone-by-cyclone, which is very significant especially for long periods of time. Important merit is also the absence of any (wide used in other studies) assumptions i.e. empirical thresholds, which more or less affect the physical objectivity of the procedure. Most obvious drawback is the limitation to only one, ‘bulk’ characteristic of the circulation state, which constrains the analysis possibilities only over this metrics.

3. USED DATA AND PERFORMED CALCULATIONS

The data used in this study are the time series of 6-h wind produced during National Centers for Environmental Prediction (NCEP) National Centre for Atmospheric Research (NCAR) 40-year reanalysis project (Kalnay et al., 1996), converted in plain ASCII format in the Climatic Research Unit, University of East Anglia. The data set consists of grid point values of the 850 hPa level real (not geostrophic!) wind in a grid of $2.5^\circ \times 2.5^\circ$, allowing the study of synoptic scale cyclones. The full time span of 66 years (1948–2013) is covered at 00:00, 06:00, 12:00 h and 18:00 h co-ordinated universal time (UTC).

The modeling domain extends between latitudes 22.5°N and 55.0°N , and longitudes 12.5°W and 47.5°E including completely the Mediterranean, the surrounding territories and the Black Sea.

The finite difference method is applied to calculate the vorticity field at 850 hPa. The reasons for selection of this isobaric level hPa are manifold. First, according to the traditional concept, the (well) developed tropospheric cyclone is better expressed in the low levels. On the other hand, however, mainly the turbulent friction in the planetary boundary layer alters the flow, which makes the near surface layer unsuitable for such analysis. In the bigger part of the vorticity-based cyclone studies, the 850 hPa level is the most preferable one. Many authors (Sinclair, 1994, Picornell et al. 2001 and etc.) point out the inherent ‘noisiness’ of the vorticity and the consequence that small-scale features can mask higher scales. Applying the Cressman filter (Cressman, 1959) is widely used in the objective cyclone analysis technique to overcome this problem. After some tests, Picornell (Picornell et al. 2001) states, that the value of 200 km of the Cressman’s filter tuning parameter, often called ‘radius of influence’, provides accurate description of Western Mediterranean cyclones. This distance is smaller than the horizontal grid resolution in the bigger part of the domain, which makes such preprocessing unnecessary in our case.

Figure 1 shows an illustrative application of the proposed approach to one case of a well-developed cyclone over the eastern Mediterranean on 31 December 2000. Due to the (general) absence of aerological soundings over Europe at 18 UTC, respectively weather map on the selected isobaric level AT850, the synoptical situation is visualized with a manual surface map from the NIMH-BAS archive, as shown on the left pane. As can be seen, the weather over the Central and Eastern Mediterranean is dominated by a deep (the MSLP in one station near the low’s minimum is 996,9 hPa) single-core cyclone eastwards from Sicily. The cyclone is surrounded by an anticyclonic belt over Central Europe in the north and over the northeastern part of the Balkan Peninsula in the northeast. A secondary low is placed over Ukraine. On the right pane of figure 1 are given the vorticity in each grid node and the cyclonic vorticity flux trough each gridcell, calculated with the proposed method, at AT850 correspondingly. The comparison between the pictures on left and right panes shows that the maximal flux is located in the cell containing the vorticity maximum, and decreasing radially, turns to zero in the gridcells, whose all corners are with negative (i.e. anticyclonic) vorticity. Again, the flux is positive near the upper right corner of the domain, over the secondary low. The continual zones with positive flux are interpreted as separate lows and their intensity is obtained by integrating the flux over them.

One of the main merits of the chosen approach, based on the above proposed method, is the indicative force of the vorticity flux over a certain area – first, it is a very robust integral (over the space) criterion of absence or presence of cyclonic activity there and, if such is present, of its magnitude. Thus, the first step in the performed calculations is to compute it for every time step for the whole 66-years period.

Past and future trends in cyclone characteristics, or, more generally, of cyclone activity, are an important issue in the discussion of climate change impacts. In this context, the knowledge of interannual and decadal variability is indispensable for assessing the importance of observed or projected trends. From climatological point of view it is essential to process ‘sufficiently’ long datasets to achieve statistically robust, respectively representative results. Many authors (Neu et al, 2013) emphasize the principal impossibility to perform comprehensive diagnosis of long-term trends using 20-year and, in some studies, even shorter datasets. The most often used criterion for time scale judgment in this sense is the standard 30-year long World Meteorological Organization (WMO) period (see, for example, Baddour and Kontongomde 2007). It is worthy to underline, that among all (at least these freely available) the NCEP-NCAR reanalysis is with the longest time coverage, which makes it preferable for climatological studies, as the presented in this paper.

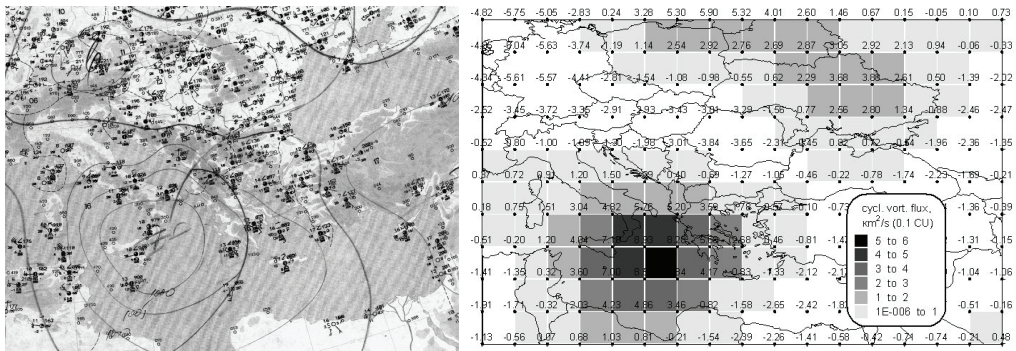


Fig. 1. Hand-drawn surface synoptic map for 31.12.2000 at 18 UTC (on left, NIMH-BAS archive) and calculated vorticity (unit: CVU) in each grid node and cyclonic vorticity flux in each gridcell (see legend) respectively for the same situation (on right).

In the more than half a century after the work of Petersen (1956), many other studies (Alpert et al. (1990a and 1990b), Trigo et al. (1999), Trigo et al. (2002)) reveal the irregular spatial, seasonal and diurnal distribution of the Mediterranean cyclones according to their cyclogenesis and lysis regions, life cycle aspects, and tracks. Therefore, from methodological point of view, the correct long term comparisons have to be performed over monthly or seasonal averages and not simply over fixed time-length (years, decades) periods. So, the calculated for each 6 hours daily means are additionally averaged for each season. The whole time span is divided equidistantly in three 22 year long time periods: 1948-1969, 1970-1991 and 1992-2013 and the traditional four meteorological seasons (December–February, DJF; March–May, MAM; July–August, JJA; September–November, SON) segmentation is applied, although some criticism to the latter (Trigo et al 1999) exists. To keep the consistency of this article however, only results for the two ‘main’ seasons, namely winter and summer, are presented here. The correct comparability between the seasonal averages is ensured with recalculation of

these quantities for standard 90-day period. Thus the inconsistency between summer and winter as a result of their different durations is avoided.

Despite the above listed considerations about the applicability of the core-point vorticity as a cyclone strength measure, this value is calculated for all detected maxima for a rough judgment of the strength. Here, the traditional manner of detecting the location, respectively of the value, of the maxima is performed: The vorticity in each node is compared with that in all eight surrounding grid points, followed by interpolation within the gridcell. The calculations show, that only in a few time frames (isolated cases) it is greater than 12 CVU ($1 \text{ CVU} = 10^{-5} \text{ s}^{-1}$). Thus, the range between 0 and greater than or equal to 12 CVU is divided into four categories and each detected maximum is allocated to one of them. The number of events in each category in each gridcell for the periods of interest is an additional statistic in the assessment of the spatiotemporal variations of the cyclonic activity in the domain.

On the first calculation step, the vorticity flux field for the current time frame and then the daily averages as mean of the corresponding four consecutive ones are obtained. Simultaneously, the vorticity maximum statistics, as prescribed above, are computed. All intermediate results are stored in catalogue and data base files, which allows further and separate processing, in particular adopting other ideas. Second, after an additional averaging procedure, the seasonal daily averages for each 22-year time period, are calculated. They express in most concise form the main results of the presented study and are shown on figures 3-5.

A logical next step is to try to assess the long-term variations of the calculated quantities. The above described 22-year seasonal means, which, in the frame of the adopted approach, can be treated as climatic representatives for the corresponding periods. As the proposed method estimates the overall cyclonic flux in fixed grid rather than of non-stationery objects (individual systems, tracks, etc.) methodologically the simplest way for such assessment is to obtain the relative changes of one time period relative to the other two. For conciseness again, only the relative changes of the last period to the first are presented here, as shown on figures 6 and 7.

To point out the zones with more robust tendencies, which are thought as most significant for the regional climate, the gridcells without monotonic (i.e. if the change of the second period to the first and the third to the second are not with the same sign) are discarded (differently color coded on the corresponding figures).

4. RESULTS AND DISCUSSION

The climatology of cyclones in the domain is highly influenced by the almost enclosed Mediterranean Sea, which is an important source of energy and moisture for cyclone development. Major role in the steering and deflecting air flows plays its complex land topography. Moreover, being located within the transition between the subtropical high-pressure belt and the mid-latitude westerlies, the Mediterranean is also subject to

strong interannual variability of cyclone activity (Lionello et al. 2006). The outcomes of the most modern automated procedures allow assessment of the cyclonic activity distribution in different terms - areas where cyclogenesis tends to occur (as, for, example in Trigo et al. 1999, 2002), storm-tracks densities (Picornell et al. 2001, Musculus and Jacob 2005, Trigo et al. 2006), cyclone centers counts (Maheras et al. 2001) or frequently combination of them. Due to the above mentioned limitation of the proposed approach, the applied estimators in the presented study are the overall cyclonic flux and the categorized number of vertices. Although the obtained results can be analyzed further, the main issues can be briefly divided and summarized in the following sections:

- Geographical and the seasonal distribution
- Long-term (inter time-period) variations.

Main result according the geographical distribution can be concise formulated as:

- Statistically the most robust in all seasons and time periods region of the cyclonic activity in is the the domain over the Ligurian, Tyrrhenian and Ionian seas, where the most intense cyclonic flux and centers with the highest core-point vorticity have been detected.

Part of the systems, originate from other regions, for instance northern Africa, as shown in Genovés et al. (2006), but obviously during their propagation and life-cycle development they reach the phase of maximal development here, causing the strongest climatologically averaged vorticity flux. As shown on figures 3-5, the gridcells with the maximum total amount (i.e. sum of counts in all four categories) of centers are located in the central Mediterranean. Second, here are concentrated those in the first two categories (with core-point vorticity above or equal to 9 CVU and between 6 and 9 CVU), although this zone is elongated in the southeast direction to Cyprus, which is a cyclogenetic region (Trigo et al. 1999, Trigo et al. 2002).

Generally, this result agrees with the conclusions of many other studies obtained with different methodologies, selection criteria and data sets (e.g. Alpert et al. 1990a,b Campins et al., 2000, Maheras et al. 2001, Picornell et al. 2001, Musculus and Jacob 2005). The relatively coarse resolution of the dataset and nature of the proposed approach, however, does not allows resolving sub-areas as in other dynamically oriented methodologies (Campins et al., 2000, Picornell et al. 2001).

The decadal averaged seasonal vorticity flux shows also another distinguishable pattern, namely:

- In all time periods a sea/land difference in the cyclonic activity is observed and as a whole it is greater over the seas. The contrast is most clearly expressed during the winter.

This fact can be explained in general with the role of latent heat release and diabatic processes. As stated in Lionello et al.(2006) this is a key issue in the Mediterranean cyclogenesis.

According many studies (see, for example Lionello et al. 2006), the overall synoptic activity over the entire basin has a well-defined annual cycle, being more intense in the

period from November to March which corresponds to the so-called storm season. This study reveals overall the same seasonal variation pattern:

- *Generally the cyclonic activity over the domain is more prominent in the winter than in the summer, especially over the above described region.*

The mechanisms typical of winter cyclogenesis in the Mediterranean exhibit contrasting characteristics with those most common in spring and summer seasons, with intermediate situations in spring and autumn. Our study reveals, that in the three time periods the average summer vorticity flux over the seas of increased activity is roughly between 3 and $6 \cdot 10^{-2}$ CU, and in winter, again roughly, it is between 5 and $9 \cdot 10^{-2}$ CU. In terms of number of detected centers this seasonality is significantly better expressed: During the summer, only in a few gridcell events in the second, and almost not at all in the first category, are realized. Opposite, in the winter, the number of events in the second category is relatively great, reaching in the internal part of the domain a couple of tens. Using the NCEP-NCAR datasets for the period 1958-1997, Maheras (Maheras et al. 2001) also reveals especially high frequency of cyclone centers in the Gulf of Genoa, which is the most discernible activity region in our study, and more preferably for the intense cyclones. The Mediterranean cyclones are in general more similar to the Atlantic cyclones in winter than in summer (Campins et al., 2005). In winter there are strong links between synoptic upper-troughs and local orography and/or low-level baroclinicity observed over the northern Mediterranean coast. As stated in Lionello et al. 2006, winter cyclogenesis occurs essentially along the northern coast in three major areas characterized by strong baroclinicity: the lee of the Alps, and over the Aegean and Black Seas, when an upper-trough moves over the relatively warm water basins. For the third and the fourth category, containing the centers with core-point vorticity greater than or equal to 3 and lower than 6 CVU, and lower than 3 CVU respectively, the picture seems converse, although not clearly expressed: in significant part of the domain the number of centers in summer is greater than in winter. Obviously during its development one cyclone traverses from one category to another and these facts alone are not sufficient for more general conclusions, but point to the known from many studies fact (Maheras et al. 2001, Picornell et al. 2001, Trigo et al. 2002), that in the summer the cyclonic activity is dominated by shallow, as a rule barotropic and short-living depressions (Ulbrich et al. 2009).

However, one clearly standing out exception of this pattern has to be emphasized: A very strong cyclonic maximum in the summer (especially in the first time period) is revealed over Anatolia. This maximum is stronger even than the winter one over the Tyrrhenian Sea – in terms of the vorticity flux and especially in terms of the number of cyclonic centers: for example in the first time period the Anatolian (summer) maximum has peak vorticity flux between 10 and $12 \cdot 10^{-2}$ CU and a number of centers in the second and third category 59 and 580 respectively. On the other hand, the Tyrrhenian (winter) maximum has a vorticity flux between 7 and $9 \cdot 10^{-2}$ CU and a little bit greater number of centers in the second category – 76, but only 169 in the third.

Usually, the Anatolian center of activity is considered rarely in most climatological studies for the Mediterranean. Fisher (1978) explains this semi permanent cyclonic center (“Anatolian low” in terms of MSLP) with the northwestern expansion of the Indian subcontinent monsoonal low combined with the intense heating over the Middle East. The formation of big overheated air mass is strengthened especially over a terrain with specific orography (the Anatolian plateau) during the summer. In the works of Kotroni et al. (1997) and Chronis et al. (2011) this low, in constellation with high pressure system over the Balkans, is considered as prerequisite for strong north-north-east winds over the Aegean Sea, known as Etesian winds. Maheras et al. (2001) treats this center as part of the eastern Mediterranean one, but, however, relation to synoptic scale cyclones was not revealed. In the means of the proposed approach this case demonstrates how the long time integration of the cyclonic fluxes of weak, but frequent (semi permanent) vertices can produce result, commensurable or even greater than those of significant, but seldom structures. This fact can be observed as limitation of the possibility for assessment, based only on the gridded vorticity flux. The method have to be applied in combination with other estimators, as for example as demonstrated in this study, the categorized number of center counts.

No significant (in comparison with the surrounding territories) cyclonic activity is detected over the Black Sea.

At first sight this conclusion contradicts to the one in Trigo et al. (2002), where the eastern part of the Black Sea is revealed as a cyclogenetic region, using, however, different datasets (origin and time span) and a different approach. Analyzing the cyclonic tracks over the Eastern Mediterranean Flocas (Flocas et al. 2010), detects noticeable number over the Black Sea, which conclusion is supported also by other studies (Neu et al. 2013). A possible reason for the apparent disagreement is the fact that the average cyclonic flux might be quite low in that area due to very early stages of cyclone development. Consequently ‘cyclogenetic area’ and ‘area of intense (overall) cyclonic circulation’ according our approach, can not be treated as synonyms.

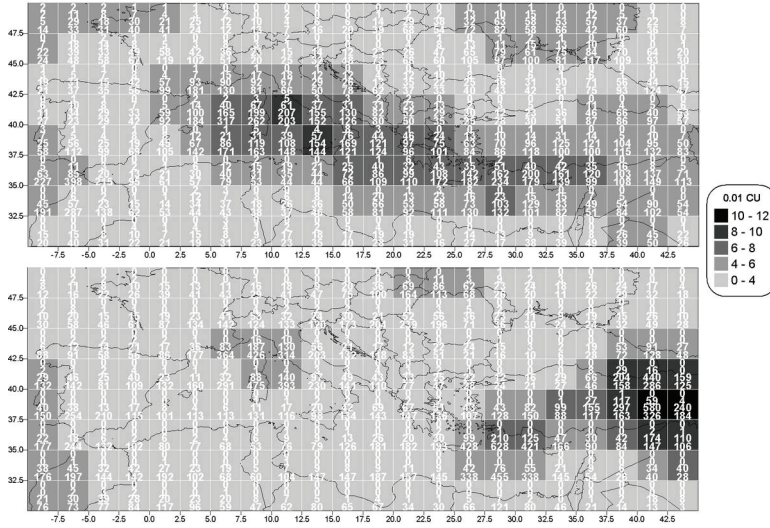


Fig. 2 Average daily cyclonic flux for the first time slice (1948-1969) during the winter (upper pane) and summer (lower pane). The number of the detected cyclone centers during all winters/ summers in the time slice with core-point vorticity below 3 CVU, between 3 and 6 CVU, between 6 and 9 CVU and greater than 9 CVU in each gridcell are shown in the first (lowest), second, third and fourth text register respectively.

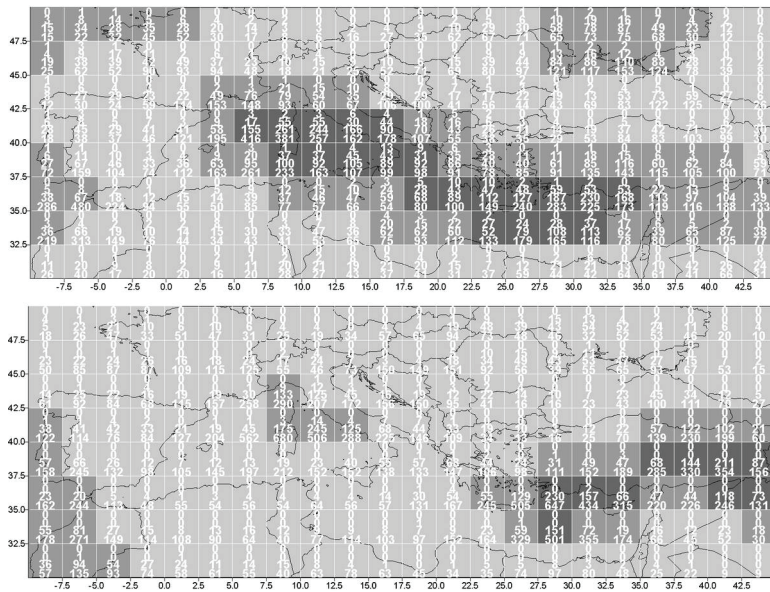


Fig. 3 Same as Figure 2, but for the second time period (1970-1991)

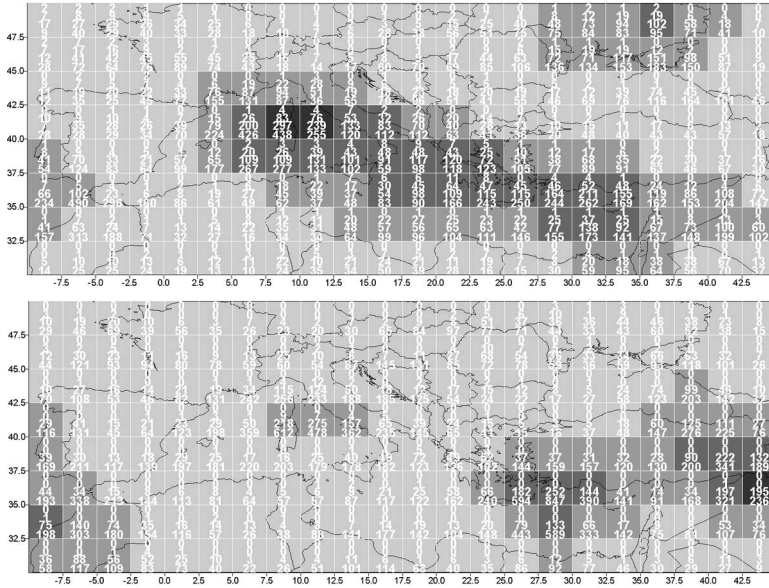


Fig. 4 Same as Figure 2, but for the third time period (1992-2013).

The long-term (inter time-period) variations assessment also highlights significant features. Continuing the concise presentation style of the previous section, the following most remarkable issues can be outlined.

Over the bigger, compact marine part of the domain (as over the bigger part of the whole domain), which, as previously stated, is the main region of cyclonic activity, the relative change of the mean winter vorticity flux of the second time period (1970-1992) to the first one (1948-1969) and that of the third (1992-2013) to the second, are not with the same sign, i.e. the time change of period-to-period vorticity flux field is not monotonic.

A monotonic increase of the mean summer vorticity flux (spatially very roughly averaged) relatively 30-50% is revealed over the bigger marine part of the domain, although this quantity varies significantly in the different seas of the Mediterranean. Monotonic increase with relative high values (over 50%) of the summer vorticity flux is revealed also over a couple of neighboring gridcells in different parts of the domain, but most significant seems the one on the south domain border, around the Gulf of Sidra. This significance is caused not only by the value of the increase, but also by the fact, that this area is a well-known cyclogenetic region, origin of some of the most severe storms over the Central Mediterranean (Genovés et al. 2006).

Accordingly, for the Anatolian centre of cyclonic activity, a discernible decrease of the vorticity flux is observed over the autumn, winter and spring (the pictures for the autumn and spring are not shown), but not for the summer, which, as discussed above, is the season of the most pronounced manifestations of this activity.

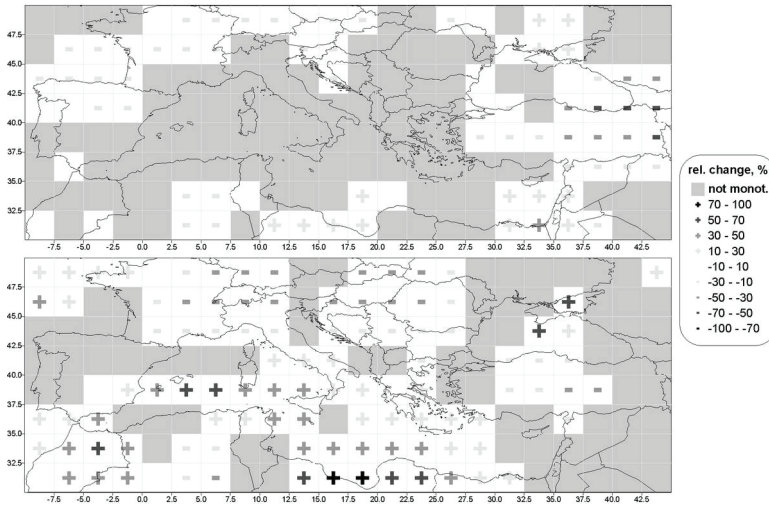


Fig. 5 Relative change of the average daily cyclonic flux of the last time period to the one of the first for the winter (upper pane) and the summer (lower pane). The gridcells without monotonic change are greyed.

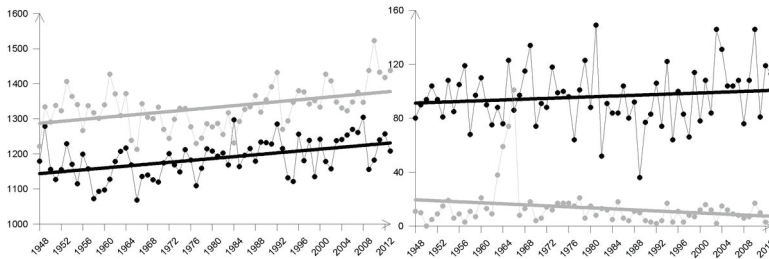


Fig. 6 Time series for the total (on left) and strong/very strong (on right) seasonal cyclone center counts. The datasets, respectively the trend lines, for the winters are shown in black and for the summers – in grey.

A basic approach for computing cyclone frequencies is counting their number of occurrence (from the identification scheme) or positions (from tracks) in grid squares (either simply on a fixed latitude-longitude grid, or referring to a fixed area size). Similar to the IMILAST long-term estimation approach (Neu et al 2013), we have constructed also the time series of the total and of the strong and very strong seasonal cyclone center counts in the domain during the winter and summer season, as shown in Figure 6. Here ‘count’ means all centers found at any time step and ‘strong’ and ‘very strong’ – cyclones with core-point vorticity between 6 and 9 CVU and above or equal to 9 CVU (the upper two bins according to our classification) respectively. The significant

seasonal difference in both ensembles is clearly outlined – in all years, except 1984, the number of all winter centers is smaller than the summer's. In contrast, the number of strong and very strong centers in winter is greater in all years, except one remarkable outlier, the year 1964.

A counting of cyclone centres (without any differentiation on intensity), based on the NCEP re-analysis, which covers the period 1958–1997, shows a reduction of the number of cyclones in western Mediterranean and an increase in the East (Maheras et al., 2001). Linear fit to the data leads roughly to a 15% increase/decrease. Changes are not seasonally homogeneous. The IMILAST-analysis reveals, that most participating methods indicate increase of the total number of (North hemispheric) cyclone centers over the winters in the 1989–2009 period and decrease of the deep (core pressure below 980 hPa) ones, although with significant differences between the methods. Further, it is emphasized, however, that hemispherically averaged trends do not provide information about regional shifts of cyclone occurrence. Thus, results obtained for a limited domain as ours, can not be directly compared with the IMILAST ones or such from other studies, for example Bartholy et al. (2006). The linear regression fit lines of our time series are with so small slope (the absolute value is smaller than 1.4 counts/year for all four) and so poor (the coefficient of determination is smaller than 25% for all) that any statements for persistence of long-term trends, at least for any statistical significance, based only on these results, would be incorrect. Exploring these intermediate outputs with a more productive method, in particular for seeking robust annual and decadal tendencies, can be a subject of further studies.

5. CONCLUSION

Combining optimally clear meteorological meaning and deep physical contents on the one hand and the possibility of relatively easy computation from freely available data on the other, the relative vorticity flux demonstrates features of a perfect cyclonic systems estimator. Main result, described in the paper is the proposed novel approach for estimating of the cyclonic flux in grid, using the wind components in the gridnodes as a part of the author's idea to assess the cyclonic activity overall for fixed region and time frame, rather as a statistic for individual lows. The method is transparent, free from empirical thresholds, conceptually simple, and, as result, computationally not demanding. It can be practically without change adapted for different datasets/regions and periods. Inspecting digital charts, it is possible to use it for dynamical analysis of separate cyclones in semi-automatic manner. The method gives the opportunity to obtain the cyclone size (horizontal extend) and mean vorticity separately, which is significant for assessment of individual systems. The study proves, that even with such a general approach, not considering individual objects, meaningful outcomes can be achieved, revealing significant features of the cyclonic activity in the Mediterranean and its long-term variations. As many times mentioned, the outcomes according the regions with

increased cyclonic activity and the annual variation of this activity generally express basic facts of the synoptical meteorology and climatology of the Mediterranean, but that does not reduce its value, rather, it can be considered as a kind of dynamical explanation. They are in principal good agreement with the modern concepts – results from computationally-oriented studies (see again Lionello et al. 2006 for a comprehensive review). As shown in the case of the Anatolian low however, the method shows, also weaknesses – retrieving only the gridded overall flux, it is not possible to discriminate between the summarized contribution of frequent and shallow from one site and rare, but significant structures from other. The use of the full 66 year (until the end of 2013) time span of the NCEP-NCAR Reanalysis dataset for such, preliminary indeed, long term objective assessment, is novel. It gives the possibility for treatment of three distinct (i.e. fully non-overlapping) 22-years time periods, which are itself with significant length for climatological analysis. The comparison between the averaged seasonal fluxes, which is also novel, for these time-periods performed in this study, reveals interesting patterns. Among them, most climatologically relevant seems the monotonically increased flux in the Gulf of Sidra, which is recognizable cyclogenetic region.

At the end, we need to emphasize that is methodologically reasonable to aspect some differences between the outcomes of the presented study and others, most of them treating every cyclone separately. Ever since the beginning it was underlined that due to various reasons the results of similar, much more sophisticated methods, can differ from each other. In this context the presented study has to be accepted as a small step toward the understanding of the complex nature of the cyclonic activity over the Mediterranean.

6. ACKNOWLEDGEMENT

To NCEP-NCAR for providing free of charge data and to the Climatic Research Unit, University of East Anglia for the reformatting of these data in convenient form and its further online redistribution. The author would like to express his gratitude to Pl. Neychev and D. Karamfilova from NIMH-BAS for their help.

APPENDIX

Applying the Stokes theorem, which states equivalence between the circulation C , defined as linear integral of some vector (in our case the velocity u) around a closed path L_s and the flux of the vector's vorticity through the area, bounded by this path S , we can write:

$$C = \oint_{L_s} \vec{u} \cdot d\vec{r} = \iint_S (\vec{\nabla} \times \vec{u}) \cdot d\vec{s} \quad (\text{A.1})$$

Due to the fact that the dot product between the horizontal vorticity components $(\vec{\nabla} \times \vec{u})_x$, $(\vec{\nabla} \times \vec{u})_y$ and the surface element $d\vec{s}$ is equal to zero, the cross product in the right side of equation (1) can be replaced with the vertical vorticity component, traditionally marked with ξ :

$$\xi := (\vec{\nabla} \times \vec{u})_z = \frac{\partial v}{\partial x} - \frac{\partial u}{\partial y} \quad (\text{A.2})$$

The integral on the right side of equation (1) can be estimated as follows:

$$C = \iint_S (\vec{\nabla} \times \vec{u}) \cdot d\vec{s} = \iint_S \xi d\vec{s} \approx \bar{\xi} \cdot S_c \quad (\text{A.3})$$

Thus, C is roughly equal to the area S_c enclosed by the curve L_s times the mean vorticity $\bar{\xi}$ over the area. If obtained separately from the mean vorticity, which is possible with the proposed method, S_c can be used as additional measure of the cyclone's magnitude.

REFERENCES:

- Alpert P, Neeman BU, Shay-El Y (1990a) Climatological analysis of Mediterranean cyclones using ECMWF data. *TellusA* 42:65–77
- Alpert P, Neeman BU, Shay-El Y (1990b) Intermonthly variability of cyclone tracks in the Mediterranean. *J Clim* 3:1474–1478
- Baddour O, Kontongomde H (ed.) (2007) The role of climatology normals in a changing climate WCDMP-No. 61, WMO-TD No. 1377, World Meteorological Organization, Geneva
- Bartholy J, Pongrácz R, Pattantyús-Ábrahám M (2006) European cyclone track analysis based on four geopotential fields of ECMWF ERA-40 datasets. *Int J Climatol* 26:1517–1527
- Blender R, Fraedrich K, Lunkheit F (1997) Identification of cyclone-track regimes in the North Atlantic. *Quart J R Met Soc* 123:727–741
- Buzzi A, Tosi E, (1989) Statistical Behavior of Transient Eddies near Mountains and Implications for Theories of Lee Cyclogenesis. *J. Atmos. Sci.*, 46, 1233–1249
- Campins J, Genovés A, Jansà A, Guijarro J. A., Ramis, C. (2000). A catalogue and a classification of surface cyclones for the Western Mediterranean. *Int. J. Climatol.*, 20, 969–984
- Campins J, Jansà A, Genovés A (2006) Three-dimensional structure of western Mediterranean cyclones *Int. J. Climatol.* 26: 323–343
- Chervenkov H (2012) The Winter of 2011/2012 – Synoptical Aspects and Weather Events Proc. of IX-th scientific-technical conference “ECOLOGY and HEALTH”, ISSN 1314-1880 511-516 (in Bulgarian)
- Chronis T, Raitsos D, Kassis D, Sarantopoulos A. (2011) The Summer North Atlantic Oscillation Influence on the Eastern Mediterranean *Journal of Climate* vol 24: 5584-5596
- Cressman GP. 1959. An operational objective analysis system. *Monthly Weather Review* 87: 367–374.
- Fisher, W. B., (1978) *The Middle East*. 7th ed. Cambridge University Press, 5–47.

- Flocas H, Simmonds I, Kouroutzoglou J, Keay K, Hatzaki M, Bricolas V, Asimakopoulos D, (2010) On Cyclonic Tracks over the Eastern Mediterranean. *J. Climate*, 23, 5243–5257.
- Genovés A, Jansà A (1989). Statistical approach to mesoscale non-alpine West Mediterranean cyclogenesis. *WMO/TP num*, 298, 77–85
- Genovés A, Campins J, Jansà A (2006) Intense storms in the Mediterranean: a first description from the ERA-40 perspective *Adv Geosciences*, 7, 163–168
- Hewson T, Tittley H (2010) Objective identification, typing and tracking of the complete life-cycles of cyclonic features at high spatial resolution *Met App*, vol 17, 3:355–381
- Hodges KI (1994) A general method for tracking analysis and its application to meteorological data. *Mon Wea Rev* 122:2573–2586
- Hodges KI, Hoskins BJ, Boyle J, Thorncroft C (2003) A comparison of recent reanalysis datasets using objective feature tracking: storm tracks and tropical easterly waves. *Mon Wea Rev* 131:2012–2037
- Jansà A, Alpert P, Buzzi A, Arbogast, P (2001a). MEDEX, cyclones that produce high impact weather in the Mediterranean, available at <http://medex.inm.uib.es>.
- Jansà A, Genovés A, Picornell M. A., Campins J., Riosalido R., Carretero, O (2001b). Western mediterranean cyclones and heavy rain. Part 2: statistical approach. *Meteorol. Appl.*, 8, 43–56
- Kalnay E, Kanamitsu M, Kistler R, Collins W, Deaven D, Gandin L, Iridell M, Saha S, White G, Woolen J, Zhu Y, Chelliah M, Ebisuzaki W, Higgins W, Janowiak J, Mo KC, Ropolewski C, Wang J, Leetmaa A, Reynolds R, Jenne R, Joseph D (1996) The NCEP/NCAR 40-year reanalysis project. *Bull Am Meteorol Soc* 77:437–471
- Klein, W.H. (1957) Principal tracks and frequencies of cyclones and anticyclones in the Northern Hemisphere. U.S. Weather Bur., Res. Paper num. 40
- Kotroni V, Kallos G, Lagouvardos K (1997) Convergence zones over the Greek peninsula and associated thunderstorm activity *Q. J. R. Meteorol. Soc.* 123, pp. 1961–1984
- Lionello P, Dalan F, Elvini, E (2002). Cyclones in the Mediterranean region: the present and the doubled CO2 climate scenarios. *Clim. Res.*, 22, 147–159
- Lionello P., Bhend J., Buzzi A., Della-Marta P. M., Krichak S., Jansà A, Maheras, P., Sanna, A., Trigo, IF., and Trigo, R.(2006) Cyclones in the Mediterranean region: climatology and effects on the environment *Developments in Earth and Environmental Sciences*, Elsevier, 4, 325–372
- Maheras P, Flocas H, Patrikas I, Anagnostopoulou C (2001) A 40-year objective climatology of surface cyclones in the Mediterranean region: spatial and temporal distribution. *Int J Climatol*. 21:109–130
- Maheras, P., Flocas, H. A., Anagnostopoulou, Ch., & Patrikas, I. (2002). On the vertical structure of composite surface cyclones in the Mediterranean region. *Theor. Appl. Climatol.*, 71, 199–217
- Murray RJ, Simmonds I (1991) A numerical scheme for tracking cyclone centres from digital data. Part I: development and operation of the scheme. *Aust Meteorol Mag* 39:155–166
- Musculus M, Jacob D (2005) Tracking cyclones in regional model data: the future of Mediterranean storms. *Adv Geosciences* 2:13–19
- Neu U., M.G. Akperov, N. Bellenbaum, R. Benestad, R. Blender, R. Caballero, A. Coccozza, H.F. Dacre, Y. Feng, K. Fraedrich, J. Grieger, S. Gulev, J. Hanley, T. Hewson, M. Inatsu, K. Keay, S.F. Kew, I. Kindem, G.C. Leckebusch, M.L.R. Liberato, P. Lionello, I.I. Mokhov, J.G. Pinto, C.C. Raible, M. Reale, I. Rudeva, M. Schuster, I. Simmonds, M. Sinclair, M. Sprenger, N.D. Tilinina, I.F. Trigo, S. Ulbrich, U. Ulbrich, X.L. Wang, H. Wernli, (2013) IMILAST – a

- community effort to intercompare extratropical cyclone detection and tracking algorithms. *Bull. Amer. Meteor. Soc.*, 94, 529–547
- Pettersen S. (1956) *Weather Analysis and Forecasting*, Vol I. McGraw-Hill: New York, 428.
- Picornell MA, Jansà A, Genovés A, Campins J (2001) Automated database of mesocyclones from the Hirlam (INM)-0,5° analyses in the Western Mediterranean. *Int J Climatol* 21:335–354
- Pisarski, A. (1955) The Mediterranean cyclones and their impact on the weather in Bulgaria (in Bulgarian) *Hydrology and Meteorology* (issue of the Bulgarian Institute of Meteorology and Hydrology) vol II, no. 6
- Radinovic D, Lalic D (1959) Cyclonic Activity in the West Mediterranean (in Serbian) *Rasprave i studije Saveznog hidrometeorološkog zavoda*. no. 7
- Radinovic, D. (1978) Numerical model requirements for the Mediterranean area, *Riv. Met. Aer.*, 38, 191–205
- Radinovic D. (1997) The basic concept of the methodologies on Mediterranean cyclones and adverse weather phenomena studies. In INM:WMO Symposium on Cyclones and Hazardous Weather in the Mediterranean, Ministerio de Medio Ambiente:Universitat Illes Balears, Palma de Mallorca; 45–53; available at Instituto Nacional de Meteorologia, Palma de Mallorca
- Raible CC, Yoshimori M, Stocker TF, Casty C (2007) Extreme midlatitude cyclones and their implications to precipitation and wind speed extremes in simulations of the maunder minimum versus present day conditions. *Clim Dyn* 28:409–423
- Rudeva I, Gulev SK (2007) Climatology of cyclone size characteristics and their changes during the cyclone life cycle. *Mon Wea Rev* 135:2568–2587
- Simmonds I, Keay K, Lim EP (2003) Synoptic activity in the seas around Antarctica. *Mon Wea Rev* 131:272–288
- Sinclair MR (1994) An objective cyclone climatology for the southern hemisphere. *Mon Wea Rev* 122:2239–2256
- Sinclair MR (1997) Objective identification of cyclones and their circulation intensity, and climatology. *Weather Forecasting* 12:595–612
- Tosi E, Buzzi E (1989) Characteristics of high-frequency atmospheric eddies over the mediterranean area in different seasons. *Il Nuovo Cimento C* 12:4, 439-452
- Trigo IF, Davies TD, Bigg GR (1999) Objective climatology of cyclones in the Mediterranean region. *J Clim* 12:1685–1696
- Trigo IF, Bigg GR, Davis TD. (2002) Climatology of cyclogenesis mechanisms in the Mediterranean. *Monthly Weather Review* 130: 549–569
- Trigo IF (2006) Climatology and interannual variability of storm-tracks in the Euro-Atlantic sector: a comparison between ERA-40 and NCEP/NCAR reanalyses. *Clim Dyn* 26:127–143
- Ulbrich U, Leckebusch G. C., Pinto J. G. (2009) Extra-tropical cyclones in the present and future climate: a review *Theor Appl Climatol* 96:117–131



Classification of macrocirculation processes of the northwest Black sea region, which contribute to surface wind strengthening

**Zubkovych* S.O., Ivus G.P., Ahayar E.V., Horska L.M.,
Semerhey-Chumachenko A.B.**

Department of Meteorology and Climatology, Odessa State Environmental University, Ukraine

Abstract. Features of the geographical position of Ukraine, synoptic processes and a variety of climatic conditions conduce to frequent occurrence of natural hydrometeorological phenomena (OHSS) and create extreme complexity of their distribution in space and time. Today the problem of storm winds is quite actual. One of the conditions for successful forecasting of strong winds is the knowledge of wind characteristics on the studied area and synoptic conditions that cause them (Bagrov 1973, Gruza G.V., Rankova., Oesterle 1976, Ivus 2012, 2014, 2015). Synoptic analysis of the material reveals the general regularities of such processes. The results presented below are the continuation of work (Katz 1959, Klimenko 1976, Kononova 2009, Martazinova, Ivanova 2004, Martazinova 2005, Rossby 1939, Vasiukov, Zverev, Ped 1962) on search for the best synoptic classification that reflects the completeness of the macro scale baric processes that lead to the formation of the wind, including strong wind, over the south of Ukraine and allows predicting it as accurate as possible.

Keywords: synoptic analysis, circulation indexes, storm winds forecasting

LITERATURE REVIEW

The first twenty years of the XXI century is the transition period from the domination of the most unstable southern meridional processes to the prevalence of the northern meridional processes. Due to the fact that the length of the southern meridional processes is currently almost twice as much as the average duration (Savter 2014), the resulting probability of disaster is high, and the circulation conditions require careful study to improve the accuracy of the natural hydrometeorological phenomena forecasts (OHSS).

* szubkovych@gmail.com

General properties of the atmospheric circulation are often described using various indices, including the best known indexes of circulation of K.-G. Rossbach (1939) and A. Blinova. Later O.L. Katz (1959) developed the typing and zonal and meridional circulation indexes, which are discussed in details below.

M.A. Petrosyants and D. Hushchina proposed a new modified circulation index, which is similar to O.M. Blinova's index. With the help of this index it is calculated the speed circulation of the zonal real wind component, that reflects the large-scale features of global circulation zone and allows characterizing the features of the atmosphere motion in different latitudinal zones in more details. In this principle, M.A. Petrosyants and D. Hushchina introduced two integrated circulation indexes as integral characteristics of wind fields: 1) zonal circulation velocity vector component along a circle of latitude and 2) the circulation of wind velocity vector of the contour. These indexes are introduced to the study of distant relationships between processes in the tropics and temperate latitudes. These circulation indexes do not carry any information about weather anomalies in the relevant areas, but abnormal circulation of the wind velocity vector can be an indicator of temperature and precipitation anomalies. Despite the attractiveness of this index its further review is beyond the scope of the article.

In the paper the connection between circulation indexes of O.M. Blinova and O.L. Katz (1959) and the Northern Hemisphere circulation types of B.L. Dzerdzyevskiy (Voskresenskaia 2009) is illustrated for the first time. Because the research is (Kononova 2009) performed on output ranks of the first half of the XX century and cannot reflect present changes in circulation conditions, it is interesting to make a similar analysis.

In general, there are several classifications of large-scale atmospheric circulation of the Northern Hemisphere, among which the most famous is Dzerdzyevskiy's synoptic classification of large-scale atmospheric processes (Kononova 2009). These classifications schematize the circulation of the atmosphere, casting small parts of the baric field that simplifies the description of synoptic processes. Methods of statistical cluster analysis are used in the creation of formal classification (Martazinova 2005), which is close in physical meaning to Dzerdzyevskiy's classification. As noted by the authors of the formal classification, part of types and groups of types from synoptic classification of Dzerdzyevskiy is observed quite synchronously with the types from classification, based on formal algorithms for partitioning of observing baric fields on clusters.

Let's remind (Kononova 2009) that in Dzerdzyevskiy's classification the type of large-scale atmospheric circulation for extratropical latitudes of the Northern Hemisphere is determined by the position and nature of main synoptic processes in the lower troposphere, i.e. the movement of southern cyclones and anticyclone trajectories, connected with Arctic invasion. These processes reflect relatively stable in time the geographical position of the altitude baric basins and ridges. So called elementary circulation mechanisms (ECM) differ in number and geographical location of basins and ridges in the middle troposphere pressure field and position of baric surface formation

trajectories. The number of ECM imposed by Dzerdzeyevskiy equals 13. Slight bias of basins and ridges in space and seasons leads the variants of circulation schemes to 41. This set allows any observed state of the atmosphere attributing to a specific type of circulation, so that circulation changes in time are reduced to changes in types (during the day there is only one type). Circulation types form 15 groups that differ at AT 500 level in number and direction of prevailing airflow deviation from purely zonal. Groups are not confined to the seasons.

Calendar of successive changes of ECM for the period of 1899-2008 is represented in (Kononova 2009), and from 2008 till 2014 at www.atmospheric-circulation.ru. Classification and calendar are the most detailed and prolonged compared to other classifications.

Materials and methods of research: The aim of given research is to analyze the interaction between large-scale atmospheric circulation to unfavorable weather conditions in the Northwest Black Sea region which are manifested as strong and very strong winds. The paper uses information from the archives ARMSyn: surface weather maps, maps of baric topography AT-850, AT-500, telegram storm alerts. Research was carried out for the period of cold season (October-March) 2011-2014 in order to exclude squally wind enhancements caused by the development of convection that occurs mainly in warmer months. Therefore, for the review there were taken only cases of graded winds observed in the south of Ukraine; minor intensification of wind was not taken into account.

RESULTS AND ANALYSIS

It is known (Ivus 2014, Savter 2014) that the impact of storm winds is significant for the functioning of the national economic complex of the North-Western Black Sea region. To study this effect there were selected fifty-seven cases of wind strengthening to the criterion of a strong wind $\geq 15 \text{ ms}^{-1}$ and a very strong wind $\geq 25 \text{ ms}^{-1}$ in Odessa region starting from October till March in the period 2011 - 2014.

The main factor of wind speed change in the cold season is a change in the baric gradient. During this period there were recorded 4 cases of strong wind strengthening to 25 ms^{-1} and more on 07.02.2012, 08.02.2012, 12.03.2012 and 23.03.2013. It should be noted that under the influence of storm winds there were only southern parts of the region, especially stations, located on the sea coast and estuaries (Belgorod-Dniesterovsky, Ust-Danube, South Port, Paromna Pereprava). Strong winds have distributed quite unevenly from season to season for years. Thus, in the cold season of 2011-12 years 19 cases of dangerous winds were registered, in 2012-13 years there were 23 cases and in 2013-14 - only 15 cases. Most often strong winds blow from the northeast, north and northwest. These directions are typical for moving of cyclonic vortices from the southwest when in the zone of warm front influence the northeast, and after the passage of a cold front northwest and north winds increase. In contrast to these directions south, southwest and

western winds occur much less frequently. Very strong winds on 07-08.02.2012 had a northeast direction, 23.03.2013 – northwest direction, and 03.12.2012 the direction varied from 120 to 350 degrees.

To determine the nature of macroscale synoptic processes that lead to emergence of storm winds in the North-Western Black Sea region, we will use A.L. Katz's typing (Katz 1959). Calculations were carried out for the first sector of the temperate zone - Atlantic-European, which is between 20° west longitude and 80° east longitude and 35° to 70° north latitude.

According to the formulas (1)-(2) we define the indexes of zonal and meridional circulation and at the ratio of the meridional index to zonal one we get the index of general circulation (formula (3)):

$$I_z = \frac{\sum_1^6 (n_3 - n_c) \cdot b}{6,3,5} \quad (1)$$

where n_3 is the number of intersections of six meridians by isohypses between 35 and 70° North latitude which are directed from west to east; n_c is the number of intersections of meridians, which are directed from East to West; b is the coefficient, equal to 4 gp dam on map AT-500 hPa;

$$I_m = \left[\frac{n_{45} \cdot \frac{1}{\cos 45}}{120} + \frac{n_{55} \cdot \frac{1}{\cos 55}}{120} + \frac{n_{65} \cdot \frac{1}{\cos 65}}{120} + \right] \cdot \frac{b}{3} \quad (2)$$

where n_{45}, n_{55}, n_{65} is the number of intersections of these parallels by isohypses, regardless of their direction;

$$I_{gen} = \frac{I_m}{I_z} \quad (3)$$

where I_m and I_z are indexes of meridional and zonal circulation respectively. If $I_{gen} \geq 0,75$, it is considered to be a meridional circulation.

It is known (Zubkovych 2010) that zonal type of circulation is characterized by latitudinal orientation of isohypses on map AT-500, and meridional (m) type of circulation is divided into four forms: western (W), eastern (E), central (C) and mixed (Mix), which differ from each other significantly in territorial distribution of altitudinal ridges and basins.

As expected, strong wind over the south of Ukraine was marked mainly in the meridional type of atmospheric circulation (77.2%), the zonal type of circulation has

22.8% of all cases. Meridional type of circulation, in turn, is mostly represented by mixed (24.6%) and west (22.8%) forms. Slightly rarely the central (17.5%) and eastern (12.3%) circulation form were observed. All cases of wind strengthening up to 25 ms⁻¹ and more are connected exclusively with meridional circulation of different forms. The number of index ranges from 0.76 to 2.11. So we can assume that the meridional character of atmospheric circulation creates favorable conditions for wind strengthening in the Northwest Black Sea region to the criteria of strong and very strong wind.

Exploring the impact of baric objects on the strong and very strong wind formation, there were highlighted the main types of synoptic situations causing storm conditions in the Northwest Black Sea region (Table 1). Wind increasing up to 25 ms⁻¹ and more during cold seasons of years 2011-13 is connected with the release of southern cyclones. A common feature of the mechanism of southern cyclones occurrence is meridional character of macroscale processes that influence the formation of favorable local cyclogenesis of thermodynamic conditions. It should be noted that all the cases were characterized by extremely close location of Arctic Front system to Polar system that led to increased activity of cyclonic vortices.

Table 1 The frequency of synoptic situations in various forms of atmospheric circulation during the cold period of 2011 – 2014

Type of synoptic situation		Circulation types				
		Zonal	Meridional			
			Western	Central	Eastern	Mixed
1	2	3	4	5	6	
Western cyclone			1		1	
Southern cyclone		5	1	3	2	8
Diving cyclone		4	8		1	1
Zone of interaction	Anticyclone is in the east, the cyclone is in the west	1		5	2	3
	Anticyclone is in the west, a cyclone is in the east		4			2
	Anticyclone is in the north, the cyclone is in the south		2	2	1	

Southern cyclones also conditioned by strong wind (19 cases), and the type of atmospheric circulation was meridional in 14 cases, and in 5 cases it was zonal. Diving cyclones from the Scandinavian area caused wind strengthening to storm values 14 times. Western cyclones moving was accompanied by strong wind only twice. The zone of cyclone and anticyclone interaction of different geographical location also significantly influenced the formation of strong winds. Most often they were blocking anticyclones from the east (11 cases, both Arctic and Siberian anticyclones). In 6 cases there was an opposite picture when anticyclone was located over Western Europe, and

Classification of macrocirculation processes of the northwest Black sea region, which contribute to surface wind strengthening

the cyclone was in the east (mainly over the Volga region) and 5 cases where anticyclone was located in the north and cyclone was in the south. Thus, the peripheral processes are extremely important in storm wind forecasting in the Northwest Black Sea region.

Table 2 The repeatability combination (%) of ECM and subtypes of synoptic processes with indexes of Katz and V_{max} . Cold period of 2011-2014

Type of ECM	Subtypes of synoptic processes											
	5.1		5.2		6.1		6.2		6.3		6.4	
5 a, 5 b							5,3	0,95 m mix 0,91 m mix 1,11 m east 22				
6			3,5	0,76 m west 0,79 m east 16								
8 bz, 8 gz	1,7	0,67 zon 16					3,5	0,48 zon 1,18 m west 18				
11 a, 11 b, 11c, 11 d			3,5	1,64 m mix 2,11 m west zah 26	7,0	1,30 m zm 1,45 mc 1,71 mc 1,13 mc 25	1,7	0,59 zon 20	3,5	0,70 zon 0,97 m mix 22	5,3	1,50 m mix 0,55 zon 0,99 m ц 21
12 a	5,3	1,16 m mix 0,79 m mix 0,65 zon 20			5,3	1,10 m c 1,03 m c 0,99 m mix 20	10,5	1,32 m mix 0,97 m west 1,08 m west 0,98 m west 1,39 m west 22	5,3	0,97 m east 0,75 m east 0,72 zon 20	5,3	0,77 m mix 0,60 zon 0,77 m east 27
12 bz			3,5	1,29 m c 0,55 zon 20	3,5	0,80 m c 0,95 zon 22	1,8	0,76 m mix 25	1,8	0,76 m mix 16		
12 vz			5,3	1,02 m mix 1,05 m msx 0,53 zon 20	1,7	1,16 m west 16	1,8	0,94 m east 22				
13 z	3,5	0,82 m west 1,11 m west 20	7,0	3,01 m c 1,53 m c 1,12 m c 0,74 zon 22			1,8	0,95 m west 21			1,8	2,85 m mix 22

Note: each cell on the left indicates repeatability (%), on the right – Katz’s circulation index and value V_{max} , m s⁻¹ (below).

Table 2 shows all the cases of strong wind, observed in southern Ukraine during the cold season of 2011-2014, in the corresponding group of circulation conditions according to Katz, Dzerdzeyevskiy or classification of synoptic processes developed at the Department of Meteorology and Climatology OSEU (Kononova 2009, Martazinova 2005, Rossby 1939).

Strong wind is generally formed during synoptic processes assigned to 5 and 6 type of classification. Type 5 is peripheral atmospheric processes of atmospheric fronts. Subtype 5.1 is eastern and western transfer on the eastern-southeastern periphery of the anticyclone. Wind speed increases under the influence of the Black Sea depression and storm zone ($\partial P / \partial n \geq 3,5$ hPa / 111 km) from the front. Subtype 5.2 - east and southeast transfer occurs on the south-southwestern periphery of anticyclone during the passing of arctic or polar fronts; in the area of high pressure gradients without fronts or if there is a vague front. Type 6 is cyclonic circulation with high pressure gradient ($\partial P / \partial n \geq 2,5$ hPa / 111 km). Subtype 6.1 is eastern part of cyclone or storm zone between cyclone in the west, northwest and anticyclone in the east.

Subtype 6.2 is the type of cyclone that moves with speed ≥ 40 km h⁻¹. Subtype 6.3 is a basin with fronts, and subtype 6.4 is a southern cyclone, carrying out air masses transfer from the south. However, in its northern part it may be occurred a wind of northern and south-eastern directions, in the center of cyclone (with fronts) wind may be of all directions, including the north-eastern. Strong and very strong wind over the south of Ukraine is marked by 6 types (13 subtypes) and 2 types (6 subtypes) of ECM of the department classification. According to Table 2 the greatest repeatability of strong wind (10.5%) has a combination of ECM 12a and subtype 6.2 in the meridional type of Katz's circulation. ECM 12a provides 18 of 57 examined cases, including maximal wind speed (27 ms⁻¹) in the region on 12.03.2012, when 11 regional stations fixed the speed ≥ 20 ms⁻¹. The wind direction changed in the investigated area on stations from 170 ° (South Port) to 350 ° (Bolhrad); the atmospheric front passed with waves (subtype 6.4). Also, strong wind was often observed at ECM 13z, mainly in the meridional processes while south cyclones were moving.

Let's consider one of the typical synoptic situations, which was formed by type ECM-11 and subtypes 5.2, 6.1. Thus, on the 26-29 of January, 2014 (Fig. 1) unfavorable weather conditions in the Azov-Black Sea basin and adjacent areas were predetermined by interaction of the north-western anticyclone ridge with maximal pressure 1053 hPa that shifted from the Baltic sea region to Moscow and southern cyclone basin with minimal pressure 997 hPa, which emerged on the wave of polar front over Italy and shifted to the east of the Black sea.

Pressure drop in front of the cyclone along the coast of Turkey was insignificant (1,1-1,6 hPa / 3h), pressure increasing in the rear part near the Dardanelles Strait reached 6.7 hPa / 3h according to 09 (11)h on 29.01.2014.

Altitude cyclone outlined by one enclosed isohypse 132 dam over the northern regions of the Aegean Sea corresponded to surface cyclone on the map AT-850, on the

map AT-700 it was high-altitude basin, which axis was focused from the British Isles through central Europe to the Balkans. Geopotential gradients of altitude frontal zone over the Sea of Azov on the map CS 500/1000 was about 8-10 dam / 1000 km.

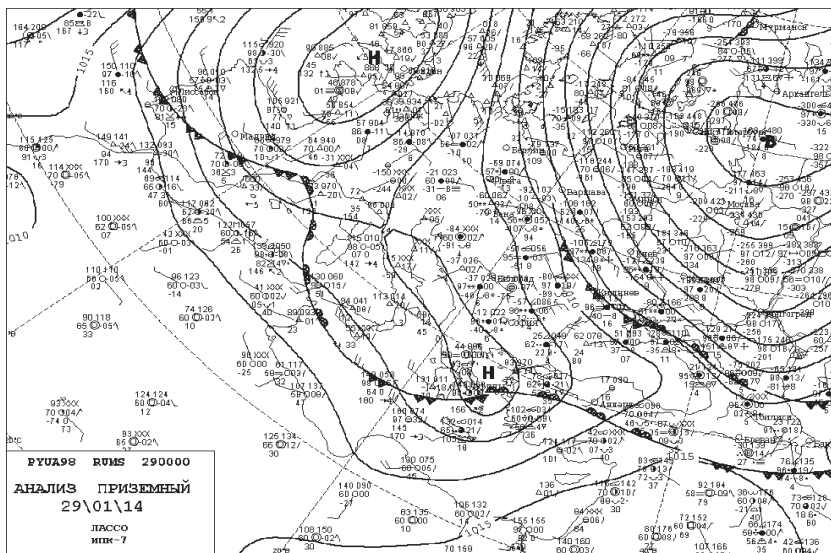


Fig.1. Surface analysis for 01.29.2014, 00 UTC

In front of the cyclone advection of heat from the eastern Mediterranean Sea held in the south-eastern regions of the Black Sea, air temperature of the Turkish and Caucasian Black Sea coast at 18 (20) hours on the 29 of Jan. was 14-18 ° C, while above the Sea of Azov it decreased to 9 ... 14 ° C. Cyclone shifted from the Sea of Marmara on the eastern regions of the Black Sea per day, the pressure at the center grew to 1010 hPa. The presence of a blocking anticyclone supported significant thermal and baric (about 5 hPa / 111 km) gradients near the Earth's surface above the Sea of Azov, which contributed to the northeastern wind strengthening to the criteria of natural hydrometeorological phenomena. In the water area of the seas wind speed reached 15-24 ms⁻¹, in Heniches, Berdyansk and Mariupol it was 25-28 ms⁻¹. The combination of strong wind with snow led to strong blizzard. Wind strengthening was accompanied by dangerous icy and wind-surge phenomena, quick icing of ships (Ivus 2014). OHSS caused damage to the ports and maritime industry enterprises located on the Azov Sea coast, cargo operations and shipping were terminated, power lines were damaged (Ivus 2014).

CONCLUSIONS

As a result of research of features of macrocirculation processes structure in the troposphere over Ukraine using Katz's circulation index, circulation classification

mechanisms by B.L. Dzerdzeyevskiy and synoptic processes typing revealed the following:

1. In the study of formation conditions of a strong wind in the cold season in the south of Ukraine it was found that strong and very strong winds often occur in southern and central regions, particularly in stations located on the shores of the seas and estuaries (Belgorod-Dniestrovskiy, Ust-Dunaysk, South Port, Paromna Pereprava).
2. Meridional nature of atmospheric circulation (77.2%) creates favorable conditions for wind strengthening in the Northwest Black Sea region to the criterion of strong and very strong, the zonal type of circulation has 22.8% of the total amount. Meridional circulation type is mainly represented by mixed (24.6%) and western (22.8%) forms according to Katz's typing.
3. There were identified the main types of synoptic situations (Ivus 2012, Katz 1959) of the department typing which caused strong winds. Often strong wind occurred during the moving of cyclonic vortices from the south (type ECM 12a, 13z) and in the area of interaction between cyclones and anticyclones. All these four cases of the wind strengthening to the criterion of very strong are connected with the southern cyclones movement.

The conclusions have a preliminary character and need confirmation on more volumetric statistical material.

REFERENCES

- Bagrov N.A. 1973, On some issues of tax collection for the image, Proceedings of the HMC USSR. – Vol. 106., pp. 78-104. (Bagrov N. A. O nekotorykh voprosakh vzyiskaniya naloga dlya dannogo obraza //Trudy GMTS SSSR. – 1973.) (In Russian)
- Gruza G.V., Rankova E.L., Oesterle G.R. 1976, Scheme of adaptive statistical forecast by the usage of the group analogue, Proceedings VNIGMI- IDC. - Vol. 13., pp. 5-25 (Gruza G. V., Ran'kova E. L., Esterle G. R. Skhema adaptivnogo statisticheskogo prognoza s ispol'zovaniyem gruppy analogova. Trudy VNIGMI-MTSD. – 1976. – Vyp. 13.) (In Russian)
- Ivus G.P. 2012, Specialized weather forecasts, tutorial, Odessa: TPP. - 407 p. (Ivus H. P. Spetsializovani prohnozy pohody: pidruchn. [dlya stud. vyshch. navch. zakl.] // Odesa: TES, 2012. – 407 s.) (in Russian)
- Ivus G.P. 2014, Conditions of formation of dangerous wind zones on the territory of Ukraine / G.P. Ivus, S.O. Zubkovych, G.V. Khomenko, I. Kovallkov // European Applied Science, Europaische Fachhochsschule. – 2014. – Ed.10. – P. 59-64.
- Ivus G.P. 2015 To the question about typification of synoptic processed over territory of Ukraine / G.P. Ivus, S.O. Zubkovych, E.V. Aqayar, L.M. Gurskaya // International Journal of Research In Earth and Environmental Sciences. - 2015. – Vol. 03. - № 1. – P. 21-27.
- Katz A.L. 1959, Index as an indicator of the zonal circulation and meredional synoptic processes, Meteorology and Hydrology. - 1959. –Vol. 5. - pp. 3-8. (Katz A. L. Indeks tsirkulyatsii kak pokazatel' zonal'nykh i meredional'nykh sinopticheskikh protsessov // Meteorologiya i gidrologiya. – 1959. – № 5. – S. 3-8.) (in Russian)

- Klimenko L.V. 1976, Synoptical-climatic typisation of atmospheric processes and its catalog, M: Moscow State University. M.V. Lomonosov, – 106 p. (Klimenko L. V. Sinoptiko-klimaticheskaya tipizatsiya atmosferykh protsessov i yeyo katalog // M: MGU im. M. V. Lomonosova, – 1976. – 106 s.) (in Russian)
- Kononova N.K., 2009, Classification circulation mechanisms of the Northern Hemisphere by Dzerdzeevski B.L. model , AB Shmakin A.B. (Ed.), Russian Academy of Sciences, Institute of Geography. - M.: Voentehinizdat, 2009. - 372 p. (Kononova N. K. Klassifikatsiya tsirkulyatsionnykh mekhanizmov Severnogo polushariya po B. L. Dzerdzeyevskomu //otv. red. A. B. Shmakin, Rossiyskaya akad. nauk, In-t geografii. – M.: Voyentekhnizdat, 2009. – 372 s.)
- Martazinova V. 2005, The Classification of Synoptic Patterns by Metod of Analog , J. Environ. Sci. Eng. – 2005. – 7. – pp. 61-65.
- Martazinova V., Ivanova E. 2004, Long-range weather forecasting in the Ukraine, 3rd European Conference on Application of Meteorology. – Th. AGU Fall Meeting. – San-Francisco. – pp. 267 - 268.
- Rosby C.-G. et al. 1939, Relations between variations in the intensity on the zonal circulation of the atmosphere and the displacements of the semipermanent centers of action. – J. Mar. Res. – 1939. – Vol. 2. – P. 38-55.
- Savter L.A. 2014, Natural meteorological phenomena that were observed in the Black and Azov seas in 2014. /L.A. Savter // Journal of Hydrometeorological Center of Azov and the Black sea. - 2014. - №2 (17). - p.13-16. (in Ukrainian)
- Vasiukov S.A., Zverev N.I., Ped D.A. 1962, Forecast of synoptic processes for the current period by usage of the analogue, Meteorology and Hydrology. - Vol. 1., pp. 27-33. (Vasyukov S. A., Zverev N. I., Ped' D. A. Prognoz sinopticheskikh protsessov na tekushchiy period s pomoshch'yu analoga // Meteorologiya i gidrologiya. – 1962. // – № 1) (In Russian)
- Voskresenskaia E.N. 2009, Classification of synoptic processes storms in the Azov-Black Sea basin of /E.N. Resurrection, VA Naumova, MP Evstigneev, VP Evstigneev // Tr. UkrNIGMI, 2009. -. 258. - S. 189 - 200. Klassifikatsiya sinopticheskikh protsessov shtormov v Azovo - Chernomorskom baseyne /Ye.N . Voskresenskaya , V.A. Naumova , M.P. Yevstigneyev , V.P. // Yevstigneyev Tr . UkrNIGMI , 2009. - Vip . 258. - S. 189 – 200 (in Russian)
- Zubkovych S. A. 2010, Typization of the synoptic processes over Eastern Ukraine, Ukrainian Hydrometeorological Journal, 2010. - Vol. 7. – pp. 103-108. (Zubkovych S. A. Tipizatsiya sinopticheskikh protsessov nad Vostochnoy Ukrainoy // Ukrainskiy gidrometeorologichniy zhurnal, 2010. – Vyp. 7) (in Russian)



Assessment of water losses from Badovc Lake, Kosovo: Isotopic implications

Skender Bublaku^{1*}, Arjan Beqiraj²

¹Faculty of Civil Engineering and Architectura, Department of Hydrotechnic, Bregu i Diellit Str, Prishtine, Kosove

²Faculty of Geology and Mining, Elbasani Str, Tirana, Albania

Abstract: This paper aims to quantitatively assess water losses of Badovc Lake – Kosovo based on both water balance of the lake and water isotopic composition of H-2 and O-18. According to lake water balance, a water loss of 3,738,905 m³ for the hydrologic year 2014, was evaluated. These consistent data favour the opinion that a continuous groundwater outflow from the lake is present and it is conditioned by the intensively developed fracture system in the lake basement formations. This was also supported by the isotopic analysis (H-2 and O-18) of the sampled waters. Most of water samples taken from hydrologic components of Lake Badovc fall on a linear plot of $\delta^2\text{H}$ versus $\delta^{18}\text{O}$ showing an isotopic variation typical for waters evaporated from a lake and fits very well with Global Meteoric Water Line (GMWL), while two rain water samples are isotopically lighter (more negative δ values). Water samples taken from water leakages on the right side of the dam, the piezometer, two wells drilled in the valley downstream of dam, Hajvalia mine gallery and the water flow downstream of the dam, have isotopic composition similar with that of the lake water. Water of Hajvalia mine well shows isotopic composition that falls between that of rain water and lake water. Considering δ values of rain water ($\delta^2\text{H} = -129.6\text{‰}$, $\delta^{18}\text{O} = -16.56\text{‰}$) and lake water ($\delta^2\text{H} = -67.2\text{‰}$, $\delta^{18}\text{O} = -9.20\text{‰}$) and mine water (mixture) ($\delta^2\text{H} = -73.3\text{‰}$, $\delta^{18}\text{O} = -10.15\text{‰}$) was found that the fraction of rain water in mine water ranges from 6% (according H-2) to 10% (according O-18), while the fraction of lake water in mine water varies from 94% (according H-2) to 90% (according O-18).

Keywords: isotopic composition, isotopic mass balance, rainfall, lake water balance, water loss.

* s_bublaku@yahoo.com; arjan.beqiraj@fgjm.edu.al

1. INTRODUCTION

Badovc Lake, that is built in 1965 along the course flow of Gračanca river, represents the main source for drinking water supply of Prishtina city. Its watershed consists of limestone, terrigenous formations (ophiolitic melange, sandstone, siltstone, mudstone), magmatic (gabbro-diabase, andesite, peridotite) and metamorphic (quartz-mica schist, chlorite schist, sericite schist, phyllite, gneiss, marble) rocks (Elezaj and Kodra, 2008). The geological formation where the dam is located is mostly composed of altered and fissured serpentinites. Water inflow in the lake for 2014 was 22,334,517 m³ (table. 1) and it comprises (i) river flow to the Lake (V_s), (ii) volume of runoff from the catchment (V_R), (iii) volume of direct precipitation on the lake (V_p) and groundwater inflow (V_{GI}). A water volume of 700,000 m³ was transferred from another lake to Badovc lake in April 2014 because of the water lack in this later and this quantity of water was considered as an additional inflow component in the lake water balance. Water outflow from the lake comprises (i) evaporation from the lake surface (V_e), water abstraction (V_A) and infiltration of water from the lake bottom (V_{GO}). The total volume of water outflow from the lake over the hydrologic year 2014 was 11,295,420 m³ (table. 1). A difference of 3,738,905 m³ water in the lake water balance for the year 2014, between inflows and outflows, was attributed to water losses from the Lake (*Bublaku and Beqiraj, 2014, 2015*). Most of loosed water from the lake was drained to Hajvalia mine voids as confirmed by the data of isotopic (H-2 and O-18) composition of water sampled. In fact, water of Hajvalia mine well shows isotopic composition that falls between that of rain water and lake water on the linear plot of $\delta^2\text{H}$ versus $\delta^{18}\text{O}$. In this case, the isotopic composition of the mixture (mine water) of various proportions of the two waters (rain and lake) will lie on the straight line connecting the δ values of the two waters and is determined by isotope mass balance (*Cook and Herczeg, 2000*):

$$\delta_1 n_1 + \delta_2 n_2 + \delta_3 n_3 \dots = \delta_f (n_1 + n_2 + n_3 \dots)$$

where δ_1 is the δ value of component 1, n_1 equals the amount of substance in component 1, and δ_f is the δ value of the product. Rain water has $\delta^2\text{H} = -129.6\text{‰}$ and $\delta^{18}\text{O} = -16.56\text{‰}$ while lake water has $\delta^2\text{H} = -67.2\text{‰}$ and $\delta^{18}\text{O} = -9.20\text{‰}$. Water of mine (mixture) has $\delta^2\text{H} = -73.3\text{‰}$ and $\delta^{18}\text{O} = -10.15\text{‰}$. By knowing the isotopic composition of two waters that are mixed, was found that the fraction of rain water in mine water ranges from 6% (according H-2) to 10% (according O-18), while the fraction of lake water in mine water varies from 94% (according H-2) to 90% (according O-18).

2. MATERIALS AND METHODS

A digital Hydrographic Echo Sounding HydroBox2010 device, with measuring frequency every 5 sec, was used for generating bathymetric data which were then interpolated

by the Arc-GIS for the construction of the Lake bathymetry. In 2013 four manual rain gauge with diameter 250mm have been installed for a daily monitoring of the rainfall in the basin. A continuous geodesic survey was applied for the monitoring of water level variations in the lake. The evaluation of the rivers flow was made across hydrometric regular profiles, where the water speed was measured with Flowatch-JDC instrument. The daily abstraction of water from the lake was provided by water supplier of Prishtina. Measurement of evaporation is made with a standard evaporation pan located close to lake. Calculation of the annual water budget components is made through direct measurements and calculations. The precipitation on the lake (V_p) is calculated from measurements rain gauge located near the lake. Amount of water surface runoff from the catchment (V_R) is calculated based on the determination runoff coefficient by measurements stream flow to the lake. Stream flow to the lake (V_s) is calculated by flows measurements in three independent perennial tributary rivers that flew into the lake. Abstraction of water from the lake (V_A) is calculated by daily amount abstraction water provided by water supplier of Prishtina. Water evaporated from the lake surface (V_E) was calculated using Penman equation (Penman, 1948) and the results were compared with values obtained using Meyer equation (Show, 2005). Changes in the water volume of Lake (ΔV) are calculated based on the fluctuations of water level in the Lake which, in turn, are a function of the balance between precipitation on the lake, runoff to the lake, evaporation, abstraction and groundwater outflow from the lake.

25 water samples were taken for isotopic analysis of H-2 and O-18 (Fig. 2). Water was filled in 50 ml, double capped, polyethylene bottle directly from the water source, without any sample filtration or preservation. Isotopic analysis of H-2 and O-18 are made at the Chemical-physical Laboratory of Institute of Geosciences and Georesources, Pisa, Italy. Deuterium was directly measured in the vapour phase of the water molecule, the instrument use was Liquid Water Isotope Analyzer (LWIA) produced by Los Gatos Research (LGR) which is based on technic of cavity ringdown spectroscopy (CRDS). Standard di riferimento: SMOW (*Standard Mean Ocean Water*) (Craig, 1961).

Oxygen-18 was determined through isotopic equilibration of water with CO_2 at $25^\circ C$ and isotopic analysis of CO_2 by mass spectrometer type MAT 252 produced by Finnigan. Standard di riferimento: SMOW (Standard Mean Ocean Water) (Craig, 1961).

3. GEOLOGICAL OVERVIEW

Badovc basin belongs to Vardar zone which represents the boundary between Drino-Ivanica (as peripheral part of Dinaride zone) and Serbia-Macedonian massif (*Elezaj and Kodra, 2008*). It consists of limestone, terrigenous formations (ophiolitic melange, sandstone, siltstone, mudstone), magmatic (gabbro-diabase, andesite, peridotite) and metamorphic (quartz-mica schist, chlorite schist, sericite schist, phyllite, gneiss, marble) rocks (fig.1). Serpentinities, which are the most spread formations at the dam

zone, occurs as irregular lenses with dimensions that range from several meters to some kilometers. Serpentinities have schist and/or netting structure and are intensively fractured where cracks and cleavages are filled with calcedone, opal, carbonate and argyle. The presence of an almost vertical tectonic zone (*Institute for Hydro-economy "Jarosllav Çerni", 1982*) in the dam profile complicates the situation of water drainage from Lake toward underground waters. Serpentine formations are separated in several big blocks due to tectonic faults and gabbro intrusions. The tectonization of serpentinites was probably caused by orogenic movements and Miocene vulcanization in this region (*Hyseni, 2000*). Tectonic faults are mainly overthrust type but there are also some strike slips. The complex geological construction of catchment area determined formation of several aquifer types (*KPMM, 2006*).

Low-permeable fissured aquifer – It is related with metamorphic schists, serpentinites, gabbros, diabases and is mainly charged by rainfalls and discharges through springs with yield under 1.0 l/s, which emerge through weak tectonic zones. Accumulation of underground water in these rocks is controlled by the development of fissure system which has conditioned a high variation of spring yields that ranges from 0.01 l/s to 1.0 l/s.

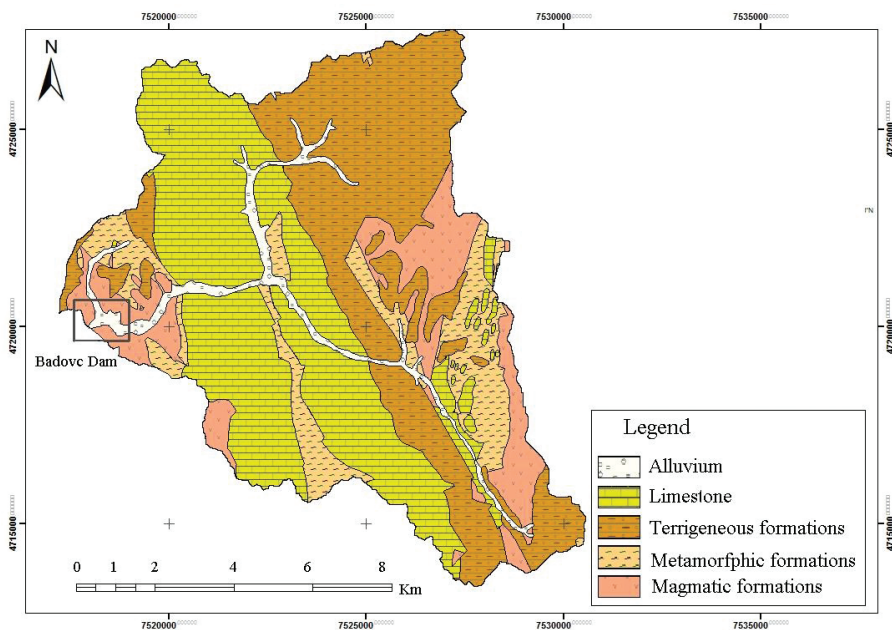


Fig. 1. Geological map of Badovc basin, scale 1:100.000 (KPMM-2006)

Karst aquifer – it is related with limestone which present an important aquifer. Springs that emerge from these rocks have yields over 1.0 l/s.

Porous aquifer – it is related with alluvial formations which present the most important aquifer of the basin. Its thickness ranges from 3 to 7m. This aquifer is mainly developed through river valleys. Water yields of wells opened in these formations ranges from 2 to 10 l/s.

4. LAKE WATER BALANCE

The water balance equations are based on the premise that the difference between water inflow and water outflow over a given time period for the hydrologic system of a lake must equal to the change in water storage in that system (*Gebreslase, Hagos and Samuel, 2012; Radwan, 2009*). All of lake's water gains and losses and the corresponding changes in the measured lake level over the same period are taken into account in order to compute the lake water budget, as it appears in the following equation (*Gebreslase et al., 2012*):

$$\Delta V = (V_P + V_R + V_S + V_{GI}) - (V_A + V_E + V_{GO})$$

where:

ΔV = change in lake volume (m³)

V_P = precipitation on the lake (m³)

V_R = surface runoff from the catchment (m³)

V_S = stream flow to the lake (m³)

V_{GI} = groundwater inflow to the lake (m³)

V_A = abstraction from the lake (m³)

V_E = water evaporation from the lake (m³)

V_{GO} = groundwater outflow from the lake (m³)

Data collection of the water balance components of the lake was carried out for 365 days. The results of Badovc lake water balance in 2014 showed that inflow volume into the Lake was 22,334,517 m³, while outflow volume from the lake was 11,295,420 m³. As it can be seen in (table. 1), where level and volume variations during 2014 are shown, the volume change during 2014 was 7,341,000 m³ which is 3,698,097 m³ less than the difference (11,039,097 m³) between inflow and outflow water volumes (table 1).

Water inflow in the lake for 2014 was 22,334,517 m³ (table. 1) and it comprises (i) river flow to the Lake (V_S), (ii) volume of runoff from the catchment (V_R), (iii) volume of direct precipitation on the lake (V_P) and groundwater inflow (V_{GI}). A water volume of 700,000 m³ was transferred from another lake to Badovc lake in April 2014 because of the water lack in this later and this quantity of water was considered as an additional inflow component in the lake water balance. The water outflow from the lake comprises (i) evaporation from the lake surface (V_E), water abstraction (V_A) and infiltration of water from the lake bottom (V_{GO}). The total volume of water outflow from the lake over the hydrologic year 2014 was 11,295,420 m³ (table. 1).

Table 1: Monthly and annual water balance for the Badovc Lake, year 2014

Month	Level (m.a.s.l)	Inflow (m ³)	Outflow (m ³)	Volum change in the lake (m ³)	Inflow-Outflow (m ³)	Groundwater outflow (losses) (m ³)
	0	1	2	4	5=(1)-(2)	(4)-(5)
January	636.65	392,622	754,602	-412,000	-361,980	-50,020
February	636.10	345,455	715,546	-422,000	-370,091	-51,909
March	635.83	791,971	771,313	-213,000	20,658	-233,658
April	641.50	7,071,817	778,195	5,834,000	6,293,622	-459,622
May	645.45	6,691,739	961,415	5,087,000	5,730,324	-643,324
June	645.26	1,308,136	1,069,970	-360,000	238,166	-598,166
July	644.77	788,884	1,119,282	-567,000	-330,398	-236,602
August	644.00	421,489	1,101,856	-1,084,000	-680,367	-403,633
September	643.50	724,771	1,031,265	-650,000	-306,494	-343,506
October	643.25	758,906	1,019,451	-678,000	-260,545	-417,455
November	643.27	1,587,383	973,002	487,000	614,381	-127,381
December	643.60	1,451,344	999,523	319,000	451,821	-132,821
Annual		22,334,517	11,295,420	7,341,000	11,039,097	-3,698,097

5. WATER LOOSES

The results of Badovc lake water balance in 2014 have shown a difference in water volume of 3,698,097 m³ between inflow and outflow into the Lake. This amount represents about 17% of annual inflow into the Lake for 2014, and is considered as water loss from Lake and can be attributed to groundwater outflow due to water infiltration through cracks and tectonic zones that involved geological formations of the lake bottom and beneath the dam. Near the Lake there are three mines, but Hajvalia mine is the nearest one and a possible hydraulic communication between lake and this mine can be assumed. In fact, a raise of 114 m of water level in abandoned Hajvalia mine was registered by the measurements performed from 2004 to 2014 (*Hajvalia Mine, 2014*). Assuming that the whole infiltrated rainfall water drained downward as groundwater prior to mine operation, we can consider that the above mine watering was related with groundwater outflow from the Lake. This can also be supported by the fact that no consolidation measures of the formations beneath the dam were undertaken during the closure of the lake. In order to confirm this opinion, the data of isotopic analysis from several hydrological water components of the Badovc watershed were confronted (Table 2).

6. ASSESSMENT OF WATER LOSSES FROM THE LAKE BY USING ISOTOPIC COMPOSITION OF H-2 AND O-18 IN WATER

Stable isotopes have been among the most used techniques for solving problems of age, origin especially of pathways of the water movement in a watershed (*Michener and Lajtha, 2007*). Stable isotopes of water (hydrogen (^2H or D for Deuterium) and oxygen (^{18}O) have been used since the pioneering work of (*Craig, 1961*). Unlike applied tracers, stable isotopes are added naturally at the watershed scale by rain and snowmelt events. These environmental isotopes can be used to trace and identify different air and water masses contributing precipitation to a watershed since the stable isotope composition of water changes only through mixing and well-known fractionation processes that occur during evaporation and condensation (*Michener and Lajtha, 2007*). Once in the subsurface, and away from evaporative effects, the stable isotopes of water are conservative in their mixing relationships. This means that isotopic composition of the mixture of two water sources will fall on a straight line and its position is dependent only on the proportions of the two sources (*Michener and Lajtha, 2007*). ^2H and ^{18}O , the elemental basis for H_2O molecules, are ideal tracers because they behave exactly as water would as it undergoes transport through a watershed. Oxygen – 18 and deuterium occurs in water at abundances of 0.204% of all oxygen atoms and 0.015% of all hydrogen atoms, respectively (*Clark and Fritz, 1997*). These relative abundances change slightly as a result of thermodynamic reactions that fractionate or partition atoms of different mass (isotopes). Isotopic fractionation is strongly temperature dependent such that it is greater at low temperature (*Majoube, 1971*). Under equilibrium conditions, the heavy isotopes are always enriched in the more condensed phases because they have lower rates of evaporation, i.e. lower rates of diffusion across the water-atmosphere layer (*Gat, 1996; Kendall and Caldwell, 1998; Mook, 2000*).

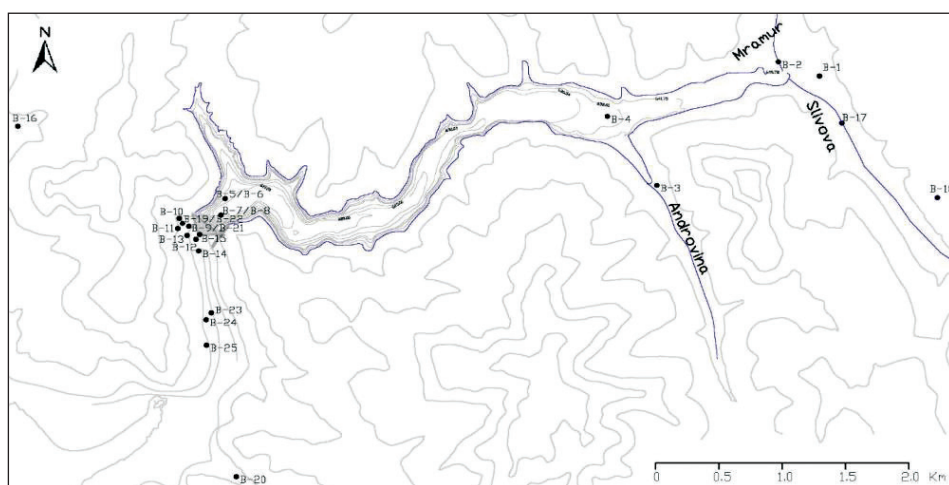


Fig. 2- Topographic map of the Badovc basin where sampling points are shown

Table 2. Isotopic composition of Oxygen-18 and Deuterium of Badovc water

No. Sample	Location	Oxygen-18	Deuterium
		(V-SMOW)	(V-SMOW)
B-1	River Mramor	-9.73	-68.1
B-2	River Slivovë	-10.15	-71.9
B-3	River Androvinë	-9.83	-68.6
B-4	Lake	-9.37	-67.9
B-5	Lake	-9.2	-67.2
B-6	Lake	-9.3	-67.3
B-7	Lake	-9.35	-67.6
B-8	Lake	-9.23	-66.9
B-9	Upper leakage	-8.85	-65.4
B-10	Lower leakage	-9.07	-66.5
B-11	Stream	-8.47	-63.3
B-12	Well no. 1	-8.7	-63.8
B-13	Gallery of Hajvali	-8.85	-64
B-14	Well no. 2	-8.78	-63.5
B-15	Pellg nën dige	-8.17	-60.2
B-16	Hajvalia well	-10.15	-73.3
B-17	Rain water	-16.56	-129.6
B-18	Rain water	-16.12	-129.1
B-19	Piezometer	-8.65	-63.6
B-20	Mine Kishnice	-9.97	-71.5
B-21	Lower leakage	-9.02	-65.4
B-22	Piezometer	-8.9	-65.7
B-23	Spring	-8.66	-64.6
B-24	Spring	-8.7	-65.1
B-25	Water flow downstream of the dam	-8.7	-64.2

Most of water samples taken from hydrologic components of Lake Badovc (fig. 2) show an isotopic variation typical for waters evaporated from a lake and fits very well with Global Meteoric Water Line (GMWL) (*Craig, 1961*) (Table 2; Fig. 3). Two rain water samples are isotopically lighter (more negative δ values) and fall below the GMWL being compatible with a high quota lake or with evaporated clouds.

Lake water shows uniform isotopic composition. Water samples fallen within blue circle have isotopic composition similar with that of the lake water that means these waters are derived from the lake (Fig. 4). Water of Hajvalia mine well shows isotopic composition that falls between that of rain water and lake water.

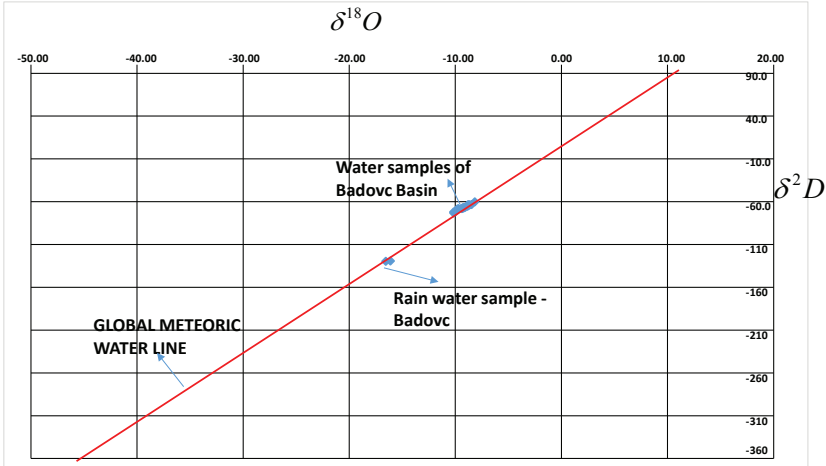


Fig. 3. Isotopic composition of sampled waters confronted with Global Meteoric Waters

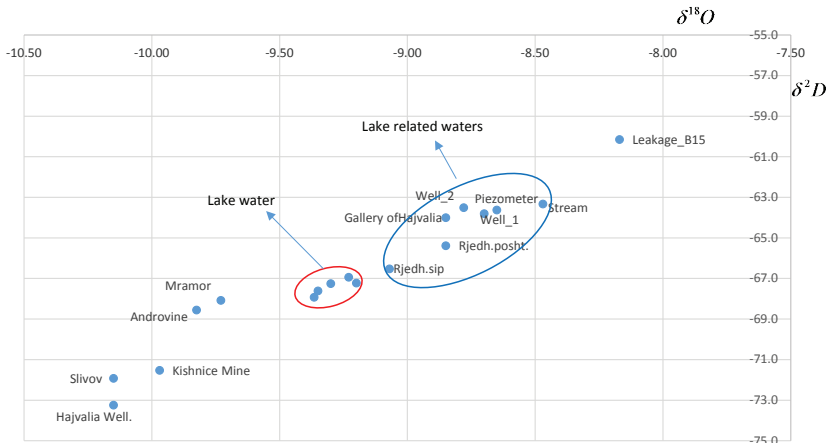


Fig. 4. Variation of δ^2D versus $\delta^{18}O$ for sampled waters

The isotopic composition of substances formed by combining two or more components with different isotopic compositions is additive, and is determined by isotope mass balance (Cook and Herczeg, 2000)(equation 1)

$$\delta_1 n_1 + \delta_2 n_2 + \delta_3 n_3 \dots = \delta_f (n_1 + n_2 + n_3 \dots) \quad (1)$$

where δ_i is the δ value of component 1, n_i equals the amount of substance in component 1, and δ_f is the δ value of the product. In our case, rain water and lake water represent two end members, while the final component is represented by Hajvalia mine water. Because all the samples fall on a linear plot of δ^2H versus $\delta^{18}O$, the isotopic composition of the

mixture of various proportions of the two waters will lie on the straight line connecting the δ values of the two waters. Rain water has $\delta^2\text{H} = -129.6\text{‰}$ and $\delta^{18}\text{O} = -16.56\text{‰}$ while lake water has $\delta^2\text{H} = -67.2\text{‰}$ and $\delta^{18}\text{O} = -9.20\text{‰}$. Water of mine (mixture) has $\delta^2\text{H} = -73.3\text{‰}$ and $\delta^{18}\text{O} = -10.15\text{‰}$. By knowing the isotopic composition of two waters that are mixed, one can determine the fraction derived from each component. Fractions of rain water and lake water in this mixture are determined by equation 2:

$$n_{rain} \delta_{rain} + n_{lake} \delta_{lake} = n_{min} \delta_{min} \dots\dots\dots (2)$$

$$(-129.6)n_{rain} + (-16.56)n_{lake} = (-73.3)(n_{rain} + n_{lake}) \quad \text{for deuterium}$$

and

$$(-16.56)n_{rain} + (-9.20)n_{lake} = (-10.15)(n_{rain} + n_{lake}) \quad \text{for oxygen 18}$$

Because we have only two end members, it is true the equation

$$n_{rain} + n_{lake} = n_{min} = 1 \dots\dots\dots (3)$$

By solving the above equations was found that the fraction of rain water in mine water ranges from 6% (according H-2) to 10% (according O-18), while the fraction of lake water in mine water varies from 94% (according H-2) to 90% (according O-18). The deviation between two estimates (H-2 and O-18) is only 4% which is lower than the range of acceptable values (5-10%) (*Cook and Herczeg, 2000*).

7. CONCLUSIONS

A difference in water volume of 3,698,097m³ between inflow and outflow into the Badovc Lake resulted by its water balance for the year 2014. This water volume is considered as water loss from Lake and can be attributed to groundwater outflow due to water infiltration through cracks and tectonic zones that involved geological formations of the lake bottom and beneath the dam. Hajvalia mine is the nearest one and a possible hydraulic communication between lake and this mine was assumed and this was confirmed by isotopic data of oxygen 18 and deuterium. Water of Hajvalia mine has isotopic composition that falls between that of rain water and lake water, showing that its water represents a mixture of rain water and lake water. The fraction of rain water and lake water in the water of Hajvalia mine ranges from 6% (according H-2) to 10% (according O-18), and from 94% (according H-2) to 90% (according O-18), respectively.

REFERENCES

- Bublaku S, Beqiraj A, 2015 Water balance and water loss implications in Badovc lake, Kosovo. *Journal of Geography and Earth Sciences*, Available online at:
<http://jgesnet.com/vol-3-no-1-june-2015-abstract-5-jges>
- Bublaku S, Beqiraj A, 2015 Assessment of Water Losses from Badovc Lake, Kosovo: Hydrochemical Implications, *Journal of Environmental Science and Engineering A1* (2015), Available online at:
<http://www.davidpublisher.org/index.php/Home/Article/index?id=13862.html>
- Bublaku, S, Beqiraj A. 2014. Preliminary indications on the factors influencing the unexpected water level lowering at Badovc Lake, Kosovo, *Proceedings of CBGA2014*, Eds. Beqiraj A., Ionescu C, Christofides G..., Vol. 2, p. 106., Tirana, Albania.
- Cook P. G. and Herczeg A. L., 2000. *Environmental tracers in subsurface hydrology*. Springer Science + Business Media New York. 534 p.
- Clark I.D dhe Fritz P., 1997. *Environmental Isotopes in Hydrogeology*. Lewis Publishers, Boca Raton, Fl.
- Craig H., 1961. Standards for reporting concentrations of deuterium and oxygen-18 in natural waters - *Science*, 133, 1833-1834
- Elezaj Z., Kodra A. 2008. *Geology of Kosovo*, 213p, University of Pristina.
- Gat J.R., 1996. Oxygen and hydrogen isotopes in the hydrologic cycle. *Annual Review of Earth and Planetary Sciences*, 24, 225-262.
- Gebreslase M. SH., Hagos Y. E. and Samuel, G., 2012. *Lake Water Balance*, Lambert Academic Publishing, Saabrucken, Germany, pp.8-88.
- Hajvalia Mine, 2014. Data from the diary on measuring of water level in the mine of Hajvalia, Trepça Mining, Mitrovicë, Kosovo.
- Hyseni S., 2000. *Metalogenic mineralization features field mine "Hajvali-Badovc-Kizhnicë"*, (Dissertation), Tirane
- Institute of Hydro-Economy "Jarosllav Černi", 1982. Book 1. Characteristics of water resources, note 1 *Geology and Hydrogeology*, page 25-26.
- Independent Commission for Mines and Minerals (ICMM) 2006: *Geological map (1:200.000)*, Prishtinë.
- Kendall C. dhe McDonnell J.J., 1998. *Isotope tracers in catchment hydrology*. Elsevier, Amsterdam.
- Majoube M., 1971. Fraccionnement en Oxygène – 18 et en deutérium entre l'eau et sa vapeur. *Journal of Chemical Physics*, 197, 1423 – 1436.
- Michener R and Lajtha K., 2007. *Stable isotopes in ecology and environmental sciences*. Blackwell Publishing LTD, USA. 566 pp.
- Mook W.G., 2000. *Environmental isotopes in the hydrological cycle: Principles and Applications*. International Atomic Energy Agency, Vienna.
- Penman HL 1948, Natural evaporation from open water, bare soil and grass, *Proc R Soc Math Phys Sci* 193(1032):120–145, London, U.K.
- Radwan G. A., 2009. Using Hydrological and Meteorological Data for Computing the Water Budget in lake Qarum, Egypt. *National Institute of Oceanography and Fisheries, Egypt*.
- Show E. M. 2005. *Hydrology in practice*, Tazlor and Francis E-Library, England, 628 pp



Experimental research on the effective water abstraction permitting regime

Krasya Kolcheva*, PhD, eng.

*National Institute of Meteorology and Hydrology - Bulgarian Academy of Sciences,
Tsarigradsko shose 66, 1784 Sofia*

Abstract: Modelling and analysis of water rights become more and more important for the adaptation to the changing management conditions of the water resources in river basin, considered as an integrated system, where the water consumers are interconnected. A measure in this sense is the development of a science-based water abstraction permit regime, consistent with the objectives of the Water Framework Directive 2000/60/EC (WFD) and the River Basin Management Plans (RBMP). The main point of the procedure is the development of an assessment tool granting water right through mathematical modeling of water distribution in a certain watershed, clarifying the degree of supply of the requested volumes and the free volumes for satisfaction of future needs. For the first time in Bulgaria a new methodological approach is proposed, based on research and analysis of foreign and own experience, including distribution of water resources, water rights analysis and estimation of free water volumes. For its practical application is selected SIMYL simulation model, developed by the former Institute of Water Problems at the Bulgarian Academy of Sciences and further modified for the purpose. The experiments carried out for the real pilot basin of Tundja river prove the contribution of the approach for taking an informed decision about a certain water request, as well as for reassessment of the current permit system, and for a risk assessment of water deficits in the river basins designated in the RBMP.

Keywords: permit regime, water abstraction, water right, methodological approach, assessment tool, integrated water management

1. INTRODUCTION

The long-term protection of the subjected to significant pressure water resources considering the increasing water consumption, taking into account the needs of aquatic

* kolchevakrasi@abv.bg

ecosystems, changed climatic factor and intensive pollution of water resources is more frequently a subject of scientific studies, adaptive strategies, plans and programs with active public participation. For that reason, the UN designated the decade 2005÷2015 under the motto „Water in Life“ to stimulate the coordinated international activities in the field of water, and the European Water Framework Directive 2000/60 defined objectives of reaching good water status by 2015 (*WFD, 2000*). This goal, though more focused on the water quality, requires an understanding of the institutional and hydrological accessibility to water and prevents the exhaustion of the water resources, affecting the amount as an integral part of the overall status. A main tool for realization is an adequate program of measures containing different types and kinds of measures in these two main aspects. Such a program is already a fact with the entry into force in March 2010 of the first River Basin Management Plans (*RBMP EABD, 2010*) in Bulgaria.

Exceptfore being planned as a key measure for reduction of the pressure on water resources, an additional reason for developing of an effective permitting regime for water consumption in Bulgaria is the subjectivity in its current implementation. Defined as a system of legislative rules and conditions, and an assessment tool supporting the decision makers (DM) or institutions in allowance or denial of water right, this regime is on the basis of the integrated water management.

The practical solution of the measure includes water distribution based on the issued permits with an evaluation of the available water resources satisfying the existing needs and determination of the free (not used) water volumes for exedance probability of future requests for water abstractions (*Wurbs, R., 2005, 2009; Wang, L., L.Fang, K.W.Hipel, 2007*). Moreover, regarding the complex configuration of the water systems, their stochastic and dynamic nature, and the numerous water consumers, the decision requires an application of a mathematical modeling, flexible priorities of water abstraction, ecological (recognition of the ecosystems as a fully legitimate consumer) and economic (”water consumer pays“) principles (*WFD, 2000*).

The such created permitting regime will identify the water users and their water shares with the corresponding probabilities of exceedence as well as the inclusion of new users, the changes in the type and amount of water consumption, and/or in the variance of river flow.

In the current paper, through experimental studies within a real water management system (WMS) in Bulgaria, the one of Tundja river basin, is proved the feasibility of the proposed methodological approach and the mathematical model, mainly for improvement and efficiency of the procedure for issuing permits for water abstractions.

2. SUMMARY OF THE APPROACH OF PERMITS ISSUEANCE

In the basis of the proposed methodical approach on a decision making for water abstraction permits issuance through justified coordination of the requested demands with the available water resources or, for modeling of the water rights at a basin/sub-basin level stands the decision

of a three-stage task with the following *formulation*: in a certain situation - available water resource in a basin/sub-basin or river section with preliminary set priorities for water use to specify how (under what conditions) and how much (annual limit or water share) should be permitted from the requested target abstraction in such a way that the ecosystems are preserved. Similar problem is already solved (*Wurbs, R. and WBWalls, 1989; Wurbs, R., 1996*), but with different formulation, other legal framework and with another mathematical model.

The solution includes:

First stage: Distribution of water resources.

Based on the distribution of the available water resources between water users and water consumers in a certain watershed, taking into account the abstraction priorities, is intended to clarify the extent of the provision of the requested demands for water and not requested free volumes in separated river sections, as well as the availability/deficit of ecological flow and the way of functioning of the WMS. Through repeated simulation experiments under different scenarios of water use a reasonable distribution of water resources for all users from the point of view of the DM can be achieved.

Second stage: Analysis of the submitted requests for obtaining of water use right based on the results from the first stage.

In case of a disagreement of the applicants with the results from the first stage or a doubt from the controlling body about the reliability of the requested abstraction amounts and/or a negative impact on the environment and neighboring users, an additional information supporting the request is required. Thus, analyzing the new data in interactive regime both parties may agree to correct the limits. The results from the new water distribution will show if the taken decision is a basis for the provision of water use right, and if it is not, a refusal or further discussion follows. In such a way every next change, for which there is a ground and agreement, is associated with a new simulation and evaluation.

Third stage: Determination of the unused water to cover additional requests.

Simulations of different variants for the water use and water resources availability is meant to give a general assessment of the free volumes in a basin/sub-basin/water body levels and the estimate „For“ or „Against“ a particular request, taking into account the interconnectivity between the users in a particular watershed, requires the implementation of the first stage.

For solving the problem is used the SIMYL simulation model, developed by the Assoc. Prof. Eng I. Nyagolov, successfully applied for distribution of water resources within a certain river basin. A graphic diagram of the WMS (water users, river and monitoring network, water abstractions with the type of water use and the related infrastructure) is made up first for the model, based on the computing (network model). The latter is a directed graph - a system of nodes and arcs, where the nodes are the points of the tributaries inflow into the main river, the discharge of wastewater and the returning water, the abstractions and the reservoirs as components of the water resources and water use. The arcs (canals, river sections, tunnels, pipelines, etc.) are the connections between the nodes. In order to represent adequately the real system, parameters and

constraints are set for the particular elements of the model, such as reservoirs volume, permitted water amounts, water-carrying capacities of the installations, priorities of the reservoirs and water users, determined by their usefulness.

Criteria for analysis and evaluation of the results in water distribution modeling are mainly the probability of exedance probability by years, months and water volumes for the respective user, and the occurrency of water shortage or deficit.

$$P_y = k/n * 100 \%, \quad (2.1.)$$

$$P_m = l/12n * 100 \%, \quad (2.2.)$$

$$P_v = V_1/V * 100 \%, \quad (2.3.)$$

where k – number of years and months without disturbance in water use; n – total number of years and months for the research period; V_1 – discharged volume and V – necessary water volume.

The same criterion, but called “reliability” (used by (Wurbs, R., 2005), R – reliability) is used in the Western-European publications in water rights modeling and it is calculated in the same way:

$$R = n/N, \quad (2.4.)$$

where n is the number of the months without disturbance in water use, and N is the total number of months for the research period.

Regulatory exedance probability (P_r) is given by years. It is different for each consumer and generally it is estimated by the economic evaluation of the losses of a particular enterprise, hydropower plant, irrigation system (IS), fish farms etc., due to the water deficits. Depending on the category of water supply system and the functional type of the settlement, the exedance probability for domestic and industrial purposes is normatively defined in (*Ordinance № 2/22.03.2005 for design, construction and operation of water supply systems*), varying from 95% for the first category and settlements of I and II functional type, 90% for the second category and settlements – III and IV functional type, to 85% for the third category and settlements – V to VIII functional types. For the irrigation water economic practice has proved $P_r = 75\%$ and for the Hydroelectric power plant (HPP) operating in an independent mode – 85%. The lower values of the exedance probability in the irrigation can be explained by the possibility of yield in dry conditions, and in the hydropower production can be explained with the possibility of substitution with Thermal power plant (TPP).

General prerequisites, assumptions and constraints of the solution:

- The hydrology of the basin is represented by the available hydrological time series for a past period assuming that it is valid also for a future period. This concerns also the data for the evaporation from reservoirs. If a climatic scenario is applied, new estimates are used for the water quantities, water use and evaporation;
- The series for the water flow are those for undisturbed (natural) flow;
- To provide data for the water flow in the nodes without information from gauging stations are used different hydrological methods and tools such as transposition of the runoff from the HMS etc.;
- From the groundwater sources are considered those located in the river terraces (floodplains), interconnected with the surface water flow;

- The issued permits are the main source of data for water consumption and therefore specified quantities are set;
- In case of water shortages in a particular node the needs are satisfied by stages according to the Bulgarian Water Act;
- To decrease the dimensionality of the task, the smaller water users are grouped into a particular node;
- The ecological water flow after the abstractions is ensured;
- The requirements of Article 62 of the Water Act (WA) regarding the new water abstractions are observed, considering the provisions of the current RBMPs, public interests and acquired water rights;
- The interval of calculation is one month;
- The new requests for water should not cause changes in the so set permitting system.

3. EXPERIMENTAL STUDY

3.1. Summary characteristics of the pilot basin

Tundja River is 390 km long, springs from the Central part of the Balkan mountain east to the Peak of Botev and being the largest tributary of Maritsa River, flows into it on Turkish territory. The catchment area is 7884 km², occupies 22% from the East Aegean region and 7% of the Bulgarian territory. The relief is hilly to flat in the western part of the basin, mostly flat in the middle and slightly hilly in the south, and the climate varies from humid continental in the western part to Mediterranean continental in the south.

River and hydrometric network – the tributaries of first order are 44 with a total length of 393,9 km, as the larger ones are: Mochuritsa, Sinapovska and Popovska, and hydrometric and meteorological gauging stations are respectively 14 and 28 (Fig. 1).

Water resources – the river flow calculated for the representative 44-years period – 1961÷2004 as an annual value for the main river at Kalofer station compared to that at the border with the Republic of Turkey should change as follows: the minimum from 7,27.10⁶m³ to 524,25.10⁶ m³; average from 14,82.10⁶ m³ to 1256.10⁶ m³ and the maximum from 30,43.10⁶ m³ to 2254,64.10⁶ m³.

The analysis of the results shows that monthly distribution of the water flow through the year is similar to the rainfall patterns, as for the above mentioned period it is indicated a decrease in the values of the minimum monthly flow compared to the period 1961÷1998 (*Water use and water resource balance of the Tundja River Basin, 2006*).

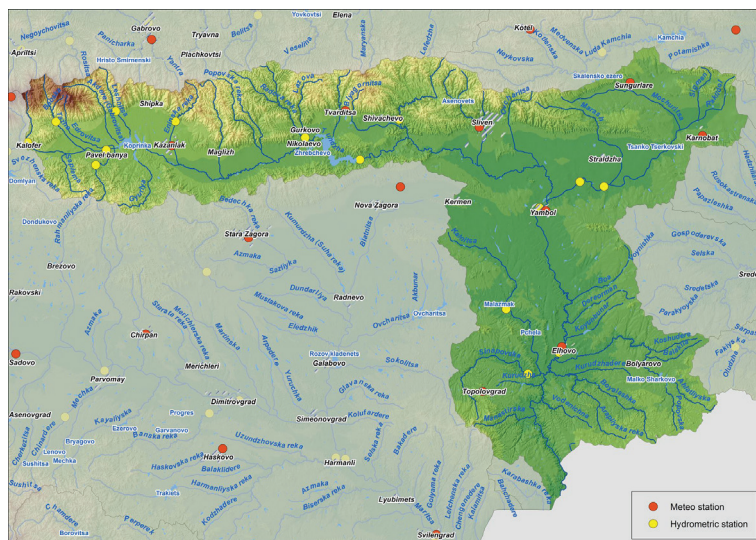


Fig. 1 – Tundja River Basin

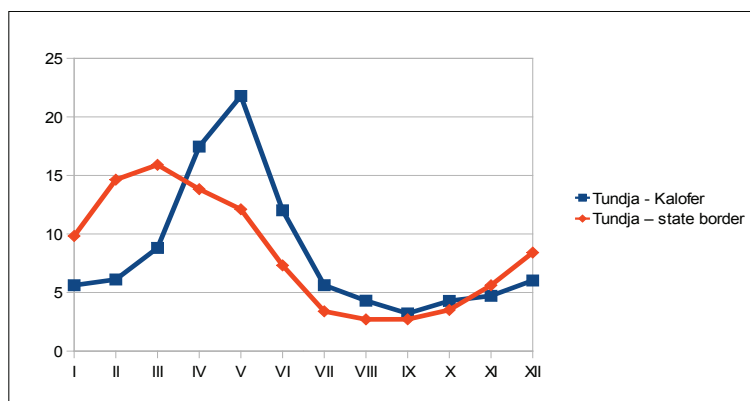


Fig. 2 – Percentage distribution of Tundja river water flow by months through the year at two stations in the period 1998÷2004

In the main aquifers of the basin is generated 8085 l/s natural flow in total, belonging mainly to the alluvial and proluvial formations and 4995 l/s exploitation groundwater resources (pore water), which is almost 10% from the average multiannual flow of the river.

The population in 2008 was 19% from that of the East Aegean region and almost 6% from the population of Bulgaria. According to the realistic forecast it is expected to drop with 21% by the year 2027.

Economy – priority economic sectors are agriculture and industry, represented by the following sectors: chemicals, metals processing and textiles.

A specific feature of the river basin is the transfer of significant water amounts of surface and groundwater from Tundja river basin into Maritsa River basin for the irrigation and industry needs in the regions of Stara Zagora and Nova Zagora, into the Danube region for drinking water supply of the town of Tryavna and back from the watershed of Kamchiya river (Black Sea region) into the catchment area of Tundja river for irrigation.

The main river is hydrotechnically assimilated and there are some hydrotechnical constructions at its larger tributaries – Asenovska, Mochuritsa and Popovska rivers. From a total number of 259 reservoirs (state and municipal property), complex and important according to the Water Act are Koprinka, Zhrebchevo, Asenovetz and Malko Sharkovo.

3.2. Water consumption and water rights

The nature and the amount of water consumption are determined by the economic and demographic development of the region. In this case, to study the dynamics of the water rights in Tundja river basin, a comparison is made between the water consumption up to 2004, considered as the base (reference) time period for the existing water users and the issued permits in the period 2004÷2008, considered as new ones.

Through review and analysis of 279 permits for water abstractions from surface and groundwaters (in the river floodplains) issued by BDWM of EAR – Plovdiv till 2008, are identified the new significant water consumers with permitted annual limit of over 150 thousands m³ and a great number of small water users. This allows to set an updated diagram for the water consumption in the studied river basin.

The biggest water consuming sector is the irrigation, with four major irrigation systems (Kazanlak, Stara Zagora, Central Tundja and Bolyarovo) and a number of smaller systems and fields. In the period 2004÷2008 are localized eleven new users joined to five of the existing irrigation systems.

The next big consumer is the household sector, provisioned primarily by groundwater sources – wells (united in water supply groups), constructed mainly around the big towns of Kazanlak, Sliven, Yambol, etc. Surface water sources are few – Asenovetz reservoir and several river intakes for partial water supply of the towns of Kalofer, Tvarditsa, Shivachevo and some smaller settlements. The dynamics of permits issuing for water consumption in this sector in the considered period shows an increase, taking into account ten new water requests and update of the annual limit of two existing users.

The industrial consumption is concentrated mainly in the large urban centers – Kazanlak, Stara Zagora, Sliven and Yambol. It is provisioned mostly from groundwater sources and has a considerable share from the total consumption in the river basin. In the period 2004÷2008 an increased intensity of the permitted requests for water consumption is observed but also a dropping out of one of the major consumers – nitrogen fertilizer factory (NFF) Stara Zagora. The availability of six fish-breeding farms by 2008, the bigger ones from which are near the towns of Nikolaevo and Yambol determines the

fish-breeding as a priority sector of the industry in the region. The industrial users in total by 2008 are with 41 more compared to 2004.

The hydropower production, considered as a water consumer, is not typical for the basin. It is represented by five hydroelectric power plants (HPP) and the significant ones are: „Koprinka“, „Stara Zagora“ and „Zhrebchevo“, operating in subordinated mode, due to the complex nature of the reservoirs and the prevailing irrigation. HPP „Taja“ and „Enina“ are daily compensators and work in energy regime only.

Water consumption and water use in the key sectors and in total for Tundja river basin in number, and the permitted annual limits in the considered two time periods up to 2004 and up to 2008, are presented in Table 1. The graph in Fig. 3 shows the abstracted water volumes in main sectors without hydropower.

Table 1 – Number of the water consumers and users, and permitted limit in the Tundja River Basin

Main sectors	Number of water consumers and users - 2004	Number of water consumers and users - 2008	Permitted limit - 2004 (m ³ /y)	Permitted limit - 2008 (m ³ /y)
irrigation	24	35	226735324	227508301
household water supply	40	50	92529192	96777468
industry	111	149	78898372	54318466
ish-breeding	3	5	10336984	11262694
hydropower plants	7	7	391500000	391500000
Total	185	246	799999872	781366929

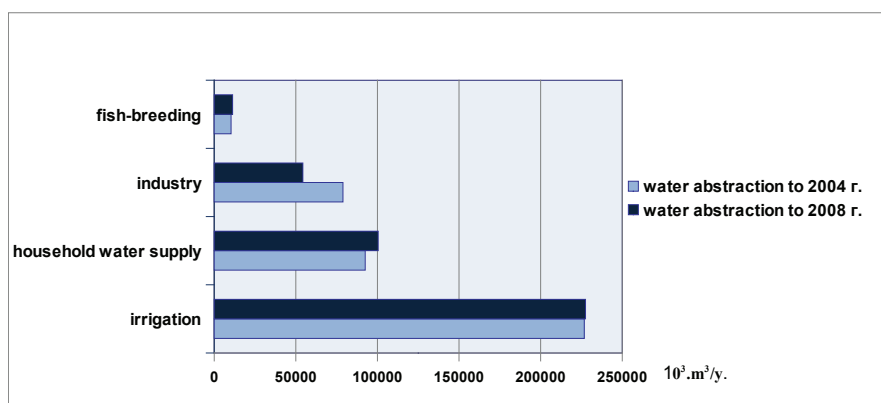


Fig. 3 – Water abstraction (without hydropower) in the Tundja river basin - 2004 and 2008

In conclusion, it can be summarized that water consumption in 2008 compared to 2004 shows an increase in household water consumption with 8,60%, for fish-breeding –

8,96%, for irrigation – 0,34% and for industry, a decrease of 45,25% due to the dropping out of NFP – Stara Zagora.

3.3. Modelling of the water rights in Tundja river basin

In accordance with the principle formulation of the problem (defined in section 2) and considering the referred in 3.1. available water resources and water consumption in Tundja river basin, formulation of a well-grounded estimation „For“ or „Against“ particular water demand includes:

- • *First stage*: water distribution between all permits in the watershed according to their needs and available water resources;
- • *Second stage*: analysis and estimate of the submitted water requests based on the results from the first stage;
- • *Third stage*: estimation and current updating of the free water resources in order to assess the compatibility with the new (future) requests for water consumption or possible redistribution of the water rights. How and to what extent will be affected the water consumption with the change of the climatic conditions is considered as a variant of the current task.

3.3.1. Compilation of graphical and computational diagram

Based on the latest data for water anstraction and water rights in the studied river basin, according to section 3.2., the graphical diagram of the consumption and use of water resources in the basin (Fig. 4), using the primary diagram from (*Water use and water resource balance of the Tundja River Basin, 2006, Niagolov, I, et al. 2007*) reflects the changes in the configuration of the water economic diagram up to 2008. To simplify the diagram, but without disturbing the adequate representation of the real WMS, an aggregation of the water consumers is done and, where possible, some of the new users (shown with dotted line) are added to the existing ones by amounts, while others are independently set at particular places. This diagram is based on the computing scheme or so called network model with 138 nodes and 143 arcs representing the real WMS. Part of it is shown in Figure 5 as the new users and the changes in the water consumption are shown in *Italic* or with dotted line.

3.3.2. Input information

The data required for the program input files by the nodes of the network model concerns, as already mentioned, water consumption and water flow. Water consumption by nodes in the two time periods is shown in Table 2 and part of it is presented with the changes. For the calculation of the surface runoff were used time series of 44-years for undisturbed monthly runoff in the period 1961÷2004, and for the calculation of the groundwater flow are used the data from the permits for the local exploitation resources.

In both points: after PS (Pump station) "Yagoda" and after Zhrebchevo reservoir are set the ecological water quantities according to the existing Water Act with the respective annual value and monthly distribution.

The modelling with a computational interval of one month was implemented by the simulation program SIMYL and the specified criteria given in section 2 were used for the assessment of the results.

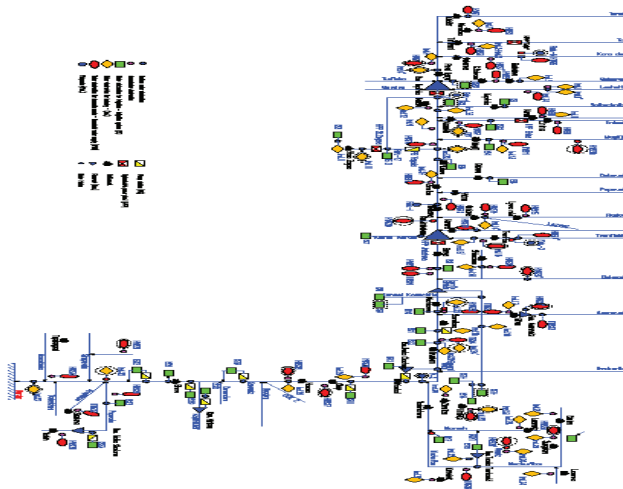


Fig. 4 – The graphical diagram of the allocation, consumption and use of water resources in the river basin of Tundja

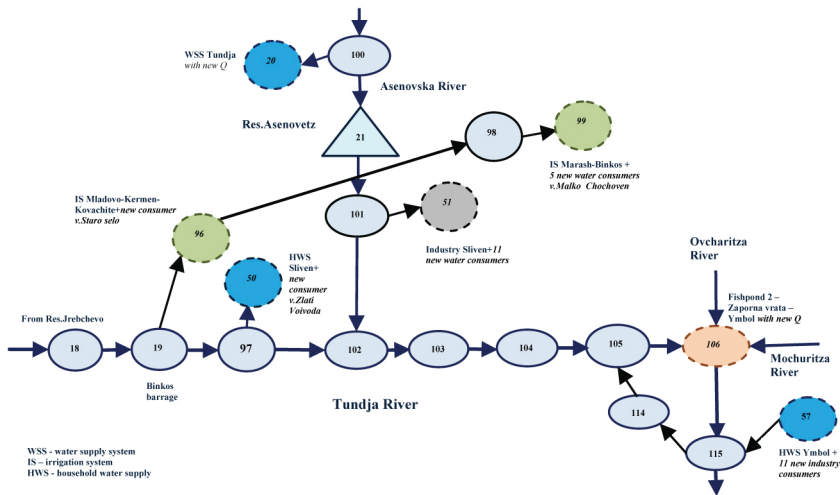


Fig. 5 – Network model of the river section after Zhrebchevo reservoir to the town of Yambol

Table 2 – Water consumers and permitted annual limit by nodes for both time periods – 2004 and 2008 (extract)

No node	Representation nodes	Water consumer	Permitted annual volume 2004 (m ³)	Permitted annual volume 2008 (m ³)
1	Tundja1+HWS 1	Household water supply of t.Kalofer from Tundja river	473040	473040
3	Tundja+HWS4+Ind.4+Ind.4'	1. To Household and industry water supply of t. Pavel Banya from GW + <i>new household water supply of villages around Pavel Banya from Sokolitza river</i> – 1261440 m ³ /y; 2. To industry water supply of Hospital Pavel Banya from GW; 3. <i>New quantity for a fishpond do Kumaks from SW</i> – 225710 m ³ /y.	956420	3991010
8	Tundja+ Irrigation 2	To IS Kazanlak + 3 new consumers from GW – 44 053 m ³ /y	14224600	14267200
138	Fishhold 4 (new)	New Fishhold of a company Throne near the v. Koprinka	0	178000
17	Tundja+Q ecol. 2	environmental needs Jrebchevo reservoir	67200000	67200000
20	HWS 21'	WSS «Tundja»– city Sliven <i>with new Q</i>	3600000	4730400
21	Res.Asenovec+HWS 21	Household water supply of Sliven from Asenovetz reservoir	15000000	15000000
24	Res.M.Sharkovo1+Irrigation 23	IS Bolyarovo	9440200	9440200
31	Irrigation 26	To Irrigation of Rouz Treiding + <i>new consumer in v.Gabarevo</i> – 78 000 m ³ /y	47000	125700
36	Ind.10+Ind.11	1. To industry water supply of t.St.Zagora + <i>new consumer</i> – 68 700 m ³ /y; 2. <i>Nitrogen fertilizer factory with 31 m³/y - dropped</i>	34103900	3172600
51	Ind.17	To industry water supply of Sliven + <i>11 new consumers from GW</i> – 5141845 m ³ /y + <i>new from SW</i> – 687000 m ³ /y	4203348	5828845
52	HWS.24+Ind.24' (new)	1. To industry water supply of Sliven and v.Krushare + <i>new household water supply of v.Panaretovci from GW</i> – 25550 m ³ /y; 2. <i>New industrial consumer from GW in v.Gergevec</i> – 394200 m ³ /y.	610000	1029750
54	Ind.23+ Ind.28	To industry water supply of t.Straldja + <i>new industrial consumer from GW in v.Devetak</i> – 65897 m ³ /y	200284	266181

Krasya Kolcheva

56	<i>HWS35+Ind. 21+Ind.29+Ind.34</i>	1. To Household water supply of t.Sungulare + <i>new household water supply of v.Lozarevo from GW – 110376 m³/y;</i> 3. To industry water supply of t. Sungulare + <i>2 new consumers – 22862 m³/y.</i>	110090	243328
57	HWS 26+ <i>Ind.25</i>	1. Household water supply of city of Yambol; 2. To industry water supply + <i>new 11 consumers from GW – 771742 m³/y.</i>	18953989	19725731
136	r.Karadere+ <i>Fishhold 5 (new)</i>	<i>New Fishhold of a company GIV on the Kara dere river</i>	0	225710
88	Tundja+ <i>HWS 39 (new)</i>	<i>Household water supply of t. Nikolaevo from GW – new consumer</i>	0	227059
89	r.Lazova+Ind.14'	Industry water supply of Gurkovo	121255	121255
93	r.Belenska+ <i>HWS20'</i>	To Household water supply of t. Shivachevo + <i>new household water supply of v.Sborishte from Dolap dere river – 110376 m³/y</i>	158000	268376
99	<i>Irrigation 14</i>	To Marash-Binkos IS + <i>5 new consumers from GW in v.Malko Chochoven – 117911 m³/y</i>	57212300	57784400
112	<i>HWS 25</i>	To Household water supply of t. Straldga+ <i>2 new consumers from GW in v.Devetak and v.Zimen – 118475 m³/y</i>	431011	549486
125	<i>Ind.35 – (new)</i>	<i>New industrial consumer from GW– v.Boyanovo</i>	0	59570
126	Irrigation 23	IF Dobrich	1311000	1311000
133	Tundja+ <i>Ind.27</i>	To industry water supply of v.Ustrem + <i>new consumer – 1500000 m³/y</i>	120000	1620000

Note: In *Italic* are shown the data from the new permits up to 2008, including; SW – surface water; GW – groundwater

3.3.3. Basic assumptions of the solution

Considering the general assumptions and limitations mentioned in section 2, the particular practical solution is based on the following assumptions:

- Water consumers with the permitted water volume in the first time period – up to 2004 are considered as existing ones and this variant is taken as a reference one, while those in the second time period – up to 2008 are considered as new ones and the requested by them water amounts will be a subject of analysis and evaluation based on the results from the simulations;

- The priorities set in the model correspond to the given normatives in the Bulgarian Water Act (Article 50, paragraphs 4 and 5);
- Twelve (12) coefficients accounting to the seasonal fluctuations in water consumption are determined through analyses.

In the experiment, considering climate changes, is accepted a conditional decrease of the water runoff with 8% due to the lack of a climate scenario for drought.

3.3.4. Simulation experiments for the basic solution of the task

- **First Stage:** Includes two variants of water distribution between all permits in the pilot river basin, corresponding to the two time periods.

In the first variant are considered the existing water consumers up to 2004, and in the second one are added newly requested volumes up to 2008. After setting the water consumption in the model with the permitted annual limits from the Table 2, simulations of the water distribution are carried out. The obtained results are presented consequently in excerpts from Table 3 (the first variant) and 4 (second variant), and analyzed.

Table 3 – Results from the first variant – First stage (excerpt)

№ node	Representation nodes	Water consumption by nodes - 2004 (*10 ² m ³ /y)	D1 (*100 m ³ /y)	P1 (%) ^v	P1 (%) ^v	P1 (%) ^m
3	Tundja+HWS 4+Ind.4+Ind.4 ⁷	9546	0	100.00	100.00	100.00
20	HWS 21	35998	955	97.35	45.45	90.91
21	Res. Asenovetz	150000	483	99.68	97.73	99.62
24	Res.M.Sharkovo1+ Irrigation 23	94402	3751	96.03	97.73	98.45
36	Ind.10+Ind.11	340908	1368	99.60	95.45	99.43
51	Ind. 17	42033	0	100.00	100.00	100.00
52	HWS 24	6098	0	100.00	100.00	100.00
54	Ind. 23+ Ind. 28	2001	12	99.40	93.18	99.24
56	Ind. 30	1099	0	100.00	100.00	100.00
57	HWS 26+Ind. 25	189540	0	100.00	100.00	100.00
77	Irrigation 3 P-17	96460	1199	98.76	93.18	98.70
78	Irrigation 3 M1-M2	439444	26468	93.98	93.18	97.08
89	r.Lazova+Ind.14 ^c	1212	24	98.02	81.82	97.73
93	r.Belenska+HWS 20	1582	6	99.62	93.18	99.24
99	Irrigation 14	572123	0	100.00	100.00	100.00
133	Tundja+Ind. 27	1197	0	100.00	100.00	100.00
134	r.Ovcharica+HWS 37	44472	1159	97.39	77.27	94.89

Explanations of the designations in the table and the subsequent tables of results: D1 is average multiannual water deficit, P1_v – average multi-annual reliability by volume,

$P1_y$ – average multi-annual reliability by years, $P1_m$ – average multi-annual reliability by months the number after D and P indicates the subsequent number of the experiment (in this case it is 1, as it refers to the first experiment).

Table 4 – Results from the second variant – First stage (excerpt)

No node	Representation nodes	Water consumption by nodes - 2004 (*10 ² m ³ /y)	D2 (*100 m ³ /y)	P2 _v (%)	P2 _y (%)	P2 _m (%)
3	Tundja+HWS 4+Ind.4+Ind.4'	39909	0	100.00	100.00	100.00
8	Tundja+ Irrigation 2	142672	439	99.69	95.45	98.94
138	Fishhold 4 (new)	1780	0	100.00	100.00	100.00
20	HWS 21'	47305	2837	94.00	15.91	79.92
21	Res. Aenovetz	150000	1252	99.17	97.73	99.05
24	Res.M.Sharkovo1+ Irrigation 23	94402	3751	96.03	97.73	98.45
31	Irrigation 26	1257	40	96.82	93.18	97.17
36	Ind.10+Ind.11	31716	300	99.05	95.45	99.05
39	HWS 7+ Ind.7	63250	0	100.00	100.00	100.00
43	Ind.32	3003	29	99.03	95.45	99.03
47	HWS 17+Ind.15	5479	52	99.05	95.45	99.05
50	HWS 22+Ind.22 (new)	33448	0	100.00	100.00	100.00
51	Ind.17	58288	0	100.00	100.00	100.00
52	HWS 24+Ind.24' (new)	10298	0	100.00	100.00	100.00
53	Ind.30+HWS 30' (new)	1716	13	99.24	97.73	99.24
54	Ind.23+ Ind. 28	2658	93	96.50	72.73	95.64
56	HWS 35+Ind. 21+Ind.29+ Ind.34	2432	0	100.00	100.00	100.00
57	HWS 26+Ind.25	197256	0	100.00	100.00	100.00
77	Irrigation 3 P-17	96460	1417	98.53	93.18	98.38
78	Irrigation 3 M1-M2	439444	21330	95.15	93.18	97.40
93	r.Belenska+HWS 20'	5605	63	98.88	86.36	98.48
96	Irrigation 9	177749	0	100.00	100.00	100.00
99	Irrigation 14	577844	1856	99.68	97.73	99.35
112	HWS 25	5494	93	98.31	81.82	97.16
113	r.Mochurica+ Irrigation 17	2790	0	100.00	100.00	100.00
125	Tundja+Ind.27	720	0	100.00	100.00	100.00
133	Tundja+Ind.27	16200	0	100.00	100.00	100.00

Note: In *Italic* are given the added nodes for the new water consumers by the end of 2008 and the new nodes.

Analysis of the results from the first experiment:

- The permitted water consumption for irrigation is almost entirely satisfied, i.e. 2/3 of the water rights of the users are provisioned at 100% and the rest at 98% ÷ 93%. There is a higher average multiannual deficit for IS “Bolarovo” (node 24), and especially for IS “Stara Zagora” – 27667.10² m³ (nodes 77 and 78);
- The most significant variations are in the permits for the household water supply, as fully satisfied with water are 71% of the water demands, 21% have an annual exceedance probability – 98÷93% and for about 9% it is below 77%. To the latter refer household water supply of the town of Sliven from the WMS Tundja (node 20) and that of the settlements from Sliven Municipality at Ovcharitsa river floodplain (node 134), which due to their disturbance for the first case in 24 years, and for the second case in 10 years of the 44-year studied period and respectively 48 and 26 from total 528 months (134) are determined as risky;
- In the *industry*, the water rights of 72% of 111 consumers are fully supplied with water, the rest 28% are disturbed slightly (92%÷98%). Of lowest annual reliability – 82% is the industrial water supply of the town of Gurkovo in the catchment area of Lazova River (node 89).

Thus summarizing the reliability of the permitted water consumption in the first time period – up to 2004, it can be concluded that, with few exceptions for the drinking water supply, it is sufficient. Yet some conditions should be included in the permits – introduction of water efficiency and annual re-estimation of the permitted limits based on the presented by the holder at the beginning of the year report for the previous year and plan for the upcoming year.

Analysis of the results from the second simulation:

- The addition of 11 new irrigation fields to the existing irrigation systems – IS “Kazanlak” and “Mladovo-Kermen-Roza”, and IS “Rose Trading”, “Terra Agro” and Binkos-Marash (nodes 8, 96, 31, 113 and 99), changes insignificantly their reliability. But here, besides the presence of the highest average multi-year deficit for the same as in the first experiment: IS “Bolyarovo” and “Stara Zagora”, a new one appears for the irrigation of “Marash-Binkos” IS (node 99), considering the new areas in Malko Chochoveni village. Therefore, compared to the first variant for satisfaction of the needs of the water users for the irrigation no significant changes were observed;
- With the inclusion of 10 new household consumers and the satisfaction of the requests for increase of the permitted limits of two existing ones, the consumers fully supplied with water are less with 1,3%, 8 users have annual reliability of 98 ÷ 93% and 4 have reliability of 86÷77%. The determined in the first experiment as a risky consumption for the town of Sliven from the WMS “Tundja” has a significantly lower value – 15.9% and three times higher deficit. Regarding the exceeding values of the deficits can be summarized, that the situation in the household water supply sector, compared to the previous period, is worse;

- Two from the new consumers in the industrial sector has 73% reliability. The water deficit has increased five times for the villages of Yagoda and Venetz and the town of Stralja in nodes 43, 53 and 54 due to the addition of new consumers, and for Stara Zagora in node 36 due to the dropping out of the significant consumer – NFP has decreased respectively. As risky water consumer is appeared to be the pig farm “Krumovo Gradishte” AD in the village of Devetak (node 54).
- Thus, decisions for the allowance of a water right have received:
- The new users in irrigation, joined to the pointed IS and IF in nodes 8, 31, 96, 99 and 113 with the inclusion of additional conditions for the application of good irrigation practices and possible reestimation of the permitted limits in case of a change in the cultivated crops and irrigated areas in drought conditions;
- Almost all new requests in the household water supply sector. To more stringent control should be subjected the permits of the villages Sborishte and Devetak, and those included to the towns Straldzha and Shivachevo (nodes 93 and 112), due to the lower annual reliability - 86% and 82%. Water deficit is distributed among more years but it is small by volume;
- The new industrial users in nodes: 3, 36, 39, 43, 47, 50, 51, 52, 53, 56, 57, 125 and 133.

No confirmation of the right have received:

- WSS “Sliven” because in case of a permit for the requested water volume by the applicant amounting at 4,7 million m³/y $P_y = 15,91\%$, there will be a deficit in 37 years and 106 months, which defines it as controversial or negotiable applicant and will be a subject of study in the second stage of solving the task;
- The request for water of the pig farm „Krumovo-Gradishte“ AD in the village of Devetaki, is added to the industry of the town of Straldzha in node 54 due to insufficient reliability, available deficit and probable pressure on the existing water users, will also be a subject of analysis in the next stage.
- The decision for allowance or denial of these applications will be a subject of the study in the second stage of solving the task.
- *Second stage*: an analysis of the submitted requests for obtaining water use right

The simulation experiments – variants 3 and 4 are meant to support the competent authorities to resolve the disputable candidates – WSS „Sliven“ and Pig Farm „Krumovo Gradishte“ AD in the village of Devetaki through discussion with them.

The Competent authority, referring to the results from the previous stage notifies both applicants that the requested water quantity can not be permitted in such volume and requires further proving information. It is assumed that WSS „Sliven“ submits a similar detailed report for five years back on the real-used water quantities with reported losses and calculations of the required amount based on the number of real consumers and water supply norm, and the industrial candidate - less water consuming technological scheme. Thus, in interactive mode both sides reach an agreement to reduce the quantity.

After the input in the data file of the new annual water consumption values for node 20 – 2 838 240 m³ and for node 54 – 259 951 m³, a new water distribution is done.

Table 5 – Results from the third variant (excerpt)

No node	Representation nodes	Water consumption by nodes - 2004 (*10 ² m ³ /y)	D2 (*100 m ³ /y)	P2 _v (%)	P2 _y (%)	P2 _m (%)
20	HWS21'	28382	482	98.30	68.18	96.40
54	Ind.23+ Ind.28	2601	87	96.66	75.00	95.83

Analysis of the results from the simulation experiment:

- HWS in node 20, despite the reestimated water volume of 2,8 million m³/y, will again, considering Py = 68%, have 14 years and 19 months with water deficit;
- The change in node 54 is insignificant – the annual exedance probability has increased only with 2% and still, during more than a half of the studied years – 29, the water consumption will be disrupted.
- The unsatisfactory results require further consideration with searching for an alternative and new water distribution.

The fourth variant, similar to the previous one estimates how the new agreement with the applicant has affected the output data from the simulation. It is assumed that WSS „Sliven“ proposes a variant with an alternative water source, and the pig farm – a scheme for reuse of the wastewater. With the new values for the water consumption of these two users, respectively, for a node 20 – 946 080 m³ and for a node 54 – 186 327 m³ a new water distribution is done.

Table 6 – Results for the fourth variant (extract)

No node	Representation nodes	Water consumption by nodes – 2004 (*10 ² m ³ /y)	D2 (*100 m ³ /y)	P2 _v (%)	P2 _y (%)	P2 _m (%)
20	HWS21'	9460	55	99.42	93.18	99.05
54	Ind.23+ Ind.28	1857	39	97.90	84.09	97.54

For both applications are reported values for the exedance probability, complying with the norms, and the average multi-annual deficit, compared to the second variant, is negligible. Although this is mainly due to the negotiated lower consumption, respectively – 946 000 m³ and 185 700 m³ compared to the initially requested, it is a cause for issuing a permit for water abstraction of WWS „Sliven“ and the pig farm „Krumovo Gradishte“ JSC.

- *Stage Three:* Estimation of the unused water to satisfy the future requests.

Through several consequent simulations is estimated the free water resource for undertaking the new requests for water abstractions in certain river sections of the main

river and some for the major tributaries, selected as being burdened with more users and respectively with a greater risk of water shortages.

The results from the simulations, shown in Tables 7 and the graphs in Figures 6 and 7, presented downstream the river (from the springs to the state border), reported availability of unused resource and its increase after the reservoirs and at the border. From the studied tributaries of highest capacity to satisfy the new requests is Mochuritsa River. But it must be taken into consideration that Mochuritsa falls within „Natura 2000“ zone according to Directive 92/43/EEC on the conservation of natural habitats and of wild fauna and flora and RBMP of EABD, where the maintenance or improvement of the state of the water is an important factor for their preservation.

Table 7 – Free water volumes for future requests from the Tundja river and the main tributaries

River Sections along the Tundja river and the main tributaries	Free water volume (*100 m ³)
from the spring up to the Koprinka reservoir	213184
Koprinka reservoir - Jrebchevo reservoir	191191
from Jrebchevo reservoir to the mouth Asenovska river	783078
from the mouth Asenovska river to the v.Zavoi	757032
from v.Zavoi to v.Hanovo	651749
from v.Hanovo to the mouth Povska river	498098
from the mouth Povska river to the border	798164
the river mouth of Gabrovica	160770
the river mouth of Asenovska	175467
the river mouth of Mochurica	437705
the river mouth of Tvardica	98791

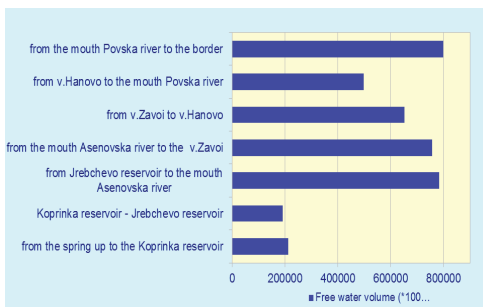


Fig. 6 – Change in the free water volumes along the Tundja river

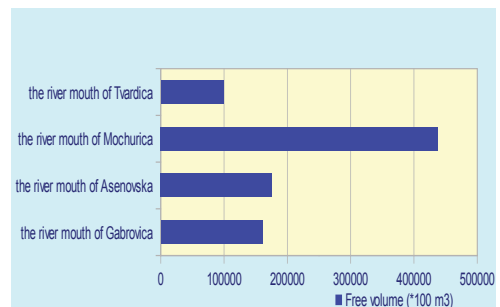


Fig. 7 – Free volume in the mouths of main tributaries of Tundja river

Such a summary evaluation is useful for the water resource management at basin and sub-basin levels, as well as for filling up of the missing estimates at this stage regarding the

quantitative status in the first water management plans, with identification of watersheds and water bodies in the so-called "water stress" or water deficit. For more detailed evaluation of a specific request, taking into account the interconnectivity between the users in a given watershed, sub-basin or river section (water body) the first stage of the task solution should be applied.

3.3.5. Solution variants of the problem

The purpose of the solution variants is to assess how the permit regime along the main river sectors will react to draught conditions, how the water deficit will change if limitations will be imposed in the permits and what mitigation measures may be proposed.

Simulation experiment was carried out under an adverse scenario – water consumption data from the second variant is used, i.e. for the second time period – up to 2008 and the input information for the water flow is the available series at all observation gauging stations reduced by 8%. As a result from the comparison of the current with the second variant in Table 9 are shown the users with considerable changes in the reliability and deficits.

Analysis of the results from the simulation experiment (comparing the current experiment 2A with the second variant):

- Water deficit in average for the whole period has risen with almost 70%. The most affected is the industry sector, which average deficit has increased with 80%, followed by the irrigation – with 75% and households – with 53%. With a new deficit compared to the second variant are the industry in the town of Sliven, IS "Shivachevo-Chervenakovo" and IS "Kazanlak", and about five times higher deficits will be sustained in the irrigated areas Marash-Binkos, Middle Tundja and Kazanlak, as well as in the planned new IS „Mlekarevo“. The risk of failure to provide the ecological flows is also increased, especially after Zhrebchevo reservoir;
- About 40% from all consumers in the basin, including also the ecological needs, have lower values of the annual exedance probability. The observed deviations in the exedance probability by volume and by months are lower (about 1% on average). With lower values of the annual reliability are: the industry of Yagoda village, Rozovo village, the towns of Sliven, Gurkovo and Straldja as for the latter it is 73%, the irrigation systems – Kazanlak, Shivachevo-Chervenakovo, Stara Zagora, Central Tundja, Bolyarovo, Koprinka and Dobrich, the irrigation of Marash-Binkos and the private grower „Rose Trading“, and for the household sector of Sliven regarding the very low value of exedance probability by years P_y – 6.82% it can be determined as the most risky consumer, followed by the settlements in the municipality and the towns of Kalofer, Kazanlak, Straldzha and Gabarevo village.

Table 9 – Variant 2 and 2A (excerpt)

№ node	Representation nodes	Water consumption by nodes – 2008 (*100m ³ /y)	Variant 2 without change in the water flow				Variant 2A with water flow decreased by 8%			
			D2 (*100 m ³ /y)	P2 _v (%)	P2 _y (%)	P2 _m (%)	D2A (*100 m ³ /y)	P2A _v (%)	P2A _y (%)	P2A _m (%)
1	T1+HWS 1	4731	129	97.27	77.27	95.45	177	96.26	75.00	94.51
8	Tundja+ Irrigation 2	142672	439	99.69	95.45	98.94	2274	98.41	93.18	97.17
17	environmental needs 2	672000	0	100.00	100.00	100.00	250	99.96	97.73	99.81
20	HWS 21'	47305	2837	94.00	15.91	79.92	3516	92.57	6,82	77.08
21	Reservoir Aenovec	150000	1252	99.17	97.73	99.05	3121	97.92	93.18	97.54
24	Yz. M. Sharkov1 + Irrigation 23	94402	3751	96.03	97.73	98.45	4688	95.03	95.45	97.67
31	Irrigation 26	1257	40	96.82	93.18	97.17	109	91.33	90.91	95.76
51	Ind.17	58288	0	100.00	100.00	100.00	256	99.56	93.18	98.86
54	Prom.23+ Prom.28	2658	93	96.50	72.73	95.64	110	95.86	72.73	95.27
89	r.Lazova+ Ind.14'	1212	25	97.94	81.82	97.35	30	97.52	77.27	96.78
93	r.Belenska+ HWS 20'	5605	63	98.88	86.36	98.48	67	98.80	84.09	98.30
99	Irrigation 14	577844	1856	99.68	97.73	99.35	9159	98.41	95.45	98.70
112	HWS 25	5494	93	98.31	81.82	97.16	105	98.09	79.55	96.97
126	Irrigation 23	13110	398	96.96	97.73	98.45	467	96.44	95.45	98.06
134	r.Ovcharica+ HWS 37	44472	1159	97.39	77.27	94.89	1258	97.17	75.00	94.13

*Note: In **Italic** are designated the consumers with changes compared to the second variant.*

4. CONCLUSION

With the experimental study carried out in the current paper is supported the first attempt to develop a permitting regime for water consumption, as a main tool to obtain water consumption rightm taking into consideration the changes in the economy, the structure of water sector and climatic changes. The proposed methodological approach, based on the available water resources in a certain time interval, water abstraction priorities and requirements for their rational distribution can be successfully used for reevaluation of the existing permitting system. This measure becomes increasingly important in the emerging trend of increased extreme events (floods and droughts) regarding the regional and temporal heterogeneity of the allocation of the water resources in Bulgaria.

The variant solution of the task in drought conditions can be a reason for reassessment of the permitted quantities as well as the conditions of the permits, but above all it is useful to identify the consumers in risk regarding their reliability. These users have to be audited, and restrictions should be discussed and applied for prevention.

Completely suitable for the three-staged problem and for the reassessment is the selected simulation model SIMIL, which has opportunities not only for consideration of the climatic changes and flexible priorities for water abstraction (the highest one is for the drinking water supply), but also for provision of the ecological needs according to the specific character of the watershed.

In conclusion, the introduction of the approach proved its applicability, considering the pilot study, and not only the current permit regime in Bulgaria could work more effectively by using it but it also could be a good basis for analysis and assessment of the quantitative status of water in the update of the first river basin management plans and the development of management plans for drought conditions. Additionally, the assessment of the pressure on neighboring consumers and the environment, and the introduction of economic principles will ensure better monitoring and control. The establishment of such models of real water management systems for other river basins in the country will facilitate the necessary revision of their current state and the future reassessments according to the continuously changing conditions, which, undoubtedly, will make contribution to their sustainable management.

REFERENCES:

Water Act, 2000

Ordinance № 2/22.03.2005 on water-supply systems design, construction and operation

Nyagolov, I., 1999, Research Tools on Water management systems, Report on UACEG Jubilee Conference, Sofia.

Nyagolov, I., O. Santurdzhiyan, 2005, Simulation modeling of water use as a tool for quantitative assessment of the water bodies in the river basins, BULAQUA-2005.

River Basin Management Plan of EABD, vol. 1, 2010, Basin Directorate for Water Management - East Aegean Region - Plovdiv

River Basin Management Plan of EABD Tundja, vol. 3, 2010, Basin Directorate for Water Management - East Aegean Region - Plovdiv

Water use and Water use and water resource balance of the Tundja River Basin, 2006, IWP (NIMH), Bulgarian Academy of Sciences, contract by the Ministry of Environment and Water



Mineral fertilizer consumption and groundwater pollution in Europe and Bulgaria

Nina Philipova^{1*}, Olga Nitcheva², Marnik Vanclooster³

¹Institute of Mechanics, Acad. G. Bonchev Str. Bl.4, Sofia 1113

²National Institute of Meteorology and Hydrology, Tsarigradsko shose 66, Sofia 1784

³Earth and Life Institute, Univeristé catholique de Louvain, B-1310 Louvain-la-Neuve, BELGIUM

Abstract. Groundwater is a main and easy water source for agriculture, industry, mining. It supplies with fresh water more than 10 megacities across the world, including London, Beijing, Mexico City, Buenos Aires. Applying great application rates of nitrogen fertilizer causes pollution of groundwater bodies with nitrates. EU observes and reports the water quality of 13000 groundwater bodies. According to the statistical survey 75% of groundwater bodies are classified as ones with good chemical status. The remaining part -25% of groundwater bodies is reported as one with poor chemical status. About 54% of the groundwater bodies with poor chemical status due their contamination to nitrates. 25% of Bulgarian groundwater bodies show a significant positive trend in increasing nitrate pollution in groundwater bodies

In this paper observation on groundwater chemical status of EU Member States in particularly Bulgaria and Belgium are reported by means latest statistical data.

Groundwater is a limited source for fresh water and measures for preventing nitrate pollution have to be applied in irrigation practice.

Keywords: groundwater pollution

1. INTRODUCTION

Fresh water on the Earth is very limited –water in lakes, streams and rivers and presents only 0.01 percent of Earth's water. Groundwater makes up another 0.6 percent. Salt water in oceans and salt lakes represents 97 percent of Earth's water.

* philipova@ibmbm.bas.bg, olga.nitcheva@meteo.bg, marnik.vanclooster@uclouvain.be

During the last decades Europe fresh water are affecting by water scarcity, droughts, floods and physical modifications (dams, wires, sluices etc.). The severe lack of water is observed particularly in South Europe.

As a consequence of droughts in EU between 1976-1990 and 1991-2006, both area and population affected have doubled [1]. Climate changes are expecting to exacerbate these impacts, with frequent and severe droughts in many part of Europe.

Over the last 50 years the world's population has doubled, the gross domestic product- has grown tenfold and the agriculture and industry has flourished. This growth and increased water usages put water resources under pressure.

During the last decades the agriculture intensifies the food production applying high input of fertilizers and pesticides. Leaching and running off a part of them, as a result of precipitations or over-irrigation leads to significant load of pollutions to ground and surface water environment.

In the developing countries the rate of increase of nitrogen fertilizer application has tripled since 1975. A quarter of growth in rice production in Asia has been attributed to increased fertilizer use. In Central and South American and South Asian regions, high rates of nitrogen fertilizer applications combined with proper irrigation technologies and favorable climatic conditions help farmers to raise three crops per year [2].

This trend of an intensified agriculture will continue during the next decades and under conditions of increasing world population and increasing demand for food and water supply.

In this paper observations on fertilizer pollution of groundwaters in Europe and Bulgaria is considered. The last statistical data for this sort of pollution are presented and commented.

2. CONTEMPORARY STATE OF NITRATE POLLUTION OF GROUNDWATER IN EUROPE AND BULGARIA

The Nitrate Directive (1991) of European Commission - Environment considers the EU recommendations for permissible nitrate concentration in groundwater that are 50 mg NO₃/l.

The chemical status of more than 13000 groundwater bodies has been monitored and their pollution is reported in 25 Member States in Europe. Good chemical status is proved to have 75% of them (by surface area), while 25 % of them are in poor status. About 3% of groundwater bodies are classified as ones with unknown chemical status [3].

Excessive nitrate concentration is responsible for 54% of groundwater bodies in Europe that have poor chemical status. Pesticides are another reason for classifying 20% of groundwater bodies as ones with poor chemical status.

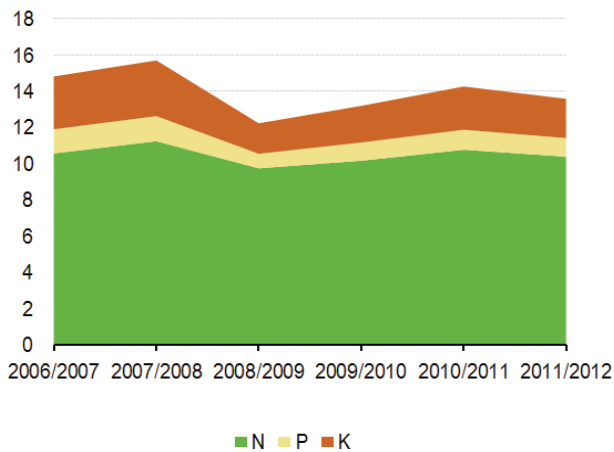


Fig.1: Mineral fertiliser consumption by agriculture in EU-27 (Fertilizers Europe), Million tonnes of nutrients, 2006-2011, [4]

Peaks of nitrogen, phosphorous and potassium fertilizer consumption for EU-27 countries are observed in 2007/2008 and 2010/2011 followed by slow decrease in 2011/2012. The mean nitrogen fertilizer consumption for EU-27 countries during the period of 2006-2012 accounts for 10.48 million tonnes of N per year. The mean phosphorous fertilizer consumption for EU-27 countries during the period of 2006-2012 is equal to 1.1 million tonnes of P per year. The mean potassium fertilizer consumption for EU-27 countries during the same period is 2.38 million tonnes of K per year.

A decreasing trend in nitrogen and phosphorous fertilizer consumption for EU-15 countries and Slovenia, Norway and Switzerland can be seen for the period of 2000-2012 but nitrogen fertilizer consumption denotes an increase for Bulgaria (BG), Czech Republic (CZ), Estonia (ES), Latvia (LT), Poland (PL), Hungary (HU) and Slovakia (SK), (Table.1).

An increasing trend in phosphorous fertilizer consumption for the same period is observed for Slovakia (SK), Romania (RO), Poland (PL) and Bulgaria (BG) (Table.2).

The data for nitrogen fertilizer consumption in Bulgaria for the period of 2000-2012 are according Table 1 and the data for 2013 are taken out from [5]. It can be seen in Fig.2 that nitrogen fertilizer consumption in Bulgaria has doubled in comperance with this one in 2000. A trend in increasing nitrogen fertilizer consumption is observed in Bulgaria for the whole observed period.

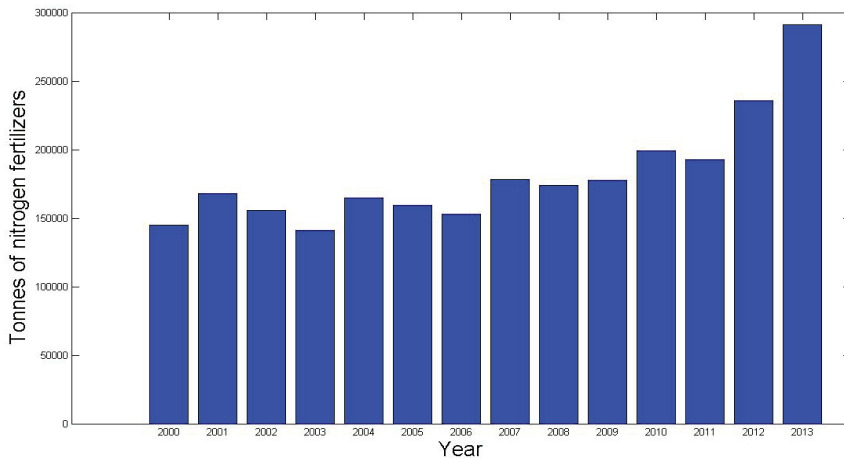


Fig.2. Consumption of nitrogen fertilizer in Bulgaria for the period of 2000-2013, [4-5]

In 2010 the maximal nitrogen fertilizer consumption per ha UAA (utilized agricultural area) is observed in Nederland (NL), Belgium (BE), Luxemburg (LU) which are respectively 120 kg N/ha, 106 kg N/ha and 103 kg N/ha.

In 2010 mean nitrogen fertilizer consumption per ha UAA for EU- 27 countries is equal to 69 kg N/ha and for EU-15 countries is correspondingly 74kg N/ha.

Nitrogen fertilizer consumption per ha UAA in Bulgaria is 56 kg N/ha.

In 2010 the maximal phosphorous fertilizer consumption per ha UAA can be observed for Poland (PL)-11kg P/ha and for Spain (EL) - 10hg P/ha. The mean phosphorous fertilizer consumptions per ha UAA for EU-27 and EU-15 countries are equal to 7 kg P/ha. Phosphorous fertilizer consumption per ha UAA in Bulgaria for the same period is 5kg P/ha.

Approximately 13% of the groundwater monitoring bodies in Europe exceed the limit of 50 mg NO₃/l. The highest proportion of the groundwater monitoring bodies, which exceed the EU Directive limit, to all monitoring ones is observed in Belgium (30%), Denmark (26%), Spain (22%) and Cyprus (19%). Bulgarian groundwater monitoring stations exceeding the accepted limit for nitrate pollution present 9% of all groundwater monitoring bodies.

Table 1: Nitrogen fertiliser consumption by agriculture, EU-27, NO and CH, 2000-2012, [4]

	Tonnes of Nitrogen												
	2000	2001	2002	2003	2004	2005	2006	2007	2008	2009	2010	2011	2012
EU-27	:	:	:	:	:	:	10 643 500 e	10 708 000 e	10 791 500 e	9 942 000 e	:	:	:
EU-15	10 037 500 e	9 350 000 e	9 078 500 e	8 968 000 e	8 931 000 e	8 469 000 e	8 297 000 e	8 184 000 e	8 201 000 e	7 499 500 e	7 853 000 e	:	:
BE	163 000	150 000	155 500	147 000	149 000	139 500	139 500	139 500	130 500	136 500	143 500 p	:	:
BG	145 000	168 000	155 500	141 000	165 000	159 500	153 000	178 000	174 000	177 500	199 000	192 500	235 500 p
CZ	262 500	311 000	289 000	242 500	303 500	293 000	309 500	335 500	341 500	254 000	270 500	352 500	349 000 p
DK	252 000	234 000	211 000	201 000	207 000	206 000	192 000	194 500	220 500	200 500	190 000	197 000	187 000 p
DE	2 014 500	1 847 500	1 791 500	1 788 000	1 828 000	1 778 500	1 785 000	1 600 000	1 807 000	1 550 500	1 569 000	1 786 500	1 640 500 p
EE	22 500	19 500	16 500	23 500	25 000	20 000	22 500	25 000	35 500	27 500	28 500	30 000 p	:
IE	407 500	368 500	363 500	388 000	362 500	352 000	345 000	321 500	309 000	307 000	362 500	345 500	296 500 p
EL (1)	285 000 e	261 000 e	253 000 e	259 000 e	246 000 e	228 500 e	207 000 e	201 500 e	149 000 e	181 000 e	196 000 e	174 000 ep	:
ES	1 279 000	1 131 000	1 026 500	1 198 500	1 073 000	924 000	970 000	986 000	740 000	781 000	941 000	846 500	843 500 p
FR	2 518 000	2 415 500	2 361 000	2 237 000	2 396 000	2 346 500	2 163 000	2 198 000	2 425 000	2 099 000	2 080 000	2 332 000	2 014 500 p
IT (1)	828 000 e	818 000 e	796 000 e	751 500 e	684 500 e	621 500 e	697 000 e	724 000 e	604 500 e	592 000 e	589 500 e	568 000 ep	:
CY (1)	:	:	:	:	:	:	8 000 e	7 500 e	4 500 e	5 500 e	4 000 e	4 000 ep	:
LV	23 000	31 500	27 500	37 500	35 000	41 000	42 500	46 000	47 500	52 000	59 500	60 000	65 000 p
LT (1)	:	:	:	:	:	:	145 000 e	147 000 e	123 500 e	134 500 e	144 000 e	147 000 ep	:
LU	18 000	15 000	16 000	13 000	16 500	14 000	14 000	13 500	13 500	13 500	13 500	15 000 p	:
HU	257 500	275 500	303 000	289 000	293 000	260 500	289 000	320 000	294 500	275 000	281 500	302 000	313 000 p
MT (2)	:	:	500 e	500 e	500 e	500 e	1 000 e	500 e	500 e	500 e	500 e	:	:
NL	339 500	298 500	292 000	290 500	300 500	279 000	288 000	257 500	238 000	225 500	219 500	214 000 p	:
AT	138 000	129 000	106 000	114 000	85 500	105 000	97 500	111 000	108 500	89 000	105 000	98 000	87 000 p
PL	861 500	895 500	862 000	831 500	895 000	895 500	996 500	1 056 000	1 142 500	1 095 500	1 027 500	1 091 000	1 094 500 p
PT	170 000	157 500	164 000	110 000	126 000	102 500	87 500	113 000	105 000	97 500	103 000	99 500 p	:
RO	239 500	268 500	239 000	252 000	270 000	299 000	252 000	265 500	280 000	296 000	306 000	313 500	290 000 p
SI	34 000	35 000	33 500	34 500	30 500	29 000	30 500	29 500	25 000	28 000	:	:	:
SK	84 500	102 500	111 500	97 500	97 000	100 000	97 000	113 500	121 500	96 500	106 500	120 500	128 000 p
FI	167 500	165 500	160 500	159 500	154 500	149 500	148 000	149 000	163 000	136 000	156 500	146 000	139 000 p
SE	189 500	197 000	185 000	180 000	177 000	161 500	160 500	167 000	186 500	142 500	168 000	170 000	148 000 p
UK	1 268 000	1 162 000	1 197 000	1 131 000	1 125 000	1 061 000	1 003 000	1 008 000	1 001 000	948 000	1 016 000	1 022 000	1 000 000 p
NO	105 500	98 500	99 000	102 500	104 000	105 500	103 000	106 500	102 000	91 000	84 000	95 500	94 500 p
CH	53 000	57 000	55 500	53 000	53 500	52 500	51 500	54 000	51 000	48 000	55 500	49 000 p	:

Special values

- :
 - p
 - e
- not available
provisional
Eurostat estimation

(1) Data from Fertilizers Europe

(2) Data from FAOSTAT

Table 2: Phosphorous fertiliser consumption by agriculture, EU-27, NO and CH, 2000–2012, [4]

	Tonnes of Phosphorus												
	2000	2001	2002	2003	2004	2005	2006	2007	2008	2009	2010	2011	2012
EU-27	:	:	:	:	:	:	1 372 500 e	1 373 000 e	1 215 500 e	881 500 e	:	:	:
EU-15	1 472 000 e	1 326 000 e	1 279 500 e	1 286 500 e	1 235 500 e	1 129 500 e	1 030 500 e	1 024 000 e	8 675 00 e	598 500 e	737 000 e	:	:
BE	16 000	11 500	12 500	11 500	12 000	11 000	9 500	10 000	6 500	4 500	5 500 p	:	:
BG	7 000	3 500	9 500	10 500	13 000	11 000	11 000	13 000	13 500	17 000	13 000	13 000	21 000 p
CZ	19 000	23 000	21 500	20 500	24 000	20 500	20 500	26 500	24 000	7 500	13 500	17 500	18 500 p
DK	18 000	16 000	15 000	14 000	15 000	15 000	13 500	14 000	14 000	7 000	11 000	11 500	13 000 p
DE	183 500	153 500	137 500	143 000	124 000	132 000	119 500	115 500	138 500	76 000	102 500	125 000	108 000 p
EE	1 500	1 500	2 000	2 500	3 000	2 500	3 500	3 500	4 000	2 500	2 500	2 500	:
IE	49 500	42 500	42 000	44 000	42 500	38 500	37 000	32 500	26 500	20 000	29 500	29 000	27 500 p
EL (1)	49 500 e	49 500 e	46 500 e	48 000 e	43 500 e	38 500 e	36 000 e	33 500 e	28 000 e	33 000 e	29 000 e	23 000 ep	:
ES	249 000	266 500	264 500	268 500	257 000	224 000	197 500	242 000	118 500	115 500	147 500	158 500	164 500 p
FR	417 500	348 500	329 500	318 500	315 500	300 500	258 500	243 500	282 500	129 000	177 000	218 500	188 500 p
IT (1)	220 000 e	199 500 e	196 000 e	197 500 e	178 000 e	151 500 e	166 500 e	142 000 e	84 500 e	114 500 e	88 000 e	78 000 ep	:
CY (1)	:	:	:	:	:	:	1500	2000	500	1000	1000	1000	:
LV	2 500	3 000	3 500	4 000	5 000	6 500	6 500	7 500	6 500	6 000	7 000	7 500	8 500 p
LT (1)	:	:	:	:	:	:	17 000 e	17 000 e	9 500 e	14 000 e	15 500 e	15 500 ep	:
LU	1 000	1 000	1 000	1 000	1 000	1 000	500	500	500	500	500	500	:
HU	19 500	25 000	27 000	29 000	32 500	26 500	33 000	38 000	27 500	19 000	20 000	22 000	25 500
MT (2)	:	:	0 e	0 e	0 e	0 e	0 e	0 e	0 e	0 e	0 e	:	:
NL	27 000	23 000	21 000	23 000	22 000	21 000	21 000	15 500	11 500	4 500	13 500	6 500	:
AT	25 500	20 000	19 000	19 500	16 000	16 000	14 500	18 000	14 000	7 500	12 500	10 000	9 500
PL	129 500	139 000	139 500	132 000	140 500	141 500	193 000	180 000	202 000	164 000	154 000	178 500	162 000
PT	39 500	34 000	34 500	39 000	52 000	33 500	22 500	29 500	18 000	11 500	18 000	14 000	:
RO	38 500	38 000	32 000	41 500	41 000	60 500	41 000	45 000	44 500	44 000	54 000	55 000	49 500
SI	8 000	7 000	7 000	6 500	6 500	6 000	5 500	5 500	5 000	3 500	:	:	:
SK	7 000	10 500	10 500	10 000	8 500	10 000	9 500	11 000	11 000	8 000	7 000	8 500	10 500
FI	20 500	21 500	20 000	19 500	19 000	18 500	17 000	16 000	16 000	11 000	12 500	11 000	10 500
SE	17 500	17 000	16 500	16 500	17 000	15 500	14 000	13 500	14 500	8 000	10 000	10 500	10 500
UK	138 000	122 000	124 000	123 000	121 000	113 000	103 000	98 000	94 000	56 000	80 000	84 000	82 000
NO	13 000	12 000	12 500	12 500	12 500	12 500	12 500	12 000	11 500	8 500	8 000	9 000	8 500
CH	5 000	5 500	6 500	5 000	6 000	5 000	6 000	6 500	5 000	4 000	4 500	4 500	:

Special values

- : not available
- 0 less than 250 tonnes
- p provisional
- e Eurostat estimation

(1) Data from Fertilizers Europe

(2) Data from FAOSTAT

Table 3: Fertiliser consumption per ha UAA, EU-27, Norway (NO) and Switzerland (CH), 2010, [4]

	N	P	UAA (4)	kg N/ha (5)	kg N/ha (5)
	tonnes	tonnes	1000 hectares	hectares	hectares
EU-27	10 308 500 e	1 032 000 e	150 059	69	7
EU-15	7 853 000 e	737 000 e	106 407	74	7
BE	143 500 p	5 500 p	1 350	106	4
BG	199 000	17 000	3 548	56	5
CZ	270 500	13 500	3 464	78	4
DK	190 000	11 000	2 548	75	4
DE	1 569 000	102 500	16 493	95	6
EE	28 500	2 500	832	34	3
IE	362 500	29 500	4 130	88	7
EL (1)	196 000 e	29 000 e	3 000	65	10
ES	941 000	147 500	18 106	52	8
FR	2 080 000	177 000	25 693	81	7
IT (1)	589 500 e	88 000 e	11 320	52	8
CY (1)	4 000 e	1000	117	34	9
LV	59 500	7 000	1 291	46	5
LT (1)	144 000 e	15 500 e	2 672	54	6
LU	13 500	500	131	103	4
HU	281 500	20 000	3 988	71	5
MT (2)	500 e	0 e	11	45	0
NL	219 500	13 500	1 828	120	7
AT	105 000	12 500	2 321	45	5
PL	1 027 500	154 000	14 163	73	11
PT	103 000	18 000	2 333	44	8
RO	306 000	54 000	11 332	27	5
SI (3)	28 000 e	3 500 e	433	65	8
SK	106 500	7 000	1 801	59	4
FI	156 500	12 500	2 268	69	6
SE	168 000	10 000	3 021	56	3
UK	1 016 000	80 000	11 865	86	7
NO	84 000	8 000	851	99	9
CH	55 500	4 500	908	61	5

Special values

p provisional
e Eurostat estimation

(1) Data from Fertilizers Europe

(2) Data from FAOSTAT

(3) Slovenia data 2009

(4) Excluding common land units, rough grazing and permanent grassland no longer used for production. Common land is included in for a minor part in Spain, Italy and Germany (minor part) and in its total in Slovenia, Cyprus and Norway.

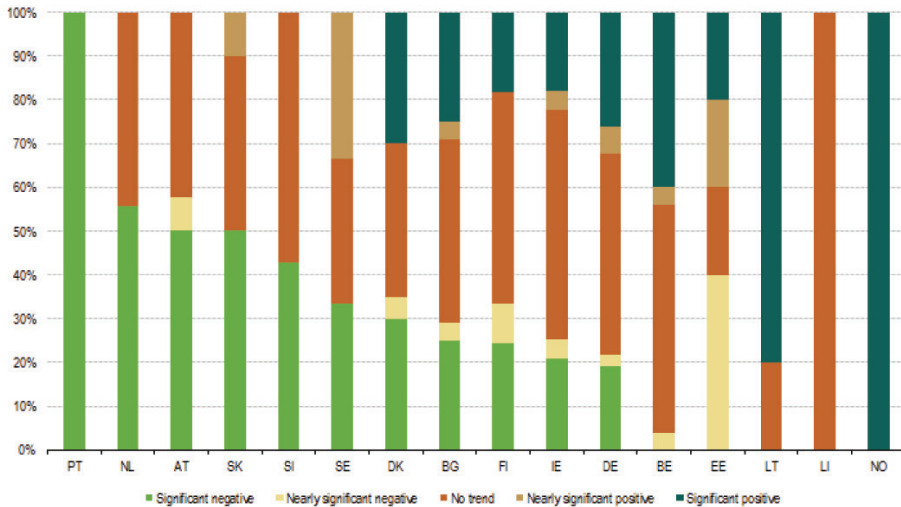
(5) Eurostat estimation

Table 4: Groundwater nitrate concentration classes (mg NO₃/l) and proportion of groundwater monitoring stations in each class per country (%), 2009, EU-27, EFTA, candidate and potential candidate countries; *Source: European Environment Agency in [6]*

	Groundwater nitrate concentration classes (mg NO ₃ /l) and number of groundwater monitoring stations in each concentration class per country				
	≤ 10	10 < ... ≤ 25	25 < ... ≤ 50	50 <	Total
BE	1024	381	534	835	2774
BG	52	21	24	15	112
CZ	385	85	70	73	613
DK	174	92	111	132	509
DE	308	107	119	88	622
EE	171	21	21	1	214
IE	130	62	21	0	213
EL	:	:	:	:	:
ES	217	100	93	114	524
FR	679	394	431	152	1656
IT	:	:	:	:	:
CY	48	12	7	16	83
LV	63	5	6	2	76
LT	162	14	6	2	184
LU	1	1	3	0	5
HU	:	:	:	:	:
MT	:	:	:	:	:
NL	244	16	16	27	303
AT	224	150	119	88	581
PL	80	10	14	8	112
PT	122	58	27	17	224
RO	476	86	51	46	659
SI	21	14	10	2	47
SK	266	72	59	37	434
FI	38	0	0	0	38
SE	23	0	1	0	24
UK	2012	441	99	31	2583
IS	3	0	0	0	3
LI	6	0	0	0	6
NO	50	7	1	0	58
CH	10	16	7	1	34
ME	4	2	1	1	8
HR	29	0	0	0	29
RS	57	8	0	0	65
TR	72	35	11	3	121
AL	10	1	0	0	11
BA	13	0	0	0	13

Special values:

: Data not available



NB: 'Negative' trend indicates a decline in concentration.
 'Positive' trend indicates a rising concentration.
 'Significant' trend indicates that a statistically significant trend is identified.
 In LT, EE, PT, SE, NO and LI the number of data series is ≤ 5 .

Fig. 3: Groundwater nitrate concentration classes (mg NO₃/l) and share of groundwater monitoring stations in each class by country (%), 2009, EU-27, EFTA, candidate and potential candidate countries *Source: European Environment Agency in [6]*

The trends in nitrate contamination of groundwater bodies of EU-27 Member States can be seen in Fig.3. A significant positive trend, that indicates a nitrate concentration rising is valid for more than 25% of Bulgarian groundwater bodies and 40% of them are with neither positive nor negative trend. Only 25% of groundwater bodies show a negative trend which means a decline in nitrate concentrations. For Norway only one groundwater body is reported which shows a significant positive trend.

According to statistical data for 2014 nitrite concentrations above 0.01 mg NO₂/l are observed in groundwater bodies of Spain, Belgium, Romania, Italy. (Fig. 4)

Nitrate concentrations above the limit of 50mg NO₃/l are reported for groundwater pollution in Spain, Belgium, Poland, Germany, Austria, Czech Republic, Greece, Bulgaria, Romania. (Fig.5).

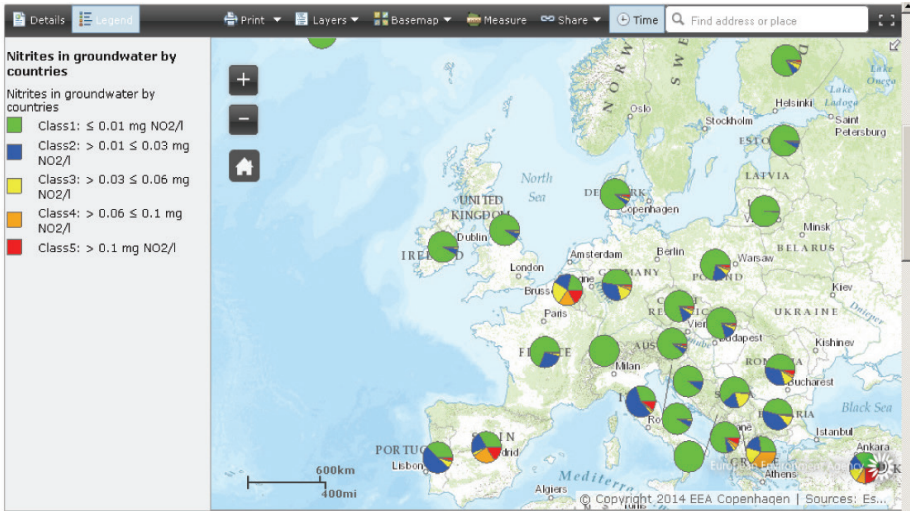


Fig.4. Map of nitrite pollution in groundwater of EU Member States, [7].

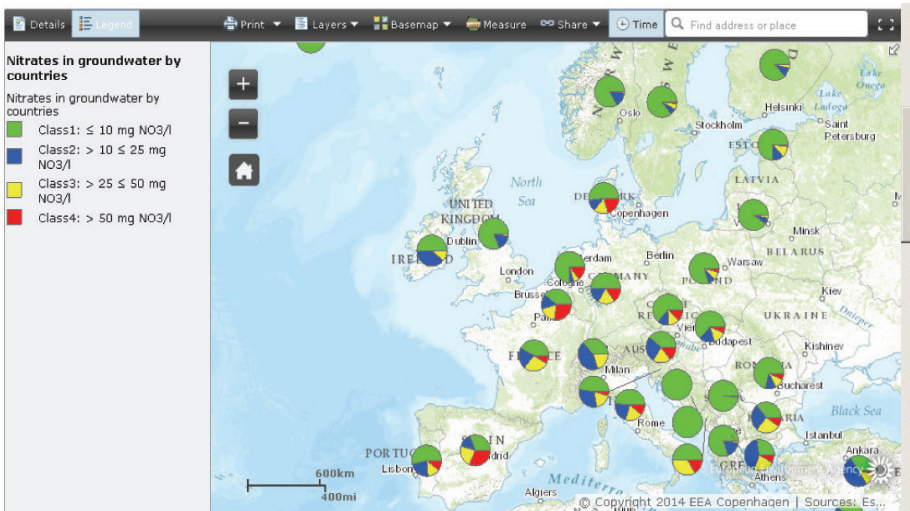


Fig.5. Map of nitrate pollution in groundwater of EU Member States, [8].

Critical concentrations of ammonium are observed in Belgium, Nederland, Spain, Estonia, Poland, Italy, Romania. (Fig.6).

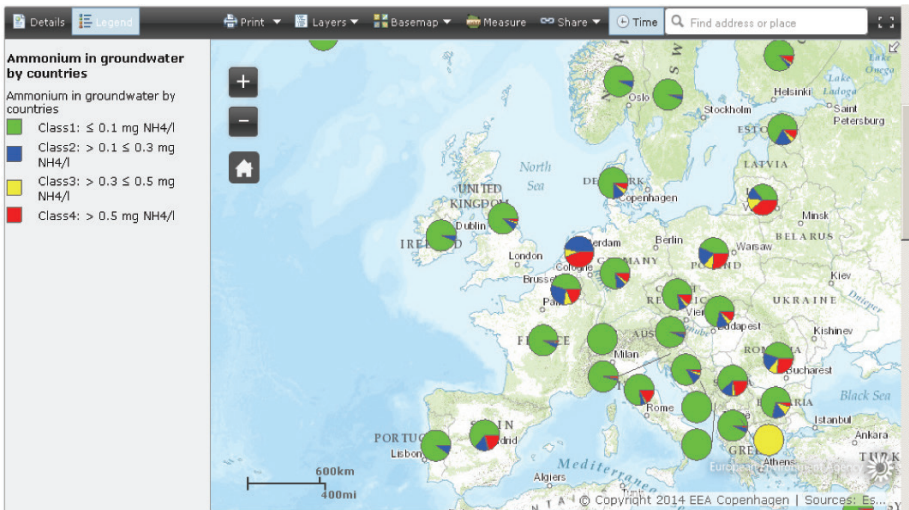


Fig.6. Map of ammonium pollution in groundwater of EU Member States, [9]

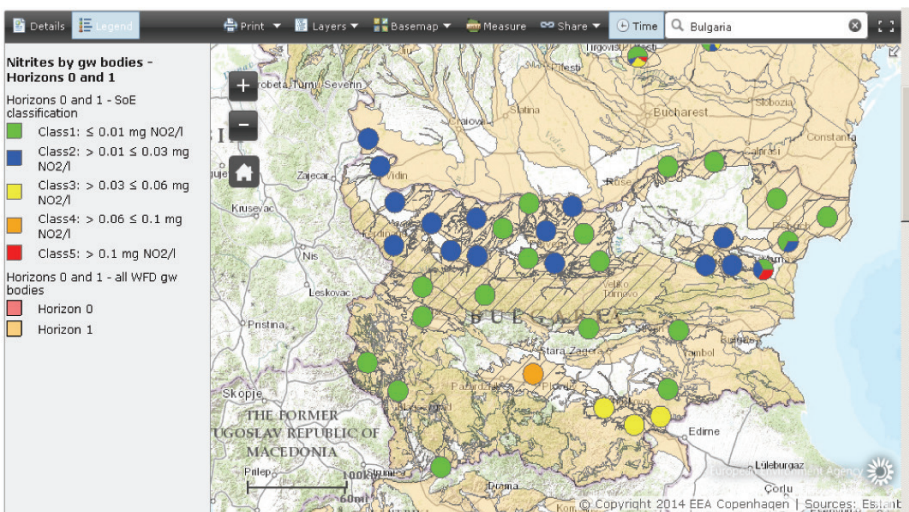


Fig.7. Map of nitrite pollution of groundwater of Bulgaria [7].

Prevailing number of groundwater bodies in Bulgaria are with lower pollution class $1 \leq 0.01 \text{ mg NO}_2/\text{l}$ and $0.01 < \text{class } 2 \leq 0.03 \text{ mg NO}_2/\text{l}$. Only one groundwater body is classified as one with class 5 $> 0.1 \text{ mg NO}_2/\text{l}$ (Fig.7).

Approximately 20 groundwater bodies in Bulgaria are classified mainly or in part with third class of nitrite pollution ($25 < \text{class } 3 \leq 50 \text{ mg NO}_3/\text{l}$). Four groundwater bodies polluted with nitrate concentration above permitted limit of class 4 $> 50 \text{ mg NO}_3/\text{l}$, (Fig.7).

The more strict caution measures should be taken into account in this regions. The farmers should follow strict recommendations for application rates of nitrogen fertilizers

Three groundwater bodies in Bulgaria are diagnosed as polluted with the highest class of ammonium concentrations (class 4 $> 0.5 \text{ mg NH}_4/\text{l}$), followed by four groundwater bodies polluted with concentration between the limits of $0.3 < \text{class } 3 > 0.5 \text{ mg NH}_4/\text{l}$, (Fig.9).

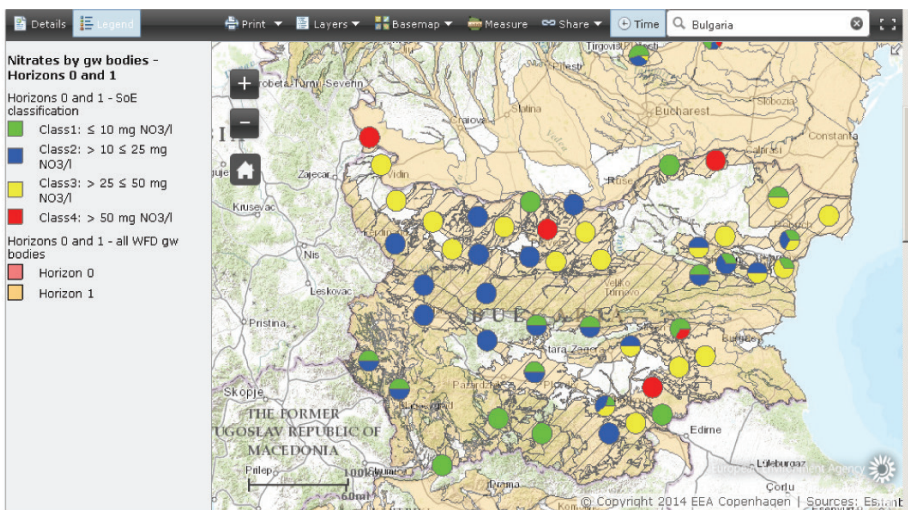


Fig.8. Map of nitrate pollution of groundwater of Bulgaria [8].

Three groundwater bodies in Bulgaria are diagnosed as polluted with the highest class of ammonium concentrations (class 4 $> 0.5 \text{ mg NH}_4/\text{l}$), followed by four groundwater bodies polluted with concentration between the limits of $0.3 < \text{class } 3 > 0.5 \text{ mg NH}_4/\text{l}$, (Fig.9).

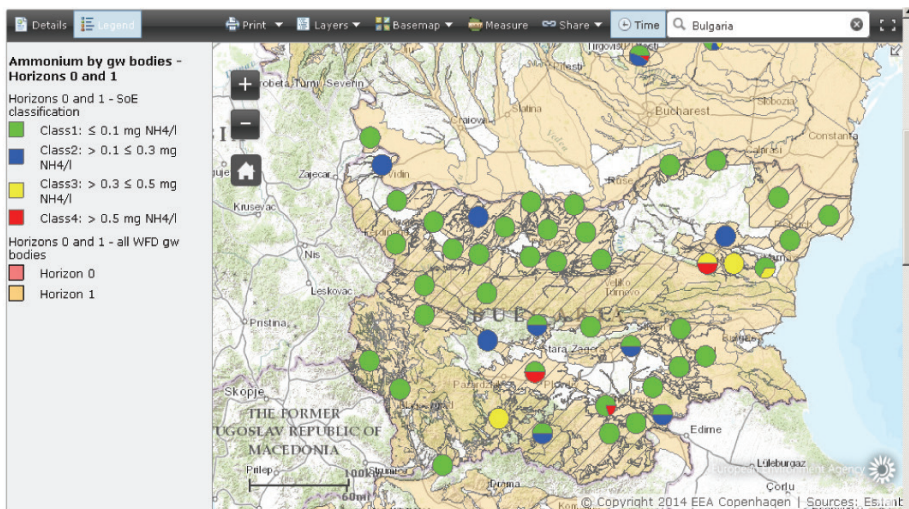


Fig.9. Map of ammonium pollution of groundwater of Bulgaria [9].

Critical is the situation with nitrite, nitrate and ammonium pollutions of groundwater bodies in 2014 in Belgium. Urgent measures should be considered and applied to pure these groundwater bodies. That could be seen correspondingly in Fig.10, Fig.11 and Fig.12.

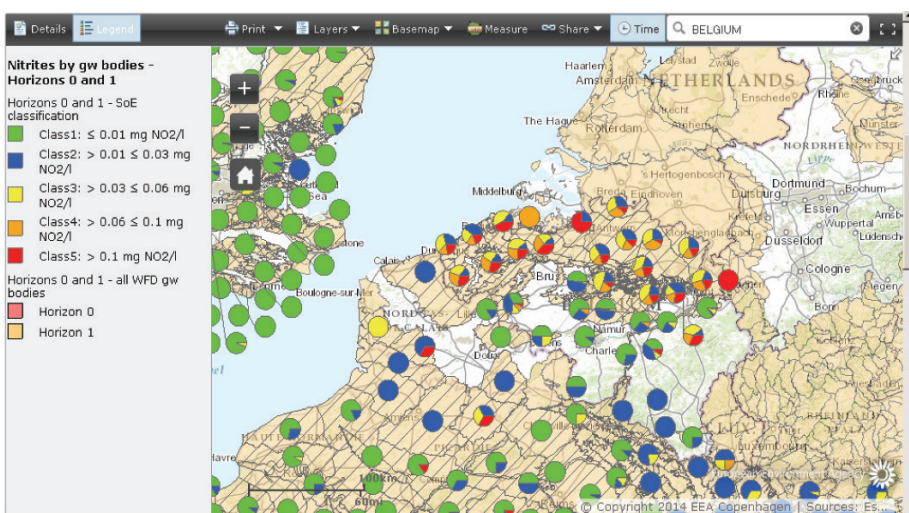


Fig.10. Map of nitrite pollution of groundwater of Belgium [7].

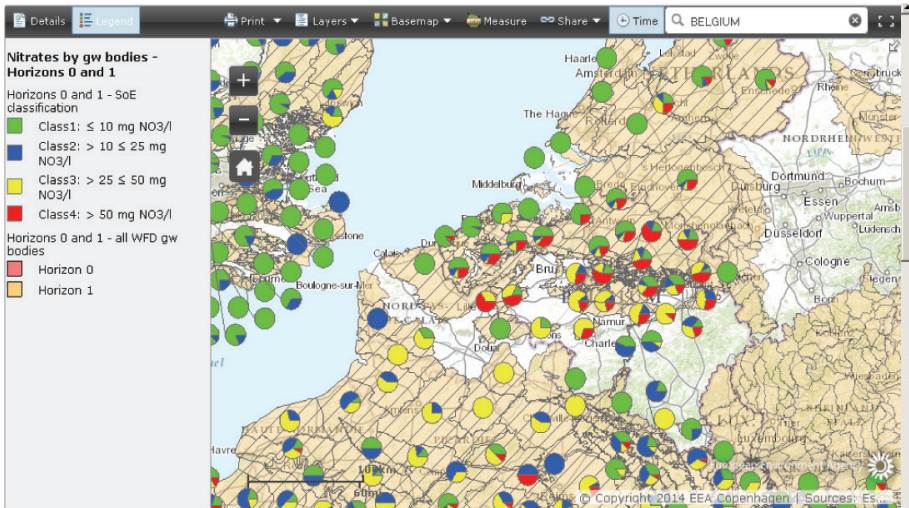


Fig.11. Map of nitrate pollution of groundwater of Belgium [8].

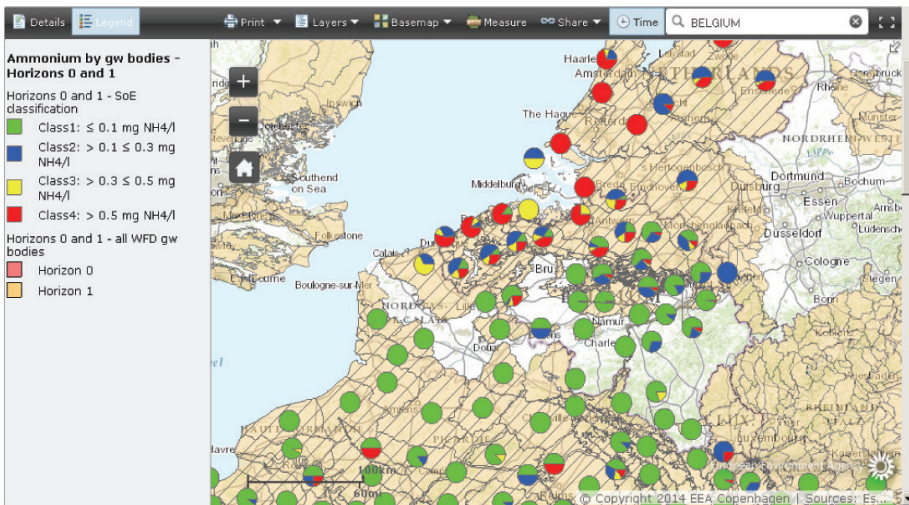


Fig.12. Map of ammonium pollution of groundwater of Belgium [9].

3. CONCLUSIONS:

Groundwater is a vital source of fresh water on the Earth. It will be of great importance as well in the future for whole human being. EU observes the contamination of groundwater bodies across Europe. Under conditions of intensified agriculture in many

parts of the Europe and particularly in Bulgaria and Belgium adequate measures should be conformed and put into practice in order future pollution of groundwater bodies to be preventing.

REFERENCES:

- The European environmental state and outlook 2010, Water resources: quantity and flows. European Environmental Agency, 2010.
<http://www.eea.europa.eu/soer/europe/water-resources-quantity-and-flows>, (Available June 2015)
- Groundwater and its susceptibility of degradation. A global assessment of the problem and options for management. United Nation Environmental Program (UNEP), 2003.
http://www.unep.org/dewa/Portals/67/pdf/Groundwater_Prelims_SCREEN.pdf, (Available June 2015)
- European waters- assessment of status and pressures, European Environmental Agency, 2012,
[http://krw.stowa.nl/Upload/European%20waters%20- %20assessment%20of%20status%20and%20pressures.pdf](http://krw.stowa.nl/Upload/European%20waters%20-%20assessment%20of%20status%20and%20pressures.pdf), (Available June 2015)
4. Agri-environmental indicator – mineral fertilizer consumption, EUROSTAT Statistics Explained http://ec.europa.eu/eurostat/statistics-explained/index.php/Agri-environmental_indicator_-_mineral_fertiliser_consumption, (Available June 2015)
- Agri-environmental indicator –Consumption estimate of manufactured fertilizer: Nitrogen, EUROSTAT Statistics, <http://ec.europa.eu/eurostat/data/database>, (Available June 2015)
- Agri-environmental indicator – nitrate pollution of water, EUROSTAT Statistics Explained,
http://ec.europa.eu/eurostat/statistics-explained/index.php/Agri-environmental_indicator_-_nitrate_pollution_of_water, (Available June 2015)
- Interactive map of nitrite pollution of groundwater of EU Member States,
European Environmental Agency, 2014,
<http://www.eea.europa.eu/data-and-maps/explore-interactive-maps/nitrites-in-groundwater-by-countries>, (Available June 2015)
- Interactive map of nitrate pollution of groundwater of EU Member States,
European Environmental Agency, 2014,
<http://www.eea.europa.eu/data-and-maps/explore-interactive-maps/nitrates-in-groundwater-by-countries>, (Available June 2015)
- Interactive map of ammonium pollution of groundwater of EU Member States,
European Environmental Agency, 2014,
<http://www.eea.europa.eu/data-and-maps/explore-interactive-maps/ammonium-in-groundwater-by-countries>, (Available June 2015)



Simulation of the groundwater level fluctuations in riparian lowlands

Part One

Zdravko Diankov*, Sashka Stefanova

National Institute of Meteorology and Hydrology BAS, 66 Tsarigradsko shose Blvd., BG-1784

Abstract. This part one of the paper describes the groundwater level fluctuations under influence of the hydrologic regime in the neighbour river based on model experiments. The processes within saturated zone result from distribution of the hydraulic head within the highly permeable layer that transmits groundwater inside the lowland. The changes of the hydraulic head are simulated by quasi-2D groundwater model. After discretization of the domain, the respective set of discrete equations is solved numerically. For this purpose, program MATLAB is used, and the results are presented in Excel format for further processing. The model experiments are performed under boundary condition in the river presenting both the rising and falling branches for the period of 55 days, and the model parameters are from the Baley-Kudelin lowland. The groundwater level fluctuations in respect to time as a function of the distance from the riverbank are presented and analysed.

Keywords: groundwater level, hydraulic head, quasi-2D groundwater model, riparian lowland

1. INTRODUCTION

Areas with pronounced flat character are usually formed around the middle and lower stretches of the river courses. In Bulgaria, 13 lowlands with total area of 68000 hectares are identified along the Danube River.

In riparian lowlands protected by dikes from direct flooding the attention is focused on the groundwater level variations under influence of hydrologic regime of the river and

* corresponding author, e-mail: zdiankov1@gmail.com

recharge from precipitation and irrigation. In general, the groundwater level in riparian lowlands is very close to the land surface, and its rising may lead to waterlogging and swamping of the area, irrespective of the drainage canals.

The influence of the changing water level in the Danube River on the groundwater level fluctuations has been analyzed for the Bulgarian lowlands based on observations in wells (*Spasov and Mollov, 1964; Spasov, 1979* as examples).

The aim of the paper is to present the results of model experiments (based on the quasi-2D groundwater flow model) to define the groundwater level fluctuations for Bulgarian lowlands near the Danube River (with parameters of the Baley-Kudelin lowland).

2. DESCRIPTION OF THE MODEL

2. 1. Groundwater flow in riparian lowlands

Groundwater flow in Bulgarian lowland near to the Danube River occurs under influence of several factors: changing water level in the river, precipitation, irrigation and evapotranspiration (*Diankov, 1981*). In this study the two-dimensional flow is considered transverse to the river flow, as the aquifer is under strong influence of the hydrologic regime in the Danube River.

The quasi-2D groundwater flow in riparian zone is described by equation:

$$\mu \frac{\delta h}{\delta t} = -T \frac{\delta^2 h}{dx^2} + w \quad (1)$$

where h is the hydraulic head, μ is the specific yield, T is the transmissivity of the aquifer, x is the distance; w is the groundwater recharge, and t is time. The hydraulic head in the aquifer as a function of time and distance from the river is described by solving this equation.

2. 2. Conceptual model

The conceptual model (2D) is presented in Fig. 1, and the input data are from the Baley-Kudelin lowland (*Diankov and Velkovski, 1990*). The horizontal extent of the model (1000 m) spans the distance from the riverbank to the drainage canal.

The upper layer is low permeable with hydraulic conductivity $K_1 = 0,4$ m/d and thickness $T_1 = 5$ m. The lower layer is characterized with high hydraulic conductivity $K_2 = 100$ m/d and thickness $T_2 = 12$ m.

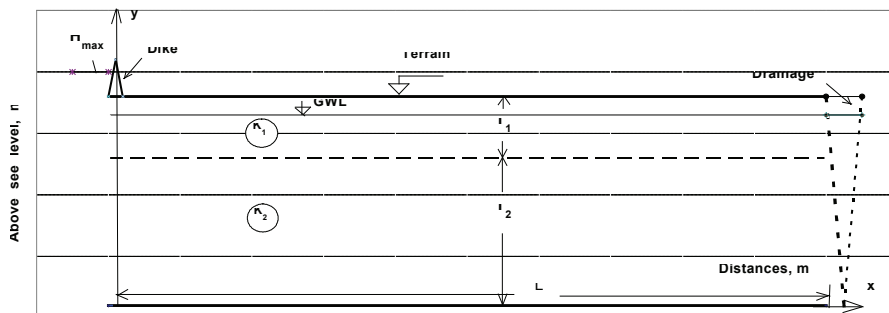


Fig. 1. Conceptual model of the 2D groundwater flow in riparian lowland

Elevation of the terrain surface is 17 m, and the protective dike at the riverbank with crest elevation is over 22,0 m.

Transient groundwater flow is considered, and a value of 0,06 is adopted for specific yield μ (typical for the Danube lowlands).

2. 3. Initial and boundary conditions

The initial condition ($h_0 = 15,5$ m) provides equilibrium state of the system with groundwater level depth 1,5 m below the land surface.

The boundary condition in the river (Table 1) describes both the rising and falling branches for the model experiments. The total duration of the studied process is 55 days within the cold period (evapotranspiration is not taken into account).

In the drainage canal, the boundary condition is specified constant hydraulic head ($h_L = 15,5$ m).

Table 1. Boundary condition – water level in the river

Period N	Duration days	Boundary conditions of the river level	Days from the start
1	8	Constant 15,5 m	8
2	14	Increasing level with a rate of 0,25 m/day, up to elevation 19,0 m	22
3	4	A constant level of elevation 19,0 m	26
4	16	Even decrease with a speed 0,25 m/day up to elevation 15,0 m	42
5	13	Constant water level at 15,0 m	55

2. 3. Space and time discretization

For numerical solution of the equation (1), discretization in space and in time is applied (Fig. 2), and a set of discrete equations is written.

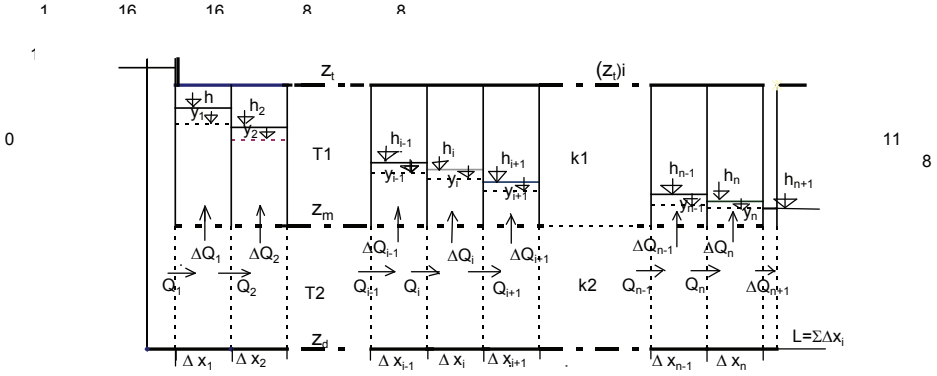


Fig. 2. Groundwater flows in elementary sections of the modelled domain

With the designations introduced in Fig. 2, the finite difference approximations of the balance equation (the inflow, outflow and the storage change) for the i -th section are as follows:

$$Q_i - Q_{i+1} = \Delta Q_i, \quad (2)$$

where:

$$Q_i = (k2)_i (T2)_i \frac{(h_{i-1} - h_i)}{(\Delta x_{i-1} + \Delta x_i) / 2} = (a1)_i (h_{i-1} - h_i), \quad (3)$$

$$Q_{i+1} = (k2)_{i+1} (T2)_{i+1} \frac{(h_i - h_{i+1})}{(\Delta x_i + \Delta x_{i+1}) / 2} = (a2)_i (h_i - h_{i+1}), \quad (4)$$

$$\Delta Q_i = (k1) \Delta x \frac{(h_i - y_i)}{(y_i - z_{mi})} = b_i (h_i - y_i) \quad (5)$$

Here y_i is the initial elevation of the groundwater level for the time period Δt and z_{mi} is elevation of the boundary between the two layers (here equal to 12 m).

Equations (2) - (5) may be written in the form:

$$(a1)_i h_{i-1} + [(a1)_i + (a2)_i + b_i] h_i + (a2)_i h_{i+1} = -b_i y_i, \quad (6)$$

or after combining the coefficients $a1_i$, $a2_i$ and b_i in a single coefficient $A_i = (a1)_i + (a2)_i + b_i$, the water balance equation for the i-th section is as follows:

$$(a1)_i h_{i-1} - A_i h_i + (a2)_i h_{i+1} = -b_i y_i. \quad (7)$$

The increase of the groundwater level for the i-th section Δy_i for the time interval Δt is defined by equation:

$$\Delta y_i = \frac{\Delta Q_i \cdot \Delta t}{\mu_i} = \frac{(K1)_i \cdot \Delta x_i}{\mu_i} \frac{(h_i - y_i)}{(y_i - z m_i)} \Delta t \quad (8)$$

2. 4. Numerical solution

The finite-difference method is chosen for solving the set of equations (7) with the specified initial and boundary conditions. For this purpose, the MATLAB program is used, and the results are presented in Excel format. The time step is equal to 1 day.

Table. 2. Procedure for solving the set equation (7) – example for the first day of simulation

Cross-section with length 1000 m																											
i-th section of the profile i											0 (ho)	1	2	3	4	5	6	7	8	9	10	11 (h _i)					
3	Length of section ΔX [m]											0	100	100	100	100	100	100	100	100	100	100	100	100	0		
4	Distance to the center of the section Xi [m]											0	50	150	250	350	450	550	650	750	850	950	1000				
5	Terrain elevation Zti [m]											17	17	17	17	17	17	17	17	17	17	17	17	17			
6	Elevation between two layers Zmi [m]											12	12	12	12	12	12	12	12	12	12	12	12	12			
7	Basis of the lower layer Zdi [m]											0	0	0	0	0	0	0	0	0	0	0	0	0			
8	Thickness of the top layer T1i [m]											5	5	5	5	5	5	5	5	5	5	5	5	5			
9	Thickness of the lower layer T2i [m]											12	12	12	12	12	12	12	12	12	12	12	12	12			
10	GW level y _{i-1} at the beginning of Δt [m]											15,75	15,5	15,5	15,5	15,5	15,5	15,5	15,5	15,5	15,5	15,5	15,5	15,5			
11	Hydraulic conductivity k1i [m/d]											0,384	0,384	0,384	0,384	0,384	0,384	0,384	0,384	0,384	0,384	0,384	0,384	0,384			
12	Hydraulic conductivity k2i [m/d]											100	100	100	100	100	100	100	100	100	100	100	100	100			
13	(a1) _i = 2*k2 _i *T2 _i /(ΔX _i +ΔX _i)											24	12	12	12	12	12	12	12	12	12	12	12	24			
14	(a2) _i = 2*k2 _i *T2 _i /(ΔX _i +ΔX _{i+1})											12	12	12	12	12	12	12	12	12	12	12	12	24			
15	b _i = (k1 _i *ΔX _i)/(y _i -Zm _i)											10,97	10,97	10,97	10,97	10,97	10,97	10,97	10,97	10,97	10,97	10,97	10,97	0			
16	(-)A _i = (a1) _i +(a2) _i +b _i											-46,97	-34,97	-34,97	-34,97	-34,97	-34,97	-34,97	-34,97	-34,97	-34,97	-34,97	-46,97	-24			
24												Matrix form of the equations											Free member	Head, m			
25	Coefficients for the section l = 1											-46,97	12												-548,057	15,642	
26	The same for the section l = 2											12	-34,97	12												-170,057	15,557
27	The same for the section l = 3												12	-34,97	12											-170,057	15,523
28	The same for the section l = 4													12	-34,97	12										-170,057	15,510
29	The same for the section l = 5														12	-34,97	12									-170,057	15,504
30	The same for the section l = 6															12	-34,97	12								-170,057	15,502
31	The same for the section l = 7																12	-34,97	12							-170,057	15,501
32	The same for the section l = 8																	12	-34,97	12						-170,057	15,501
33	The same for the section l = 9																		12	-34,97	12					-170,057	15,501
34	The same for the section l = 10																			12	-46,97					-542,057	15,500
35	h _i [m]											15,6422	15,5565	15,5224	15,5089	15,5035	15,5014	15,5006	15,5002	15,5001	15,5000						
36	Specific yield μ [-]											0,297	0,297	0,297	0,297	0,297	0,297	0,297	0,297	0,297	0,297	0,297	0,297				
37	h _i -y _{i-1} [m]											0,1422	0,0565	0,0224	0,0089	0,0035	0,0014	0,0006	0,0002	0,0001	0,0000						
38	Δ _i [d]											1	1	1	1	1	1	1	1	1	1	1	1				
39	k1/μ											1,2929	1,2929	1,2929	1,2929	1,2929	1,2929	1,2929	1,2929	1,2929	1,2929						
40	Δy _i =(k1/μ)*((h _i -y _{i-1})/(y _{i-1} -Zm _i))*Δt [m]											0,0525	0,0209	0,0083	0,0033	0,0013	0,0005	0,0002	7E-05	4E-05	0						
41	y _i =y _{i-1} +Δy _i [m]											15,75	15,5525	15,5209	15,5083	15,5033	15,5013	15,5005	15,5002	15,5001	15,5000						
42	Correction under y>h (y _i =h _i) [m]											0,0000	0,0000	0,0000	0,0000	0,0000	0,0000	0,0000	0,0000	0,0000	0,0000						

The calculation procedure is presented in Table 2 for the first day of the simulation ($t = 1$ day). The groundwater level for the new time step j is done in the row before last.

The example presented in Table 2 shows how the change of the boundary condition in the river results in subsequent redistribution of the hydraulic heads in the area and changes of the groundwater level.

3. RESULTS

3. 1. Modelled results for the groundwater level fluctuations

The results obtained from the simulation are processed to analyze variations of the groundwater level in respect to time and distance from the riverbank.

The graphs shown in Fig. 3 clearly demonstrate the influence of the changing water level in the river on the groundwater levels in riparian lowland as a result of the distance from the river and time.

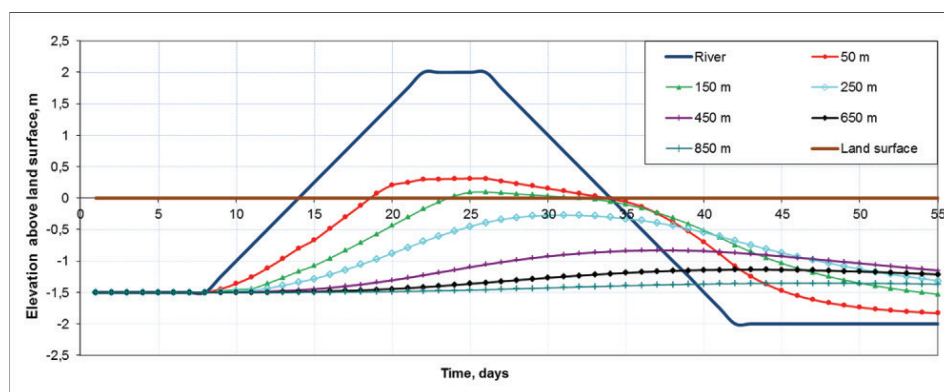


Fig. 3. Groundwater level for different distances from the river as a function of time

The high water level in the river causes temporary flooding from the groundwater, even in absence of precipitation. For example, at a distance of 250 m, the modelled results show flooding of the land surface for a period of two weeks (Fig. 3).

The graphs (shown in Fig. 4) present the groundwater level in a longitudinal section transverse to the river for different time from the beginning of the simulation. Such type of graphs is useful to define the flooded area.

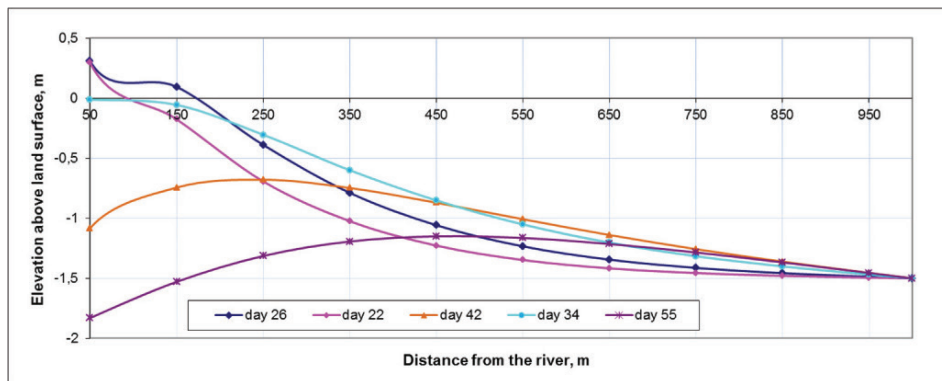


Fig. 4. Groundwater level as a function of the distance from the river

The role of the boundary conditions including the drainage canal with constant head is evident especially on Fig. 4.

3.2. Impact of the time step on the accuracy of the results

The impact of the time step on accuracy of the results concerning the groundwater level fluctuations is evaluated. It is established that the time step of one day produces satisfactory degree of accuracy in all modelled domain, compared to the obtained results with time steps $\Delta t = 0,5$ day. The respective comparisons are not presented for brevity.

With the time step of two days the calculation is faster, but on the account of inaccurate results (especially near the riverbank) that could lead to erroneous conclusions. For this reason the model is run with the time step of 1 day for the entire period of 55 days.

4. CONCLUSIONS

General features of the groundwater level fluctuations in the Baley-Kudelin lowland are analyzed based on model experiments. The changes of the hydraulic head are simulated by quasi-2D groundwater model. Numerical solutions of the equations are obtained with the aid of the program MATLAB. The model experiments are performed under boundary condition in the river presenting both the rising and falling branches for the period of 55 days.

The presented results clearly demonstrate the changes of the groundwater level depending on the distance from the riverbank and time. The amplitude of the groundwater level gradually attenuates with the distance from the river and depends on the hydraulic head in drainage canal.

The applied method could be used for other riparian lowlands based on their specific parameters and boundary conditions. Particularly, it is useful to define the areas prone to flooding by groundwater under specific hydrologic regime in the river.

REFERENCES

- Diankov, Z. (1981) Filtration in riparian lowlands – methods of modeling. Sofia, Publ. House of BAS, (in Bulgarian, with English summary).
- Diankov, Z., G. Velkovski (1990) Effect of the groundwater level on productive soil moisture in a root zone. Proceeding of the Czechoslovak-Polish seminar “Soil water physics”, Stara Lesna, 15-18 May 1990 (in Russian).
- Spasov, V., D. Mollov (1964) Groundwater regime in the Karaboaz lowland and its protection from the flooding in case of construction of a dam on the Danube River. Works on the geology of Bulgaria. Series Eng. geology and hydrogeology, III: 5 -23 (in Bulgarian).
- Spasov, V. (1979) Determining of hydrogeological parameters along the banks of the Danube River using data from groundwater regime. Eng. geology and hydrogeology, 8-9: 32-43 (in Bulgarian).



Simulation of the groundwater level fluctuations in riparian lowlands

Part Two

Zdravko Diankov*, Sashka Stefanova

National Institute of Meteorology and Hydrology BAS, 66 Tsarigradsko shose Blvd., BG-1784, Sofia

Abstract. The part 2 of the paper is focused on rising of the groundwater table caused by rainfalls, superimposed on the influence from the changing water level in the neighbour river. The WAVE model is used that simulates the 1-D unsaturated water flow in the soil profile. The lower boundary condition is obtained from the quasi-2D groundwater flow model described in part 1 of the paper. By additional post-processing of the results from the WAVE model, the water flow velocity in the unsaturated zone at different distances from the riverbank is defined as a function of time. Two periods are identified: (1) initial period when the water flow in the vadose zone is downward but the precipitation water does not reach the groundwater level, and (2) the next period when the precipitation water reaches the boundary between the vadose and saturated zones and leads to the water table rise. The parameters of the model are from the Bulgarian Baley-Kudelin lowland near the Danube River.

Keywords: unsaturated zone, groundwater level, lowland, WAVE model

1. INTRODUCTION

Groundwater level fluctuations in riparian lowlands are of special interest due to real threat of flooding. Lowlands are widespread in Bulgaria – they are located near to the Danube River. They are protected by dikes from the direct flooding from river waters. Yet the rising of the water level in the Danube River leads to subsequent rise of the

* corresponding author, e-mail: zdiankov1@gmail.com

groundwater levels, and to a real threat of swamping from groundwater. The likelihood of flooding is higher during the rainfalls.

The aim of the study is to analyze the behavior of the groundwater level under impact of fluctuations of the water level in a neighbor river in combination with rainfalls, based on the WAVE model (1-D unsaturated flow) in combination with the quasi-2D groundwater model described in the part 1 of the paper.

2. MODELING WATER FLOW IN THE VADOSE ZONE

2. 1. Water flow in the vadose zone

The one-dimensional water flow in unsaturated zone is described by equation:

$$C(h) \frac{\partial h}{\partial t} = \frac{\partial}{\partial z} \left[K(h) \left(\frac{\partial h}{\partial z} + 1 \right) \right] \quad (1a)$$

where h is the hydraulic head, K is the hydraulic conductivity, z is the vertical coordinate defined as positive upward, t is time. The differential water capacity $C(h)$ is a relation (θ is the volumetric soil moisture):

$$C(h) = \frac{\partial \theta}{\partial h} \quad (1b)$$

Equation (1) is applicable both for unsaturated and saturated media. To solve this equation, two functions should be defined: (1) the soil moisture retention characteristic and (2) the hydraulic conductivity relationship.

For the soil moisture retention characteristic, the relationship proposed by Van Genuchten (1980) is used in this study:

$$\theta(h) = \theta_r + \frac{\theta_s - \theta_r}{[1 + (\alpha|h|)^n]^m} \quad (2)$$

where θ_s is the saturated volumetric soil water content, θ_r – is the residual saturated volumetric soil water content, α is the inverse of the air entry value, and n and m are shape parameters.

The hydraulic conductivity relationship used in this study is after the hydraulic conductivity model of Gardner – power function (1958):

$$K(h) = \frac{K_{sat}}{1 + (\beta|h|)^N} \quad (3)$$

where K_{sat} is the saturated hydraulic conductivity, β and N are parameters.

2. 2. Brief overview of the WAVE model

The WAVE model (Water and Agrochemicals in the soil, crop and Vadose Environment) describes the transport and transformations of matter and energy in the soil, crop and vadose environment. The model was developed at the Institute for Land and Water Management of the Katholieke Universiteit Leuven, Belgium (*Vanclouster et al., 1994*).

WAVE is essentially a 1-D model for the description of matter and energy flow in the soil and crop system. The model may use time step smaller than a day but the model input is specified on a daily basis.

In the vertical direction, the soil layers are subdivided in space intervals called the soil compartments. The solution of the differential equations in the unsaturated zone is realized by means of the finite difference method.

The WAVE model has been applied successfully by the authors of the present study in implementation of the INCO-Copernicus Project “Development of tools, needed for an impact analysis for groundwater quality due to changing of agricultural soil use” (*Mioduszewski et al., 2005*) and in several other publications (*Diankov, Stefanova, 2011a, 2011b; Diankov et al., 2010; Nitcheva et al., 2010*).

2. 3. Input data

Input data are from the Baley-Kudelin Danube lowland (*Diankov and Velkovski, 1990*). The workflow is carried out in several stages: 1) preparation of input data for the model; 2) obtaining of the results (output files from the WAVE model), and 3) additional post-processing of the results.

For the purposes of the study, the Water Transport Module of the model is used. The input data are stored in three files:

1. file CLIMDATA – data on precipitation, irrigation and evapotranspiration during the simulated period;
2. file WATDATA for the soil characteristics data and boundary conditions;
3. file GENDATA with general information such as simulation period, time step, and parameters concerning printing of the results.

The adopted parameters for the soil moisture retention characteristic in equation (2) are: $\theta_s = 0,469$; $\theta_r = 0,08855$; $\alpha = 0,00216 \text{ cm}^{-1}$; $n = 0,4988$ and $m = 1$. For the hydraulic conductivity relationship (3), the adopted parameters are: $K_{sat} = 40 \text{ cm/d}$, $\beta = 1,33 \text{ cm}^{-1}$ and $N = 1,51$ (*Diankov and Velkovski, 1990*). The thickness of the soil compartments

is 10 cm. The lower boundary conditions for the sections located at different distances from the riverbank are obtained from the quasi-2D groundwater flow model described in part 1 of the paper.

Alluvial sediments in the lowland are presented by a two-layered system. The thickness of the upper and the lower layers is 5 m and 12 m, and the hydraulic conductivity is 0,4 m/d and 100 m/d respectively. Typical value of the specific yield μ for the area is equal to 0,06.

The modeled area is 1000 m long transverse to the Danube River. Elevation of the terrain surface is 17 m, and of the crest of the dam – over 22 m. The initial water level (and hydraulic head) in the river as well as in the total area is set at 15,5 m.

The boundary conditions in the river are as follows:

- Period 1 with duration 8 days – constant hydraulic head 15,5 m.
- Period 2 with duration 14 days – linear increase up to 19,0 m (rate 0,25 m/day).
- Period 3 with duration 4 days – constant hydraulic head 19,0 m.
- Period 4 with duration 16 days – even decrease up to 19,0 m (rate 0,25 m/day).
- Period 5 with duration 13 days – constant hydraulic head 15,0 m.

The total simulated period is 55 days.

3. RESULTS

3. 1. Defining flow rate in the unsaturated zone

As a result of rising water level in river, water table in riparian lowland may reach the land surface and produce flooding. To define the depth to the groundwater level in the lowland, the 1-D unsaturated flow is simulated for several distances from the river.

The reporting of the calculated results is done in the WAT_SUM.OUT file. The data on the volumetric soil moisture θ , the hydraulic head h and the unsaturated hydraulic conductivity k for the 10-cm soil compartments are of special interest for the objectives of this work. The output data are used to evaluate the rate of the vertical water flow and the depth to the water table in the lowland.

As an example, data for a section at a distance $X = 450\text{m}$ are presented in Table 1 that refer to for the 10th day from the start of simulation. To calculate the values of the hydraulic gradient and flow rate between neighbor soil compartments, two columns are inserted (after the CONDOC column) for additional processing of data. The negative values of the flow velocity mean the downward flow.

For the hydraulic conductivity between the nodal points, the arithmetic mean is taken.

According to the data in Table 1, the simulated values of the flow velocity for the day 10th are negative up to the depth of 0,95 m. This means that the downward flow reaches

only this depth and does not cross the water table at depth of 1,443 m. This example show the possibility to define the water flow in the vadose zone based on the results from the WAVE model.

Two main periods of the soil moisture distribution under influence of precipitation are identified: (1) initial period when the water flow in the vadose zone is downward but the precipitation water does not reach the groundwater level, and (2) the next period when the precipitation water reaches the boundary between the vadose and saturated zones and leads to the water table rise.

Two examples for distribution of the water flow velocity for the initial period are shown in Table 2 – for days 15th and day 20th from the beginning of the simulation period (at distance of 450 m from the river).

The results for days 45th and 50th from the beginning of the simulation period refer to the second period, when the downward flow reaches the saturated zone (Table 3).

Table 1. Determination of the flow velocity between the soil neighbor compartments in the vadose zone from the WAT_SUM.OUT data

PROFIL	E							
-----	-	<i>Day from</i>	<i>Beginning</i>	<i>10-th</i>				
A	B	C	D	E	F	G	H	I
COMP	DEPTH	THETA	PR,HEAD	CONDUC	<i>Hyd gradient</i>	<i>Velocity</i>		
	(MM)	(M ³ /M ³)	(CM)	(MM/DAY)	-	(mm/day)		
1	-50	0,368	-60,40	0,53				
2	-150	0,363	-69,70	0,43	1,93	-0,92		
3	-250	0,358	-78,70	0,36	1,90	-0,74		
4	-350	0,355	-85,10	0,32	1,64	-0,55		
5	-450	0,354	-87,30	0,30	1,22	-0,38		
6	-550	0,355	-85,20	0,32	0,79	-0,24		
7	-650	0,357	-79,70	0,35	0,45	-0,15		
8	-750	0,361	-72,00	0,41	0,23	-0,09		
9	-850	0,366	-63,00	0,50	0,10	-0,05		
10	-950	0,373	-53,10	0,64	0,01	-0,01		
11	-1050	0,38	-42,70	0,89	-0,04	0,03		
12	-1150	0,39	-31,90	1,38	-0,08	0,09		
13	-1250	0,402	-20,80	2,63	-0,11	0,22	<i>GW Depth</i>	
14	-1350	0,421	-9,76	8,13	-0,10	0,56	<i>mm -1443</i>	
15	-1450	0,469	0,40	400,00	-0,02	3,27		
16	-1550	0,469	10,40	400,00	0,00	0,00		
17	-1650	0,469	20,40	400,00	0,00	0,00		
18	-1750	0,469	30,50	400,00	-0,01	4,00		
19	-1850	0,469	40,50	400,00	0,00	0,00		
20	-1950	0,469	50,50	400,00	0,00	0,00		
21	-2050	0,469	60,50	400,00	0,00	0,00		
22	-2150	0,469	70,60	400,00	-0,01	4,00		

Table 2. Simulated results for days 15th and 20th

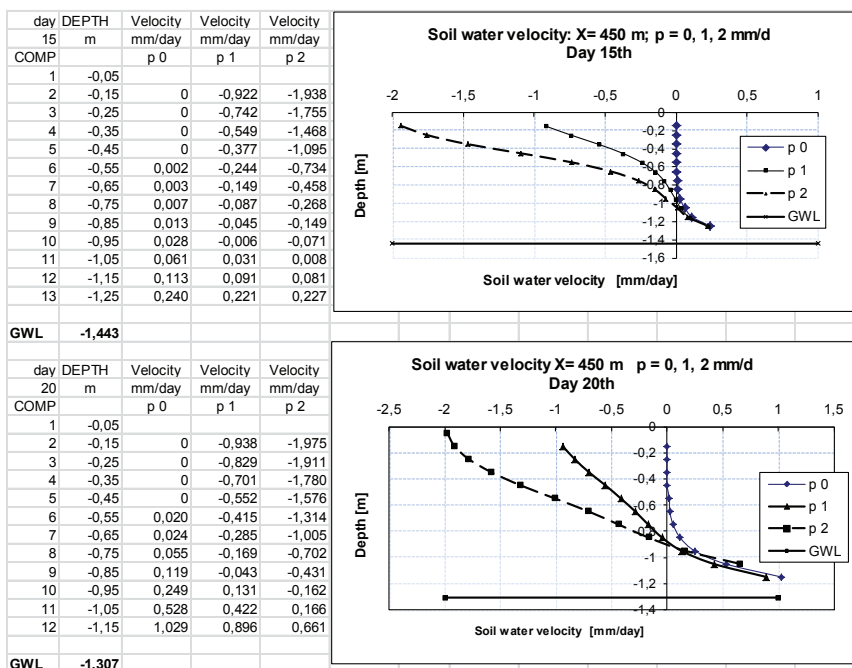
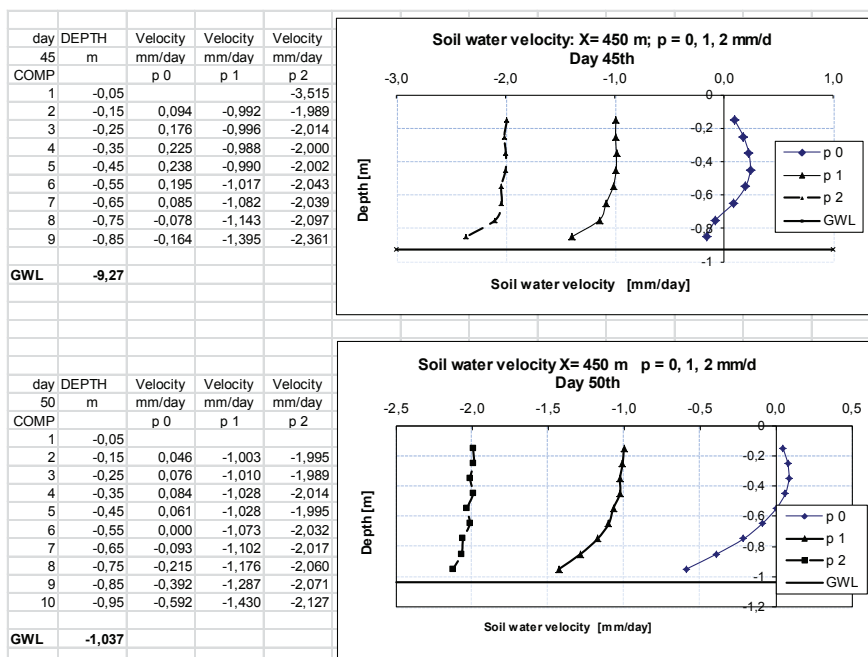


Table 3. Simulated Processes for day 45th and day 50th



3.2. Rising of the groundwater level in response to recharge from precipitation

In periods when rainfall water does not reach the surface of the saturated zone, the groundwater level is formed only under the influence of the variations of the river water level. In cases when precipitation water reaches the saturated zone, the WAVE model allows two possibilities for the processes in the vadose zone depending on the boundary conditions.

Boundary condition 1: constant head boundary at the bottom. In this case, the water table change with time $\Delta H_k = 0$.

Boundary condition 2: zero flux at the bottom. This condition leads to the groundwater level rise for the time interval K according to equation:

$$\Delta H_k = \Delta t \frac{v_k}{\mu}, \quad (4)$$

where v_k is flow rate in the saturated zone and μ is the specific yield, also known as the drainable porosity, with adopted value of 0,06.

3.2.1. Calculation scheme

The contribution of precipitation water to the groundwater level rise (when it reaches the saturated zone) is represented schematically on Fig. 1. The modelled period is divided in K time intervals from the beginning of the simulation with time step $\Delta t = 5$ days ($K = 11$).

The sequence of the data processing according to this scheme (Fig. 1) is shown in Table 3. It is assumed that the precipitation water reaches the saturated zone for the first time during the j^{th} 5-day interval from the beginning of the simulated process. During this interval (with number K), the groundwater level rises with a value of

$$\Delta H_k = \Delta t \frac{v_k}{\mu}.$$

In the end of the first 5-day interval (K_1) it rises up to $Z_1 = Z^{0,0} + \Delta H_1$, where $Z^{0,0}$ is the water table unaffected by precipitation. During the next time interval K_2 the rising starts from the previous value Z_1 .

The variations of the groundwater level unaffected by precipitation are taken into account. It is supposed that the effects on the groundwater level from precipitation and from fluctuations of the water level in the river are independent, and the total effect is calculated by the mathematical principle of superposition. For the end of the second interval the groundwater level is $Z_2 = Z^{0,2} + (Z_1 - Z^{0,1}) + \Delta H_2$.

The general recurrent equation (for time interval K) for the groundwater level is as follows:

$$Z_K = Z_{K-1} + (Z^{0,K} - Z^{0,K-1}) + \Delta H_K \quad (5)$$

The computation details are presented in Table 3, including the interval K of the first contact of the water flow that reaches the groundwater level (influenced only by the hydrological regime in the river). Two variants are described with different rainfall intensity p : 1 mm/d and 2 mm/d ($p1$ and $p2$ respectively). The computed depth of the groundwater level is presented in the last row of Table 3.

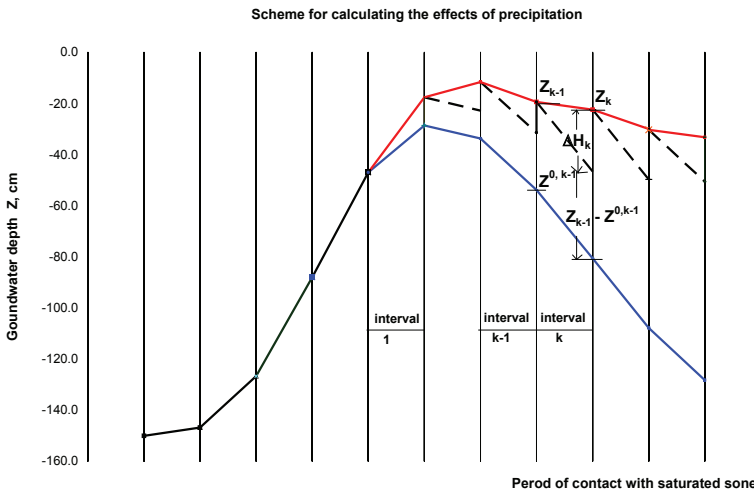


Fig. 1. Scheme for calculating the effect from precipitation

Table 3. Computations of the groundwater level depth (examples for distance of 450 m)

X=450 m														
p = 1 mm/d														
Interval (j)	0	1	2	3	4	5	6	7	8	9	10	11		
Day	0	5	10	15	20	25	30	35	40	45	50	55		
Z ⁰ без валеж p=0 от WAVE,WATSUM_OUT	450 p0	-2	-1,5	-1,47	-1,44	-1,31	-1,1	-1	-0,846	-0,848	-0,927	-1,037	-1,151	
Compartment reached								0	5	10	15	20	25	
Flow rate V _k , mm/day								0	0,22	0,94	1,39	1,43	1,5	
Δh _k =V _k /μ, mm/d								0	3,67	15,67	23,17	23,83	25,00	
ΔH _k =5*Δh _k								0	18,33	78,33	115,83	119,17	125,00	
Groundwater level														
Z _k =Z _{k-1} +(Z _{0k} -Z _{0(k-1)})+ΔH _k	450 p1	-2	-1,5	-1,5	-1,5	-1,5	-1,5	-1,5	-1,481	-1,403	-1,287	-1,168	-1,168	
X=450 m														
p = 2 mm/d														
Interval (k)	0	1	2	3	4	5	6	7	8	9	10	11		
Day	0	5	10	15	20	25	30	35	40	45	50	55		
Z _{0k} without rainfall from WATSUM_OUT	450 p0	-2	-1,5	-1,47	-1,44	-1,31	-1,1	-1	-0,846	-0,848	-0,927	-1,037	-1,151	
Compartment reached									8	8	9	10	12	
Flow rate V _k , mm/day									0	2,01	2,06	2,36	2,126	2,35
Δh _k =V _k /μ, mm/d									0	33,50	34,33	39,33	35,43	39,17
ΔH _k =5*Δh _k									0	167,50	171,67	196,67	177,17	195,83
Groundwater level														
Z _k =Z _{k-1} +(Z _{0k} -Z _{0(k-1)})+ΔH _k	450 p2	-2	-1,5	-1,47	-1,44	-1,31	-1,1	-1	-0,679	-0,509	-0,391	-0,324	-0,242	

Variations of the groundwater levels as a result of recharge from precipitation with different intensity are presented on Fig. 2 (for the same distance 450 m).

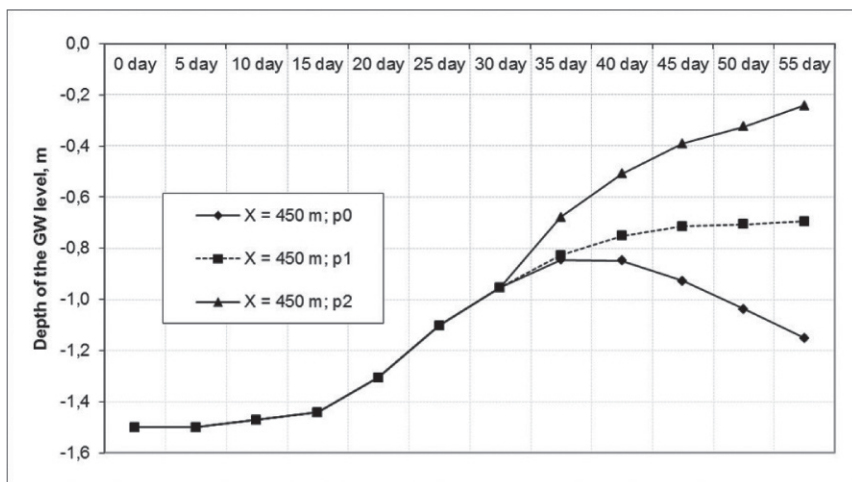


Fig. 2. Groundwater level fluctuations at distance X = 450 m under precipitation intensities p0, p1 and p2. GWL influenced by rainfall since day 30th.

It is shown in Fig. 3 that under precipitation intensity $p = 3$ mm/d the groundwater level “crosses” and swamps the land surface after the 37th day from the beginning of the process, for intensity $p_0 = 4$ mm/d – after the 32nd day, and for intensity $p = 5$ mm/d – after the 28th day.

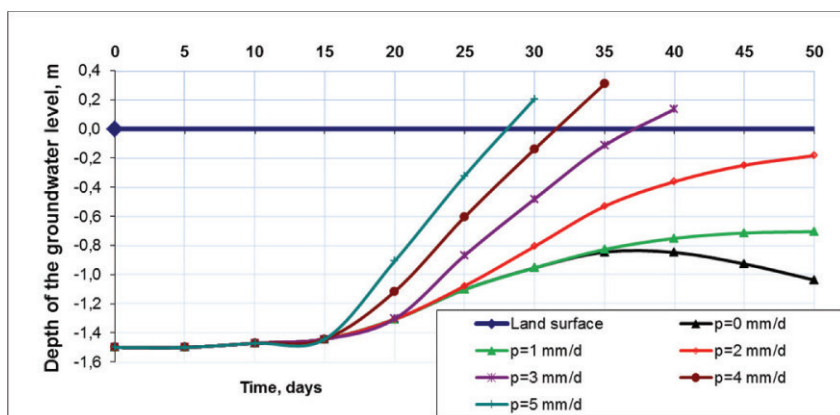


Fig. 3. Variations of the water table depth at distance 450 m from the river under different rainfall intensity values.

Really, the long term precipitation with intensity values higher than 2 mm/d is unlikely event and the respective modeled examples during the 55-day period serve for demonstration purposes only.

3.2.2. Impact of precipitation on the groundwater level rise

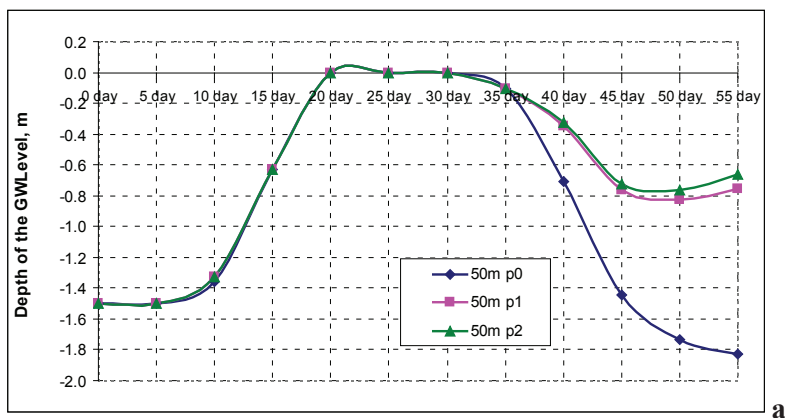
The obtained results describe variations of the groundwater level influenced both from the hydrological regime in the river and precipitation. As an example, in Table 4 are presented results on the evolution of the hydraulic heads for different distances under precipitation intensity values: 0, 1 and 2 mm/d (p_0 , p_1 and p_2 respectively).

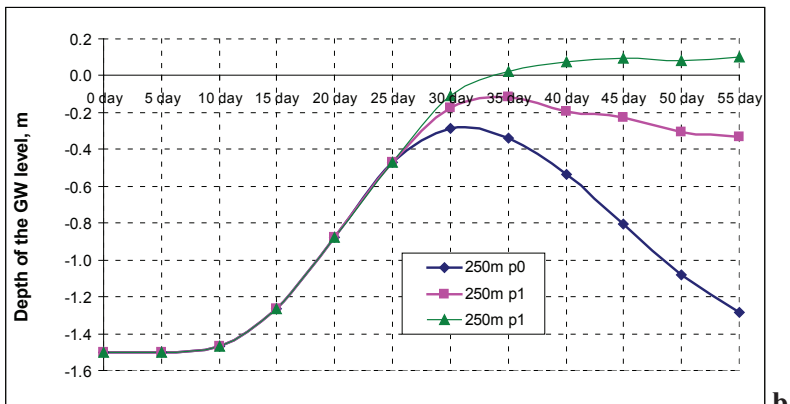
The data in Table 4 are base for the analyses for the groundwater level fluctuations both in time and in space (for different distances from the riverbank).

Table 4. Evolution of the hydraulic heads (in cm) for the defined depths as a result of recharge from rainfalls with intensity values: $p_0 = 0$; $p_1 = 1$ and $p_2 = 2$ mm/d

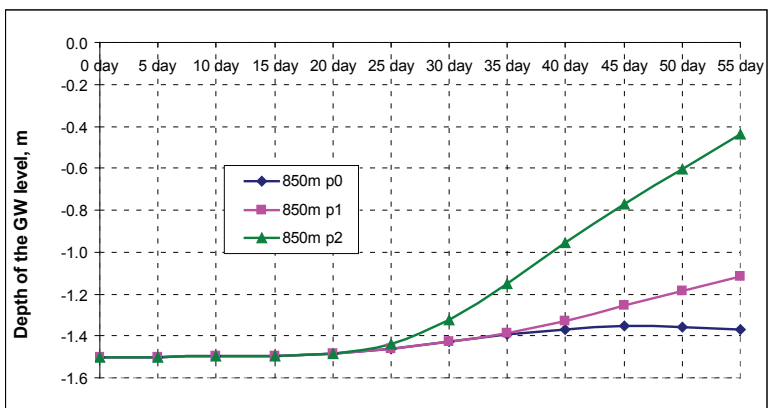
	X, m	day 0	day 5	day 10	day 15	day 20	day 25	day 30	day 35	day 40	day 45	day 50	day 55
p0	50	-150	-150	-132,6	-63	0	0	0	-10,3	-70,8	-144,5	-173,1	-183
p0	250	-150	-150	-146,6	-126,7	-88,03	-47,08	-28,633	-33,8	-53,7	-80,7	-107,9	-128,2
p0	450	-150	-150	-147,1	-144,3	-130,7	-110,2	-95,4	-84,6	-84,8	-92,7	-103,7	-115,1
p0	750	-150	-150	-149,9	-149,4	-147,0	-142,4	-136,3	-130,7	-126,7	-125,3	-126,1	-128,5
p0	850	-150	-150	-149,9	-149,6	-148,6	-146,3	-142,8	-139,4	-136,9	-135,5	-135,6	-136,7
p0	950	-150	-150	-149,9	-149,9	-149,6	-148,9	-147,8	-146,7	-145,8	-145,3	-145,2	-145,5
p1	50	-150	-150	-132,6	-63	0	0	0	-10,3	-35,0	-76,5	-82,9	-75,8
p1	250	-150	-150	-146,6	-126,7	-88,0	-47,1	-17,7	-11,7	-19,5	-22,5	-30,3	-33,3
p1	450	-150	-150	-147,1	-144,3	-130,7	-110,2	-95,4	-82,8	-75,1	-71,5	-70,5	-69,4
p1	750	-150	-150	-149,9	-149,4	-147,0	-142,4	-136,3	-129,7	-122,3	-115,0	-108,4	-103,3
p1	850	-150	-150	-149,9	-149,6	-148,6	-146,3	-142,8	-138,9	-132,7	-125,7	-118,4	-111,6
p1	950	-150	-150	-149,9	-149,9	-149,6	-148,3	-146,0	-142,3	-137,2	-131,0	-125,0	-117,4
p2	50	-150	-150	-132,6	-63	0	0	0	-10,3	-32,8	-72,3	-76,5	-66,1
p2	250	-150	-150	-146,6	-126,7	-88,0	-47,1	-11,2	2,3	7,3	9,5	7,9	10,3
p2	450	-150	-150	-147,1	-144,3	-130,7	-110,2	-95,4	-67,9	-50,9	-39,1	-32,4	-24,2
p2	750	-150	-150	-149,9	-149,4	-147,0	-140,5	-125,7	-105,4	-85,1	-67,0	-51,0	-32,4
p2	850	-150	-150	-149,9	-149,6	-148,6	-144,1	-132,3	-114,9	-95,8	-77,1	-60,4	-44,0
p2	950	-150	-150	-149,9	-149,9	-148,5	-144,5	-135,1	-120,0	-102,2	-84,5	-66,9	-49,8

Temporal variations of the water table at different distances from the riverbank are presented on Fig. 4abc. The areas close to the riverbank are the most threatened from swamping. For example, at a distance $x = 50$ m from the bank (Fig. 4a), the land surface is flooded even in the absence of precipitation during the period from the 20th to the 30th day. At the distance of 250 m the flooding would occur only under rainfall rate of 2 mm/d from the 35th day up to the end of the modelled period. Without any rainfall, at the same distance the groundwater level would show gradual decline from 0,3 m up to 1,28 m below the land surface.



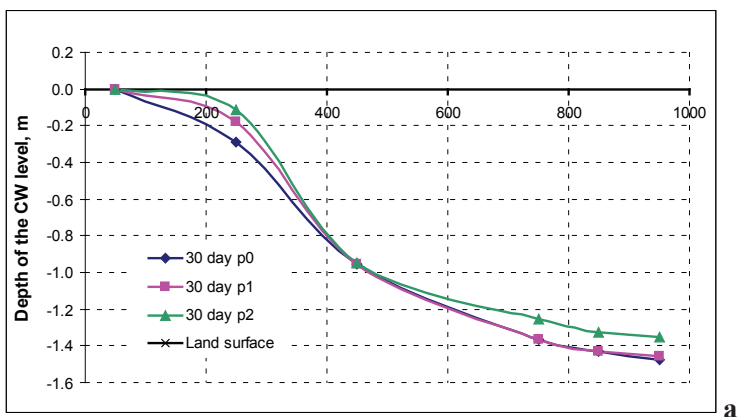


b



c

Fig. 4abc. Groundwater level fluctuations at different distances from the riverbank:
a) X = 50 m; b) X = 250 m; c) X = 850 m



a

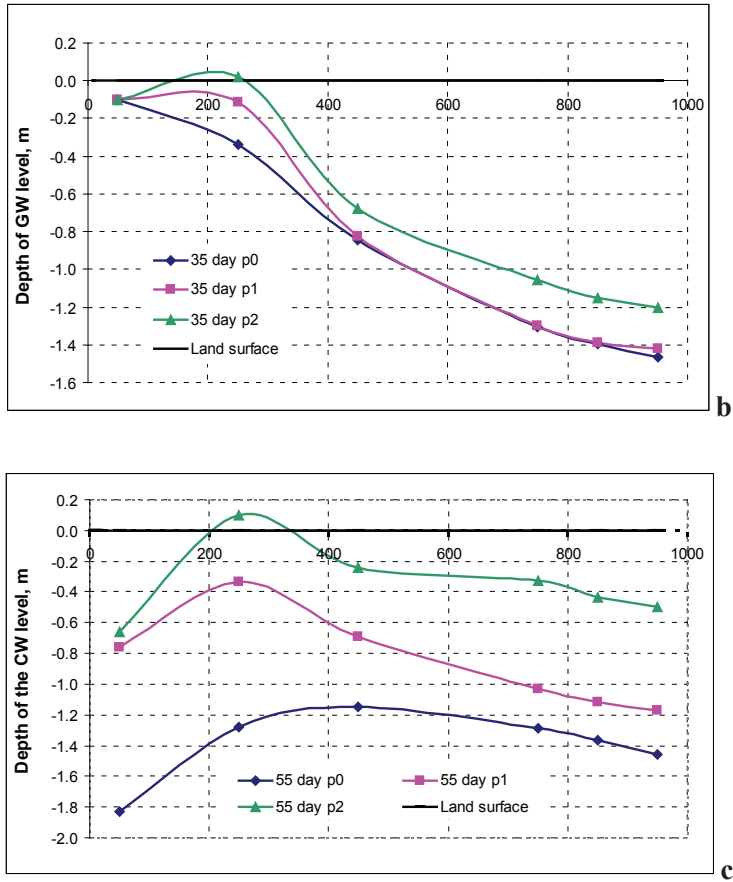


Fig. 5abc. Groundwater level as a function of the distance for various rainfall intensity values: a) for day 30th; b) for day 35th; c) for day 55th.

Figures 5abc show the groundwater levels as a function of distance from the river for various rainfall intensity values. They allow to assess the impact on the water table from precipitation and to compare the groundwater levels affected by rainfalls with the intensity 1 mm/d and 2 mm/d to those without any rainfall. The propagation of the wave inside the lowland gradually attenuates towards the drainage canal. This manner of presentation most possibly is the best to express more clearly the set objectives of modelling.

4. SUMMARY AND CONCLUSIONS

The behavior of the groundwater level in riparian lowlands is an issue of significant practical interest related to management of these areas. The necessity of protection of

the lowlands from flooding and swamping should be based both on *in-situ* observations and measurements and theoretical considerations including simulation.

The groundwater level in riparian lowlands is influenced by changing water level in a river, recharge from precipitation and irrigation and evapotranspiration.

In this study the major factors affecting the groundwater fluctuation are examined and simulated based on both the WAVE model for 1-D unsaturated water flow and the quasi-2D groundwater flow model. For this purpose a series of model experiments is run with different rainfall rates. The hydrogeological parameters used are from the Baley-Kudelin lowland and are typical for a number of riparian Bulgarian lowlands near to the Danube River.

A 55-day period has been simulated, which includes gradual rising and lowering of the water level in the river and a period of constant head.

The combined effect from hydrological regime in the river and precipitation on the groundwater level is analyzed based on model experiments. Additional processing of data from the output file (WAT_SUM.OUT) allowed quantifying the rate of the water flow in unsaturated zone as a result of precipitation in lowland affected by hydrological regime in the river. The visualization of the results clearly shows the general features of the temporal and spatial variations of the groundwater level.

The applied methodical approach could be used in practice for solving various engineering problems under specific natural conditions.

The presented case studies demonstrate the power and usefulness of the model WAVE to describe the flow processes in riparian lowlands. In addition to the simulated impacts from variable water level in the river and precipitation, the WAVE model allows modeling of the root water uptake from plants and the plant growth. Furthermore, the program WAVE includes the solute transport and the nitrogen fate modules that are important for agricultural studies.

ACKNOWLEDGMENTS

The authors would like to express their gratitude to Assoc. Prof. Dr. Tatiana Orehova for her constructive suggestions and assistance in editing the paper.

REFERENCES

- Diankov, Z., S. Stefanova (2011a) Contamination of groundwater with nitrates, predicted with the WAVE simulation model (Part One). Bulgarian Journal of Meteorology and Hydrology: 16 – 37.
- Diankov, Z., S. Stefanova (2011b) Contamination of groundwater with nitrates, predicted with the WAVE simulation model. Simulation of a long period of process development. (Part Two). Bulgarian Journal of Meteorology and Hydrology: 38 – 52.

- Diankov, Z., O. Nitcheva, S. Stefanova (2010) Estimation of the expected contamination of groundwater with nitrates agricultural land use at different rates of fertilisation in different conditions and irrigation, in view of the nitrate directive (96/676/EEC) to protect water from pollution. Report, phase of development 2. Archive of the Department MUW at NIMH-BAS (In Bulgarian).
- Diankov, Z., G. Velkovski (1990) Effect of the groundwater level on productive soil moisture in a root zone. Proceeding of the Czechoslovak-Polish seminar "Soil water physics", Stara Lesna, 15-18 May 1990 (in Russian).
- Gardner, W. R. (1958) Some steady-state solutions of the unsaturated moisture flow equation with application to evaporation from a water table. *Soil science*, 85(4): 228-232.
- Nitcheva, O., Z. Diankov, S. Stefanova (2010) Estimation of the expected contamination of groundwater with nitrates agricultural land use at different rates of fertilisation in different conditions and irrigation, in view of the nitrate directive (96/676/EEC) to protect water from pollution. Report, phase of development 1. Archive of the Department MUW-NIMH-BAS (In Bulgarian).
- Van Genuchten, M. T. (1980) A closed-form equation for predicting the hydraulic conductivity of unsaturated soils. *Soil science society of America journal*, 44(5): 892-898.
- Vanclooster, M., P. Viaene, J. Diels, K. Christians (1994) WAVE a mathematical model for simulating water and agrochemicals in the soil and vadose environment. Reference & user's manual (release 2.0). Institute for Land and Water Management, Katholieke Universiteit Leuven, Leuven, Belgium.
- Mioduszewski, W., Fic, M., Slesicka, A., Zdanowicz, A., Walther, W., Paetsch, M., Reinstorf, F., Weller, D., Diankov, S., Velovski, G., Radoslavov, S., Marinov, W., Nicheva, O., Querner, E.P., Roelsma, J. (2005) Development of tools needed for an impact analysis for groundwater quality due to changing of agricultural soil use, Lidi Razowska-Jaworek & Andrzej Saduski (eds), IAH-Books, A.A. Balkema Publishers, 295 p.



15th Annual Meeting of the European Meteorological Society and the 12th European Conference on applications of meteorology, 07-11 September 2015, Sofia, Bulgaria

From 7 to 11 September 2015, the meteorological community in Bulgaria hosted the largest European forum in the field of research and service to society with meteorological and hydrological information - 15th Annual Meeting of the European Meteorological Society and the 12th European Conference on applications of meteorology (15th EMS&12th ECAM). The conference was organized in cooperation with the Bulgarian Meteorological Society (BMS), Aviometeorological club of Bulgaria (AMC), the National Institute of Meteorology and Hydrology at the Bulgarian Academy of Sciences (NIMH-BAS), EUMETNET WG of European forecasters, EUMETNET Climate Programme and EMS. Leading local organizer, member of the Organizing, Scientific and Steering Committees was Prof. DSci E. Batchvarova. The Ministry of Education and Science supported the participation of 10 young Bulgarian scientists.

About 500 distinguished and young researchers and operational meteorologists from all meteorological services in Europe and other countries worldwide (China, Australia, Korea, USA, etc.) gathered in Sofia for a week. Researchers and professors from universities, representatives of private organizations, producers of meteorological equipment and providers of hydrometeorological information services actively participated in both events.



The President of the European Meteorological Society, Mr. Horst Böttger inaugurated the meeting, welcomed the participants and wished successful work. Greetings were offered from the President of the Republic of Bulgaria, Ministry of Environment and Water, Ministry of Regional Development, Bulgarian Academy of Sciences, NIMH-BAS, Bulgarian Air Traffic Services Authority (BULATSA), World Meteorological Organization, European Centre for Medium Range Weather Forecasts, European Space Agency, Association of Hydro-Meteorological Equipment Industry and others.

In the context of the more frequent extreme weather events during past decades in Europe and worldwide, such as heavy rains and floods, heat waves and droughts, hurricanes and storms that took thousands of lives and caused damages for hundreds of

millions of euros, the theme of the Conference on Applications of Meteorology “High impact weather and hydrological hazards: from observation to impact mitigation” was highly relevant and very welcome.

MAIN SESSIONS OF THE EVENT: *From observations and numerical weather prediction to warnings and impact mitigation; *Climate change detection, assessment of trends, variability and extremes; *Delivery and communication of impact based forecasts and risk based warnings; *Understanding and improving the socio-economic benefits of forecasts; *Meteorological observations from ground and space-based Global Navigation Satellite System; *Climate prediction and scenarios on decadal to centennial timescales; *Boundary-layer physics and parameterizations in weather and climate models; *Coastal meteorology and oceanography; *Phenology and agrometeorology; *Meteorological processes, atmospheric composition and pollution; *Education; *Media and communication; *Biometeorology; *and many other...



Particular attention was paid to the presentation of meteorological and hydrological information, forecasts, warnings and analyzes to the general public, media and government, so that each group could take full advantage of it.

The European Meteorological Society (EMS) had chosen Anton Eliassen as Laureate of the EMS Silver Medal 2015. He had been honoured for his scientific contribution to environmental meteorology, his outstanding service to the European and international meteorological community that was e.g. central for the success of the Convention on Long-Range Trans-boundary Air Pollution, and his major role in increasing and enhancing the public understanding of meteorological information through his effort to make meteorological data freely available.



The Harry Otten Prize for Innovation in Meteorology encourages individuals and groups to come forward with new ideas on how meteorology in a practical way can further move society forward. It was given in 2015 to Olivier Boucher for his idea of “Low-cost humidity observations for weather prediction from automated detection of aviation contrails”. Prizes for honours outstanding achievements in biometeorology, for best poster, for young scientist, for TV Weather Forecast, Tromp award, etc. were also awarded.

Leading world companies such as Scintec and Kipp Zonen exposed modern meteorological equipment. The American Meteorological Society presented the newest scientific journals and books in meteorology.



The events became possible with the generous sponsorship of the EMS, BMS, EUMETNET, AMC, BAS, NIMH at BAS, BULATSA. For more information <http://www.ems2015.eu/>

Ekaterina Batchvarova, Tatiana Spassova